

# Comparison of the Technical and Economic Feasibility of Devulcanisation Processes for Recycling Waste Tyres in South Africa

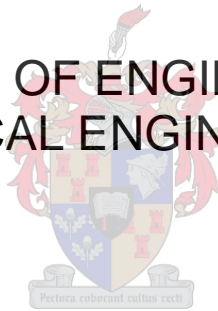
*by*

Devon William Edwards

Thesis presented in partial fulfilment  
of the requirements for the Degree

*of*

MASTER OF ENGINEERING  
(CHEMICAL ENGINEERING)



in the Faculty of Engineering  
at Stellenbosch University

*Supervisor*

Dr. P van der Gryp

*Co-Supervisor*

Prof. JF Görgens

March 2016

## ***Declaration***

By submitting this thesis electronically, I declare that the entirety of the work contained therein is my own, original work, that I am the sole author thereof (save to the extent explicitly otherwise stated), that reproduction and publication thereof by Stellenbosch University will not infringe any third party rights and that I have not previously in its entirety or in part submitted it for obtaining any qualification.

Date: .....

*Copyright © 2016 Stellenbosch University*

*All rights reserved*

## Abstract

The problem of the accumulation of waste tyres is receiving increased attention in the 21<sup>st</sup> century as a result of environmental concerns as well as the economic undesirability of discarding the valuable materials still present in tyres at the end of their useful life. The difficulty associated with recycling waste tyres is linked to the stable thermoset network structure of the vulcanised rubber comprising the majority of a waste tyre's mass.

The recovery of value from tyres via incineration for their relatively high calorific value has been a popular method of diverting tyres from landfills and stockpiles in the past, although newer methods such as pyrolysis and devulcanisation aim to recover more value than merely the energy content of tyres. Pyrolysis processes aim to recover and purify valuable chemicals generated by the thermal decomposition of the rubber compounds in tyres. Devulcanisation processes aim for the controlled breakdown of the vulcanised rubber network in such a way that the rubber regains its thermoplastic properties and can be moulded and revulcanised into new products, without a significant loss of the important mechanical properties associated with vulcanised rubber products.

The shortcomings identified in the literature include the lack of comparable technical data between devulcanisation technologies, and the near absence of any form of energy consumption and economic data associated with devulcanisation processes. This study aimed to identify promising devulcanisation technologies and address the shortcomings identified in the literature by generating comparable technical and economic data for the selected devulcanisation technologies. The devulcanisation technologies identified for further analysis included the extrusion-based mechanical and mechanochemical devulcanisation processes.

The experimental work showed that increasing extrusion temperature has a strong effect on increasing the extent of devulcanisation in both devulcanisation processes. Varying screw speed in the mechanical devulcanisation process showed a very weak effect on the extent of the devulcanisation reaction. Increasing concentration of the devulcanisation chemical in the mechanochemical devulcanisation process caused an increase in the extent of the reaction, although the effect was rather weak. Overall, the mechanochemical devulcanisation process resulted in a substantially higher selectivity for crosslink scission and therefore higher product quality in comparison to the mechanical devulcanisation process.

Economic analysis of the processes was conducted assuming various scales of operation from approximately 400 tons/year to 7000 tons/year, using scaled-up power consumption data generated during the experimental work. The mechanical devulcanisation process was found to be likely to outperform the mechanochemical devulcanisation process from an economic

perspective due to the high costs of the extra chemicals required for the mechanochemical devulcanisation process. It should be noted, however, that the economic analysis did not take into account the potentially higher market value of the reclaimed rubber produced by the mechanochemical devulcanisation process. Therefore, further market research will be required in order to come to a firm conclusion as to which process will be more economically viable. A sensitivity analysis also showed that the economics of both processes are very sensitive to the power consumption, which could be a major problem for devulcanisation processes in South Africa.

## Opsomming

Die probleem van die opeenhoping van afval bande ontvang baie aandag in die 21<sup>ste</sup> eeu as gevolg van hulle effek op die omgewing, sowel as die ekonomiese onwenslikheid van die weggooi van die waardevolle materiaal wat nog steeds teenwoordig in die bande is. Die probleem wat verband hou met die herwinning van afval bande is gekoppel aan die stabiele termoset netwerk struktuur van die gevulkaniseerde rubber in die bande.

Die herwinning van waarde van afval bande volg gewoonlik 'n roete van verbranding vir hulle hoë energie-inhoud, maar nuwe metodes soos pirolise en devulkanisasie probeer om meer waarde te herwin as net die energie-inhoud. Devulkanisasie prosesse mik vir die beheerde uiteensetting van die gevulkaniseerde rubber netwerk in so 'n manier dat die rubber sy termoplastiese eienskappe herwin en kan gevorm word en hervulkaniseer in nuwe produkte, sonder om die meganiese eienskappe te verminder.

Die gapings wat in die devulkanisasie literatuur voorkom is die skaarsheid van vergelykbare tegniese data tussen devulkanisasie prosesse, asook die afwesigheid van metings van die elektriese krag verbruik. Die doel van hierdie werk was om die vereisde data te skep vir twee onderskeide devulkanisasie prosesse, en daarna die prosesse te vergelyk. Die prosesse wat gekies is vir die studie was meganiese devulkanisasie en meganochemiese devulkanisasie.

Die eksperimentele werk het getoon dat die verhoging van ekstrusie temperatuur 'n sterk invloed op die verhoging van die mate van devulkanisasie in beide devulcanisation prosesse. Wisselende skroef spoed in die meganiese devulkanisasie proses het 'n baie swak invloed op die mate van die devulkanisasie reaksie. Toenemende konsentrasie van die chemikalieë in die meganochemiese devulcanisation proses veroorsaak 'n toename in die mate van die reaksie, alhoewel die effek swak is. Oor die algemeen het die meganochemiese devulkanisasie proses gelei tot 'n aansienlik hoër selektiwiteit vir kruis-skakel verdeling en dus hoër kwaliteit van die produk in vergelyking met die meganiese devulkanisasie proses.

Ekonomiese analise het gewys dat die meganiese devulkanisasie proses meer waarskynlik winsgewend sal wees in vergelyking met die duurder meganochemiese proses op 'n skaal van 400 tot 7000 ton/jaar. Dit moet egter daarop gelet word dat die ekonomiese analise nie rekening gehou het met die potensieel hoër markwaarde van die herwonne rubber vervaardig deur die mechanochemical devulcanisation proses nie. Daarvoor sal verdere marknavorsing benodig word om by 'n vaste gevolgtrekking te kom. A sensitiviteitsanalise het ook getoon dat die ekonomie van beide prosesse baie sensitief is vir die krag verbruik, wat 'n groot probleem vir devulkanisasie prosesse in Suid-Afrika kan wees.

## Acknowledgements

I would like to express my sincere thanks to my supervisors, Dr. Percy van der Gryp and Prof. Johann Görgens for their guidance and motivation throughout the duration of the work.

Dr. Bart Danon, thank you for the TGA analyses of my samples and for helping me bounce fundamental ideas and assumptions around until they made sense.

Mr. Jos Weerdenburg and the rest of the workshop staff, thank you for the opportunity to learn from you, and for hands-on development work that could not have been done without your help.

Thank you to the Recycling and Economic Development Initiative of South Africa (Redisa) for funding and for providing the opportunity to do this research. I would also like to thank Mr. Ika van Niekerk and Dr. Ziboneni Godongwana for their assistance with sourcing of materials and contacts within the rubber and recycling industries.

Most importantly, I would like to thank my family, friends and colleagues within the Department of Process Engineering at Stellenbosch University for their support and motivation that helped me to strive on in the face of adversity.

*“That wasn’t flying, that was falling with style” – Sheriff Woody*

# Contents

Abstract.....	ii
Opsomming .....	iv
Acknowledgements.....	v
Abbreviations .....	xi
Glossary.....	xi
List of symbols .....	xii
List of figures .....	xiii
List of tables.....	xv
1 Introduction.....	1
1.1 Background and motivation for research.....	1
1.2 Key questions .....	3
1.3 Aims and objectives.....	3
1.4 Scope and limitations of study .....	4
1.5 Layout of this thesis .....	4
2 Literature study .....	5
2.1 Automotive tyres .....	5
2.1.1 Tyre composition .....	5
2.1.2 Vulcanisation .....	6
2.2 Tyre recycling .....	7
2.2.1 Energy recovery.....	7
2.2.2 Crumbing .....	7
2.2.3 Pyrolysis of rubber .....	8
2.2.4 Devulcanisation .....	8
2.3 Characterisation of devulcanised rubber .....	9
2.3.1 Crosslink density.....	9
2.3.2 Sol fraction.....	10
2.3.3 Horikx's analysis .....	10

2.3.4	Revulcanisation and physical properties .....	11
2.4	Devulcanisation technologies.....	12
2.4.1	Thermal reclamation .....	13
2.4.2	Chemical probes.....	13
2.4.3	Microbial devulcanisation.....	14
2.4.4	Mechanical devulcanisation .....	15
2.4.5	Mechanochemical devulcanisation.....	16
2.4.6	Ultrasonic devulcanisation .....	18
2.4.7	Microwave devulcanisation .....	19
2.5	Concluding remarks.....	20
2.5.1	Devulcanisation feedstock description .....	20
2.5.2	Selection of devulcanisation technologies.....	20
2.5.3	Product characterisation .....	23
2.5.4	Novel research contribution .....	23
3	Experimental.....	25
3.1	Materials used .....	25
3.2	Devulcanisation equipment and methodology .....	25
3.2.1	Mechanical devulcanisation methodology.....	27
3.2.2	Mechanochemical devulcanisation methodology .....	27
3.3	Experimental design and planning .....	28
3.3.1	Mechanical devulcanisation experiment design .....	28
3.3.2	Mechanochemical devulcanisation experiment design.....	29
3.4	Analytical equipment and methodology.....	30
3.4.1	Soxhlet extraction equipment and procedure .....	30
3.4.2	Swelling procedure .....	31
3.5	Statistical analysis.....	31
3.6	Error analysis.....	32
4	Results and Discussion.....	33
4.1	Crumb characterisation.....	33

4.1.1	Fundamental assumptions.....	33
4.1.2	Crosslink density and sol fraction of the crumb rubber.....	35
4.2	Mechanical devulcanisation.....	38
4.2.1	Sol fraction.....	38
4.2.2	Crosslink density.....	42
4.2.3	Horikx analysis.....	45
4.2.4	Power consumption.....	46
4.3	Mechanochemical devulcanisation.....	50
4.3.1	Sol fraction.....	50
4.3.2	Crosslink density.....	53
4.3.3	Horikx analysis.....	56
4.3.4	Power consumption.....	58
4.4	Concluding remarks.....	61
5	Economic Analysis.....	62
5.1	Economic modelling strategy.....	62
5.1.1	Key performance indicators.....	64
5.1.2	Capital cost estimations (TCI).....	65
5.1.3	Variable cost estimations.....	66
5.1.4	Fixed costs.....	66
5.1.5	Revenue.....	67
5.1.6	Scale-up considerations.....	67
5.2	Preliminary economic analysis.....	69
5.3	Effect of scale on MASP.....	70
5.4	Economic trade-off between operating parameters.....	73
5.5	Sensitivity analysis.....	75
5.6	Conclusions from economic analysis.....	80
5.6.1	Mechanical vs mechanochemical devulcanisation.....	80
5.6.2	Economies of scale.....	80
5.6.3	Effect of operating conditions on economics.....	80

5.6.4	Economic sensitivity.....	81
6	Conclusions and Recommendations.....	82
6.1	Conclusions.....	82
6.1.1	Identification of promising devulcanisation technologies.....	82
6.1.2	Technical performance modelling.....	82
6.1.3	Techno-economic comparison.....	83
6.2	Recommendations.....	84
6.2.1	Experimental work.....	84
6.2.2	Scale-up methodology.....	85
6.2.3	Fundamental research into RR characterisation.....	85
	References.....	86
	Appendix A: Calculation of Horikx curves.....	91
	Appendix B: Economics.....	92
	B.1. Assumptions and clarifications.....	92
	B.2. Selected DCF sheets.....	93

## Abbreviations

DADS – Diallyl disulfide

DAE – Distillate aromatic extract (process oil)

DArDS – Diaryl disulfide

DCF – Discounted Cash Flow

DPDS – Diphenyl disulfide

GTR – Ground tyre rubber (crumb)

MASP – Minimum acceptable selling price

NR – Natural rubber

PCT – Passenger car tyre

phr – Parts per hundred parts of rubber polymer, by weight.

SBR – Styrene-butadiene rubber

SSE – Single screw extruder

TDAE – Treated distillate aromatic extract (process oil)

TSE – Twin screw extruder

TT – Truck tyre

## Glossary

Crumb – Granular rubber produced by various grinding processes (GTR).

Rubber compound – A blended compound comprising rubber polymer as a major ingredient.

Rubber polymer – Specifically the macromolecular hydrocarbon portion of rubber compounds.

Vulcanisate – A product consisting wholly or partly of vulcanised rubber.

## List of symbols

$M$	Number-average molecular weight of the rubber polymer before vulcanisation
$N$	Number of primary polymer molecules per gram of rubber
$\gamma$	Crosslinking index of a vulcanised rubber network
$\nu_0$	Number of network chains in a vulcanised network
$\nu_e$	Number of elastically effective network chains
$s$	Sol fraction of rubber polymer
$g$	Gel fraction of rubber polymer
$V_R$	Apparent volume fraction of rubber in a swollen network containing fillers
$V_{R0}$	True volume fraction of rubber in a swollen network containing fillers
$m_R$	Mass of rubber polymer network (gel) in a sample
$m_{polymer}$	Total polymer mass in a sample (sol + gel)
$\rho_R$	Density of rubber polymer
$m_F$	Mass of filler in a sample
$\rho_F$	Density of filler (carbon black)
$m_S$	Mass of solvent in a swollen network
$\rho_S$	Density of solvent
$\underline{V}_S$	Molar volume of solvent
$\chi$	Flory-Huggins polymer-solvent interaction parameter
$\phi$	Volume fraction of filler in an unswollen polymer network
$c$	Kraus correction parameter

## List of figures

Figure 2.1: Network structure of vulcanised rubber. Redrawn from (Flory, 1944) .....	6
Figure 2.2: Typical plot of the relationships between sol fraction and relative decrease in crosslink density (Horikx, 1956) .....	11
Figure 3.1: Brabender Plasti-Corder PLE 651 used for devulcanisation experiments. (1: Feeder outlet; 2: Extruder hopper; 3: Extruder driver; 4: Extruder) .....	26
Figure 3.2: Screw feeder used to feed GTR into the extruder. (1: Feeder outlet; 5: Feeder hopper; 6: Feeder speed controller) .....	26
Figure 3.3: Diagram of the single screw extruder used for experimental work. ....	27
Figure 3.4: Soxhlet extractors used for rubber analysis. ....	30
Figure 4.1: Fractional composition of GTR. The dark green section is the total extractable portion composed of crumb extract and the negligible sol fraction of the polymer. ....	33
Figure 4.2: Fractional composition of reclaimed rubber. The dark green section is the extractable portion of the sample composed of crumb extract and the sol fraction .....	34
Figure 4.3: Pareto chart indicating the significance of operating parameters on modelling the sol fraction of samples produced by mechanical devulcanisation .....	39
Figure 4.4: Surface plot of the sol fraction model for mechanical devulcanisation .....	40
Figure 4.5: TGA data confirming partial devolatilisation of the GTR used in experiments at $T > 250^{\circ}\text{C}$ .....	40
Figure 4.6: Pareto chart indicating the statistical significance of operating parameters on modelling the crosslink density of samples produced by mechanical devulcanisation .....	43
Figure 4.7: Surface plot of the crosslink density model for mechanical devulcanisation .....	44
Figure 4.8: Horikx plot of data from the mechanical devulcanisation experiment along with theoretical curves .....	45
Figure 4.9: Power consumption of the mechanical devulcanisation process at a constant screw speed (55 RPM) .....	47
Figure 4.10: Power consumption of the mechanical devulcanisation process at a constant temperature ( $225^{\circ}\text{C}$ ) .....	47
Figure 4.11: Pareto chart showing the statistical significance of the effects of operating parameters on the power consumption of the mechanical devulcanisation process. ....	48
Figure 4.12: Surface plot of the power consumption model for the mechanical devulcanisation process. ....	49
Figure 4.13: Pareto chart showing the statistical significance of various factors on modelling the sol fraction of samples generated by mechanochemical devulcanisation .....	51
Figure 4.14: Surface plot of the sol fraction model for mechanochemical devulcanisation ...	52

Figure 4.15: Pareto chart showing the significance of various factors on modelling the crosslink density of samples produced by mechanochemical devulcanisation ..... 54

Figure 4.16: Surface plot of the crosslink density model for the mechanochemical devulcanisation process..... 55

Figure 4.17: Horikx plot of experimental data from the mechanochemical devulcanisation experiment along with theoretical curves..... 56

Figure 4.18: Power consumption of the mechanochemical devulcanisation experiments at constant temperature of 185°C ..... 59

Figure 4.19: Power consumption of the mechanochemical devulcanisation at constant DPDS concentration of 17.5 g/kg rubber..... 59

Figure 4.20: Pareto chart showing the statistical significance of the various factors of the full quadratic model in terms of modelling the power consumption of the mechanochemical devulcanisation process..... 60

Figure 4.21: Surface plot of the power consumption model for mechanochemical devulcanisation process..... 60

Figure 5.1: Overview of the economic model for a devulcanisation plant including the flow of numerical information (shaded blocks) through calculations (unshaded blocks)..... 62

Figure 5.2: The MASP as a function of increasing throughput for mechanical devulcanisation ..... 72

Figure 5.3: The MASP as a function of increasing throughput for mechanochemical devulcanisation ..... 72

Figure 5.4: Effect of varying temperature and screw speed on the MASP and associated extent of devulcanisation for mechanical devulcanisation ..... 74

Figure 5.5: Effect of varying temperature and DPDS concentration on the MASP and associated extent of devulcanisation for mechanochemical devulcanisation ..... 74

Figure 5.6: Sensitivity of the mechanical devulcanisation model to changes in economic factors..... 76

Figure 5.7: Sensitivity of the mechanochemical devulcanisation model to changes in economic parameters..... 77

Figure 5.8: Sensitivity of IRR to variation of variable cost factors in the case of mechanical devulcanisation ..... 78

Figure 5.9: Sensitivity of IRR to variation of variable cost factors in the case of mechanochemical devulcanisation..... 78

## List of tables

Table 2.1: Typical compounding recipes for rubber used in the manufacture of tyres .....	6
Table 2.2: Qualitative comparison of various devulcanisation technologies.....	12
Table 2.3: Summary of chemical probes exhibiting selective reactivity to crosslinks .....	14
Table 2.4: Summary of the technical performance of vulcanisates containing RR produced via various devulcanisation technologies.....	20
Table 3.1: Summary of materials used in this study .....	25
Table 3.2: Mechanochemical devulcanisation preparation recipe.....	27
Table 3.3: Full central composite design for mechanical devulcanisation experiment.....	29
Table 3.4: Full central composite design for mechanochemical devulcanisation experiment. ....	29
Table 4.1: Composition of the GTR feedstock.....	35
Table 4.2: Sol fraction and crosslink density measurements of vulcanised rubber .....	37
Table 4.3: Sol fraction measurements of samples produced by mechanical devulcanisation .....	38
Table 4.4: Crosslink density measurements of samples generated by mechanical devulcanisation .....	42
Table 4.5: Validity of Kraus correction.....	43
Table 4.6: Electrical power consumption measurements from the mechanical devulcanisation experiment.....	46
Table 4.7: Sol fraction measurements of samples generated by mechanochemical devulcanisation .....	50
Table 4.8: Crosslink density measurements of samples from the mechanochemical devulcanisation experiment.....	53
Table 4.9: Power consumption measurements from the mechanochemical devulcanisation experiment.....	58
Table 5.1: Estimated capital costs associated with a devulcanisation plant.....	65
Table 5.2: Summary of variable costs associated with the devulcanisation economic model .....	66
Table 5.3: Annual fixed costs associated with the devulcanisation economic model .....	66
Table 5.4: Summary of scale-up parameters for plastic extrusion processes .....	68
Table 5.5: Summary of the preliminary economic analysis of a devulcanisation plant .....	69
Table 5.6: Throughput of devulcanisation processes with varying extruder configurations ..	70
Table 5.7: Effect of scale on MASP at 10% IRR for the mechanical devulcanisation process .....	71

Table 5.8: Effect of scale on MASP at 10% IRR for the mechanochemical devulcanisation process .....	71
Table 5.9: Base case values of the major economic parameters for the sensitivity analysis	76
Table 5.10: Base case values for variable cost sensitivity analysis .....	78

# 1 Introduction

This chapter aims to introduce the reader to the field of waste rubber recycling, with a specific focus on waste tyre devulcanisation. After developing the context within which this thesis lies, this chapter discusses some shortcomings that have been identified in the field of devulcanisation technology and proposes potential solutions to these.

## 1.1 Background and motivation for research

The accumulation of waste tyres is a global problem leading to considerable environmental and economic problems. It is reported that approximately 1.5 billion waste tyres are discarded globally each year (Danon et al., 2015) and approximately 11 million of these are produced in South Africa (Danon et al., 2015). At the end of a tyre's useful life, only a small fraction of the rubber has been eroded while the majority of the remaining rubber is discarded (Adhikari, De & Maiti, 2000). In the past most of these tyres were disposed of by landfilling, but recently disposal has taken other forms due to the high cost of landfilling tyres and economic undesirability of discarding the valuable materials remaining in these tyres (Adhikari, De & Maiti, 2000). In addition to economic considerations, the disposal and stockpiling of waste tyres also creates environmental problems such as forming breeding grounds for disease-carrying pests and the risk of uncontrollable fires leading to serious air, soil and groundwater pollution (Danon et al., 2015).

Vulcanised rubber, used in tyres, is a very stable thermoset compound, meaning that it cannot be remoulded by heating as in the case of thermoplastics (Adhikari, De & Maiti, 2000). This thermoset property of rubber makes tyres difficult to recycle. Current attempts to recover value from waste tyres are focused on size reduction, pyrolysis and devulcanisation (Myhre et al., 2012).

Size reduction processes aim to break bulky tyres down into more manageable sizes (shreds) and often take the process further by separating the steel, fibre and rubber compounds that make up a tyre. While waste tyre shreds are sometimes sold as a low-value fuel, further processing produces steel and fibre that can be processed to value-added products, as well as cleaner rubber crumb of various size fractions that can be used as a filler in concrete and other applications (Isayev, 2013).

Pyrolysis processes aim to generate more value from waste tyres by producing fuels and other valuable chemicals from the thermal decomposition of size-reduced tyre products such as shreds and coarse crumb feedstocks (Danon et al., 2015).

Devulcanisation processes aim to convert fine-mesh grades of rubber crumb into high-value reclaimed rubber (RR) that can be remoulded and vulcanised to produce new rubber products, with physical properties comparable to those of the original vulcanisate (Myhre et al., 2012).

Many devulcanisation processes have been developed since the invention of vulcanisation, but research into the topic has recently accelerated due to increased environmental concerns. The majority of research to date has been directed at developing new methods of devulcanisation and describing the product properties at various operating conditions, in an attempt to improve the properties of RR to the point where the recycled material can be used at higher loadings in new rubber compounds, without a significant drop in physical properties (Myhre et al. 2012).

Some of the major obstacles to commercial implementation of devulcanisation technologies include the increasing quality requirements of rubber products (Mangili et al., 2015) as well as the absence of useful economic data associated with the various devulcanisation processes. It has also been shown that the performance of a devulcanisation process depends quite strongly on the particle size (Isayev, Liang & Lewis, 2013) and chemical composition (Yun et al., 2003) of the crumb fed to the process, making it difficult to compare technical performance between publications using different rubber feedstocks. The difficulty of comparing technical and economic performance between the available devulcanisation technologies could be a significant factor preventing more widespread adoption of devulcanisation technologies.

In order to bridge the gap between academic interest and industrial implementation, comparative techno-economic information will be needed in order to prove or disprove the viability of industrial-scale implementation of devulcanisation processes. This study aims to take a step towards analysing viability of industrial-scale devulcanisation by comparing the technical and economic performance of some of the most prominent devulcanisation technologies discussed in the academic literature.

## 1.2 Key questions

The key questions to be answered in this thesis include the following:

- Which devulcanisation technologies have been developed sufficiently to warrant further investigation into techno-economic performance?
- How do the operating conditions of each devulcanisation technology affect the product properties and power consumption?
- How do the selected devulcanisation processes compare from a technical and economic perspective?

## 1.3 Aims and objectives

The main aim of this study is to generate comparative techno-economic assessments for two selected devulcanisation technologies.

Specifically, this will be achieved via the following objectives:

1. Identify devulcanisation technologies that have been studied in academic literature and rule out those technologies that show obvious flaws in terms of environmental impact, excessive operating costs and lack of substantial technology development. Select the two most promising technologies for further assessment.
2. Design and conduct experiments for the selected technologies so that response surface models can be generated for power consumption and selected product characterisation metrics.
3. Use response surface models to generate technical and economic data within the experimental domain of each devulcanisation technology and compare the advantages and disadvantages of the devulcanisation technologies from a technical and economic viewpoint.

## 1.4 Scope and limitations of study

The scope of the project is the evaluation and comparison of the techno-economics of waste-tyre rubber devulcanisation processes. In order to ensure comparability between processes it is necessary to use a single source of rubber crumb for all experiments. Therefore, the investigation will focus on the devulcanisation of ground tyre rubber (GTR) from truck tyres (TT) which consists of mostly natural rubber in terms of polymer composition, which will also avoid complications associated with the technical analysis of blends of various types of rubber.

Product characterisation can present a significant challenge due to the complexity of rubber compounds. Some of the methods and calculations used to characterise rubber compounds are based on theoretical models and assumptions, but have been shown to be effective at characterising fresh vulcanisates. These methods are still widely used to characterise vulcanised and devulcanised rubber compounds, although the applicability of these methods to devulcanised rubbers have not been proven yet, and caveats are issued where relevant.

## 1.5 Layout of this thesis

This thesis starts with a review of the relevant literature in Chapter 2, during which the various available devulcanization technologies are identified and discussed, culminating in the selection of two technologies for further consideration (Objective 1). Objective 2 is then addressed in Chapters 3 and 4, with Chapter 3 describing the design of the experiments and associated analytical methods, followed by Chapter 4 presenting experimental results and the development of response surface models. The response surface models developed in Chapter 4 are then applied to a detailed techno-economic analysis in Chapter 5, which addresses Objective 3. The thesis ends by presenting the overall conclusions drawn from the project and presents recommendations for future work in Chapter 6.

## 2 Literature study

This chapter provides an introduction to the theoretical concepts within the field of devulcanisation and builds a foundation of previous work from which this thesis will proceed. The chapter begins with Section 2.1 describing the composition and properties of the rubber compounds used to build automobile tyres. Section 2.1 is followed by a brief overview of the currently used methods for attempting to recover value from end-of-life tyres in Section 2.2, after which the focus is shifted to the characterisation of devulcanised rubber in Section 2.3 and an overview and comparison of various devulcanisation technologies in Section 2.4.

### 2.1 Automotive tyres

Section 2.1 describes the recipes and processes used in the production of tyres. As will be discussed, the chemistry of the vulcanisation process and the resultant thermoset network structure are the reasons behind the difficulties associated with recycling tyre rubber.

#### 2.1.1 Tyre composition

Automotive tyres consist mostly of a thermoset rubber compound reinforced with steel wires and textile fibres (Rodgers & Waddell, 2013a). The rubber compound is mostly made up of the rubber polymer itself and carbon black which acts as a reinforcing filler. Small amounts of sulfur, zinc oxide and accelerating agents are added to enable the vulcanisation process. Various oils and waxes are also added in order to aid processing and moulding of the rubber compound. Proportions of the various ingredients are varied according to the properties required of the compound, depending on which part of the tyre the compound is to form, such as the tread or sidewall of the tyre.

Natural rubber (NR) and styrene-butadiene rubber (SBR) are two of the most commonly used rubbers for the manufacture of automotive tyres. In general, truck tyres (TT) are usually made using mostly NR for the polymer portion of the rubber compound, while passenger car tyres (PCT) are made of blends of NR, SBR and other synthetic rubbers such as butadiene rubber (BR) (Rodgers & Waddell, 2013a). The preference for NR in truck tyres is reflected in the example compound formulations in Table 2.1.

Table 2.1: Typical compounding recipes for rubber used in the manufacture of tyres

Component	Composition (phr) <sup>1</sup>			
	TT tread	PCT tread	TT tread	PCT tread
Natural rubber (NR)	100	50	100	50
Styrene-butadiene rubber (SBR)	0	50	0	50
Carbon black	50	45	50	50
Oils and waxes	5.5	10	5	12
Sulfur	1.75	1.6	1.2	1.75
Zinc oxide	4	3	5	4
Vulcanisation additives	4.25	4.2	3.5	3
Other	4	3	1.5	4.25
<b>Total (phr)</b>	<b>169.5</b>	<b>166.8</b>	<b>166.2</b>	<b>175</b>
Reference	(Waddell et al., 1990)		(Rodgers & Waddell, 2013b)	

The formulations in Table 2.1 are still mouldable until vulcanised as discussed in Section 2.1.2 below.

### 2.1.2 Vulcanisation

After blending the rubber compound, it is moulded into the desired shape along with additional structural components and heated up to the temperature required to initiate the vulcanisation reaction. In the case of tyre production, the tyre is held in a mould at a temperature of approximately 150 °C for approximately 20 minutes for the vulcanisation reaction to reach the required level of crosslinking (Coran, 2013). During vulcanisation, the elemental sulfur and vulcanisation additives and accelerators interact to form sulfur crosslinks between the polymer chains, as shown in Figure 2.1.

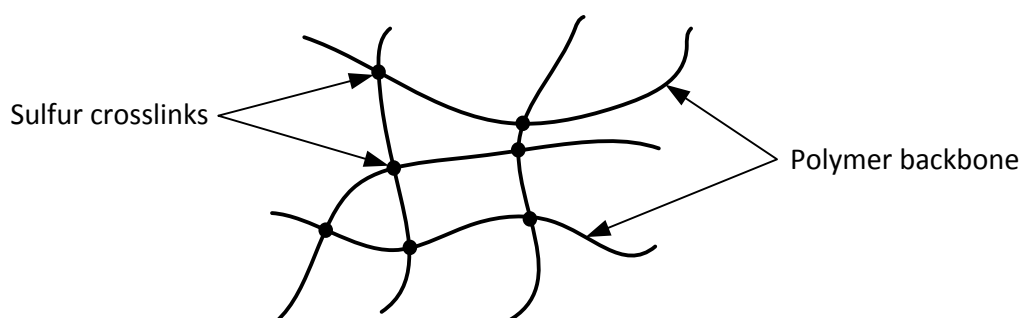


Figure 2.1: Network structure of vulcanised rubber. Redrawn from (Flory, 1944)

<sup>1</sup> Parts per hundred parts of rubber polymer, by weight

The network structure of the vulcanised rubber depicted in Figure 2.1 extends throughout the rubber compound, creating what is essentially one macromolecule comprising the rubber polymer fraction of the tyre (Flory, 1944). The macromolecular thermoset network structure of vulcanised rubber makes the compound impossible to remould without first breaking down the network into smaller, thermoplastic molecular fragments (Adhikari, De & Maiti, 2000). While there are significant challenges to recycling tyres produced by vulcanisation, a number of methods are available that attempt to recover value from waste tyres, as discussed in Section 2.2.

## 2.2 Tyre recycling

The first step to recovering value from waste tyres is usually size reduction in order to reduce bulky tyres to more manageable tyre shreds which are easier to transport (Myhre et al., 2012). The shreds are sometimes used without further processing in energy recovery processes as discussed in Section 2.2.1 or can be processed further as discussed in Section 2.2.2, Section 2.2.3 and Section 2.2.4.

### 2.2.1 Energy recovery

The calorific value of waste tyres is approximately 33 MJ/kg (Ferrer, 1997; Myhre et al., 2012). Paper mills, cement kilns and power plants are some of the largest consumers of waste tyres for energy recovery (Myhre et al., 2012). An advantage of using waste tyres for energy recovery in cement kilns is that the ash and ferrous by-products from the combustion of tyres are incorporated as a raw material in the production of the cement (Ferrer, 1997).

While waste tyres may be an attractive fuel source, the use of waste tyres for energy recovery is considered to be a very low-value application considering the high production costs of tyres (Ferrer, 1997). Therefore, further processing of tyre shreds is considered a higher-value use for waste tyres, as discussed in the following three sections.

### 2.2.2 Crumbing

The net value of tyre shreds can be improved by the separation of the steel, fibre and rubber fractions of the tyre in crumbing (grinding) facilities. The separated components of the tyre typically have a higher net market value than that of the tyre shreds (Ferrer, 1997).

The coarse fractions of the rubber particles (GTR) produced by crumbing facilities can be used in the construction of sports surfaces, while the finer fractions are used as cheap fillers in moulded products where mechanical properties are not too important (Ferrer, 1997). Rubber

chips and crumb have also found wide use in many civil engineering applications such as road construction and surfacing (Myhre et al., 2012).

While crumbing facilities add value to otherwise low-value tyre shreds, the value of rubber crumb is still very low in comparison to the value of the rubber compound used in for the production of new tyres. Therefore, pyrolysis and devulcanisation processes are receiving increasing attention in the academic literature and in practice as potential methods for further improvement of the recovery of value from waste tyres, as discussed in Section 2.2.3 and Section 2.2.4, respectively.

### 2.2.3 Pyrolysis of rubber

Pyrolysis of tyre shreds or GTR involves the generation of gas, oil and char by the thermal decomposition of the organic components of the rubber compound in the absence of oxygen (Myhre et al., 2012). Both the gas and the tyre-derived oil (TDO) have very high calorific values of 40 to 65 MJ/m<sup>3</sup> for the gas and 42 MJ/kg for the TDO, which makes them attractive for use as alternative fuels (Myhre et al., 2012). However, the high energy consumption of pyrolysis processes and poor market acceptance of the TDO and char products usually makes pyrolysis of waste tyres uneconomical (Adhikari, De & Maiti, 2000; Myhre et al., 2012). Therefore, research interest in the waste tyre pyrolysis field has shifted recently in the direction of recovering and purifying valuable chemicals, most notably dipentene, from the TDO (Danon et al., 2015).

### 2.2.4 Devulcanisation

Devulcanisation refers to any process that attempts to convert vulcanised rubber, typically in powder form with particle size of 20 – 40 mesh (400 – 841 µm), into a secondary raw material that can be moulded and revulcanised in a manner similar to that of virgin rubber (Myhre et al., 2012; Isayev, 2013). Ideally, devulcanisation processes would break the sulfur crosslinks in the vulcanised network without modifying the polymer chains. Selective scission of the sulfur crosslinks would return the rubber to a state that can be remoulded and vulcanised, to yield a product with properties similar to those of the original vulcanisate. However, due to the complex nature of rubber vulcanisates and the chemistry involved in reclaiming processes, selective scission of crosslinks is rather unlikely (Myhre et al., 2012). Therefore, the term devulcanisation is loosely applied to reclaiming processes that revert vulcanised rubber to a thermoplastic, mouldable state, known as reclaimed rubber (RR).

In order to discuss and compare the performance of currently available devulcanisation technologies, a theoretical basis for the characterisation of devulcanised rubber is provided in Section 2.3.

## 2.3 Characterisation of devulcanised rubber

Due to the complexity and variety of important characteristics of reclaimed rubber, a large number of methods of product characterisation are available. Some of the most prevalent methods identified in the devulcanisation literature include crosslink density, sol fraction, Horikx analysis and tensile testing, as discussed in Section 2.3.1, Section 2.3.2, Section 2.3.3 and Section 2.3.4, respectively.

### 2.3.1 Crosslink density

As devulcanisation processes aim to break crosslinks in the rubber network, quantification of the crosslink density in the vulcanised rubber network before and after devulcanisation serves as an indication of the extent to which the network was broken down during the treatment. Measurement of the crosslink density is typically done by swelling the rubber sample in an appropriate solvent such as toluene and then calculating the crosslink density using the widely used Flory-Rehner equation (Flory & Rehner, 1943; Horikx, 1956). The mass-basis form of the Flory-Rehner equation is given by Equation (2.1) (Horikx, 1956):

$$v_e = \frac{V_{R0} + \chi V_{R0}^2 + \ln(1 - V_{R0})}{\rho_R \underline{V}_S^3 \sqrt{V_{R0}}} \quad (2.1)$$

where  $v_e$  is the number of elastically effective polymer chains per gram of rubber (mol/g), which is commonly referred to as the crosslink density due to the relationship between  $v_e$  and the extent of crosslinking (Flory & Rehner, 1943).  $V_{R0}$  is the volume fraction of rubber polymer in the swollen rubber network,  $\chi$  is the Flory-Huggins polymer-solvent interaction parameter,  $\rho_R$  is the density of the rubber polymer (kg/m<sup>3</sup>), and  $\underline{V}_S$  is the molar volume of the swelling solvent (m<sup>3</sup>/mol).

While the Flory-Rehner equation is well-known and still widely used, practical limitations of the tetrafunctional model of rubber networks (Erman & Mark, 2013) – from which the Flory-Rehner equation is derived – lead to significant errors when Equation (2.1) is applied to real carbon-black filled rubber compounds (Kraus, 1963). The details of the Kraus correction (Kraus, 1963) to the Flory-Rehner equation are discussed in Section 4.1.2 as appropriate for the particular GTR used in this study.

Since the crosslink density of vulcanised rubber can vary significantly, a normalised indication of the extent of network breakdown (percent devulcanisation) is commonly reported as the relative decrease in crosslink density, described by Equation (2.2) (Mangili et al., 2014):

$$\text{Devulcanisation} = \frac{\nu_{e1} - \nu_{e2}}{\nu_{e1}} \quad (2.2)$$

where  $\nu_{e1}$  is the crosslink density of the vulcanised rubber network before devulcanisation and  $\nu_{e2}$  is the crosslink density of the rubber network after devulcanisation.

An alternative method for indicating the extent of breakdown of the polymer network is given by the sol fraction, discussed in Section 2.3.2.

### 2.3.2 Sol fraction

The sol fraction ( $s$ ) of a rubber compound is defined as the mass fraction of the rubber polymer portion of the rubber compound that is soluble in a suitable solvent such as toluene (Horikx, 1956; Alemán et al., 2007), while the insoluble network fraction of the polymer is referred to as the gel fraction ( $g$ ).

During vulcanisation, the sol fraction of the rubber decreases with increasing crosslink density (Charlesby, 1954). When crosslink density is decreased during devulcanisation, the sol fraction increases again and can therefore serve as a secondary indication of the extent to which the rubber network is broken down during the devulcanisation.

The sol fraction and crosslink density are not independent of each other, but are related to each other as discussed in Section 2.3.3.

### 2.3.3 Horikx's analysis

Although the ideal case of devulcanisation is that only sulfur crosslinks are broken, practical reclaiming technologies exhibit varying degrees of polymer chain scission (Myhre et al., 2012). It is therefore of interest to be able to compare the selectivity for crosslink scission achieved by various processes, for which Horikx's theory is a popular indicator (Horikx, 1956).

Using the tetrafunctional model of a rubber network (Flory, 1944; Erman & Mark, 2013), Horikx determined that for selective crosslink scission, the generation of sol from gel would be much slower than if random C-C bond scission had taken place, due to the large number of crosslinks that need to be broken before a polymer fragment can be freed from the network (Horikx, 1956). The consequence of Horikx's analysis is summarised in Figure 2.2.

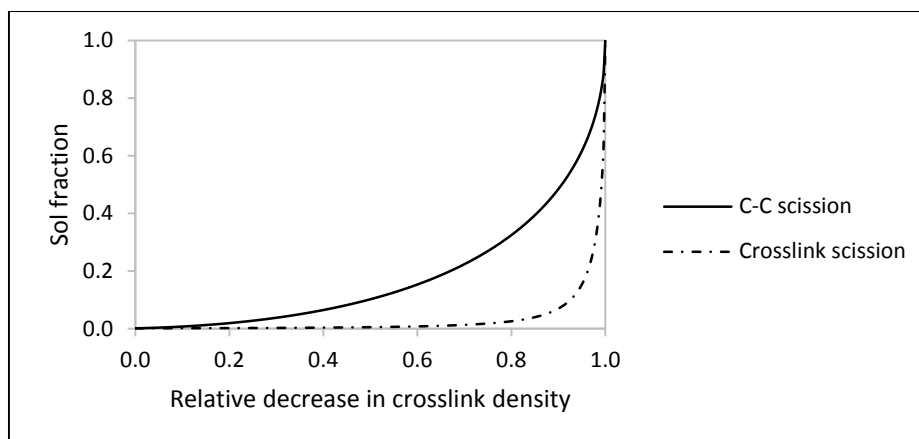


Figure 2.2: Typical plot of the relationships between sol fraction and relative decrease in crosslink density (Horikx, 1956)

Figure 2.2 shows that, for the same value of the relative decrease in crosslink density, the sol fraction of RR will always be higher if the network is broken via the scission of the polymer backbone than in the ideal case of scission of crosslinks only. Therefore, experimental data plotted against Figure 2.2 can provide a qualitative indication of the selectivity for crosslink scission exhibited by the devulcanisation process.

The aforementioned characterisation methods only describe the properties of the RR and don't necessarily give a good indication of how the RR would perform when re-vulcanised. Therefore, another commonly reported method of characterising RR is the tensile testing of the rubber after re-vulcanisation as discussed in Section 2.3.4.

### 2.3.4 Re-vulcanisation and physical properties

The mechanical properties considered important for rubber compounds include the tensile strength, hardness, elastic modulus, and many others depending on the application of the compound (Coran, 2013). There is often a trade-off between properties, which further complicates the specification of an ideal set of desirable physical properties for rubber compounds.

The physical properties of vulcanisates containing RR are typically degraded with higher loadings of RR in the compound formulation, most notably the tensile strength (Myhre et al., 2012). Therefore, the technical performance of various devulcanisation processes is also compared by reports of the tensile properties of vulcanised compounds containing RR at varying loading (Adhikari, De & Maiti, 2000; Myhre et al., 2012; Isayev, 2013).

Having established product characterisation methods associated with devulcanised rubber, a review of the devulcanisation literature is given in Section 2.4.

## 2.4 Devulcanisation technologies

The purpose of Section 2.4 is to describe the devulcanisation technologies identified in the literature and compare them in terms of the characterisation methods discussed in section 2.3. Several excellent reviews in the field of rubber recycling are available (Winkelmann, 1926; Adhikari, De & Maiti, 2000; Myhre et al., 2012; Isayev, 2013), covering qualitative advantages and disadvantages of the various devulcanisation technologies, as summarised in Table 2.2.

*Table 2.2: Qualitative comparison of various devulcanisation technologies*

Technology	Advantages	Disadvantages
<b>Thermal</b>	<ul style="list-style-type: none"> <li>• Long history of application</li> <li>• Low equipment costs</li> </ul>	<ul style="list-style-type: none"> <li>• Long batch time</li> <li>• Excessive air and water pollution</li> <li>• Poor mechanical properties of devulcanised rubber</li> </ul>
<b>Chemical probes</b>	<ul style="list-style-type: none"> <li>• Potential for very high selectivity</li> </ul>	<ul style="list-style-type: none"> <li>• Lab-scale experiments only</li> <li>• High cost and toxicity of probes</li> </ul>
<b>Microbial</b>	<ul style="list-style-type: none"> <li>• High selectivity for crosslinks</li> <li>• Low equipment and operating costs</li> </ul>	<ul style="list-style-type: none"> <li>• Very long batch time (30 days)</li> <li>• Only surface treatment</li> <li>• Very fine-mesh crumb required (~200 mesh = 74 <math>\mu\text{m}</math>)</li> </ul>
<b>Mechanical</b>	<ul style="list-style-type: none"> <li>• Fast, continuous process</li> </ul>	<ul style="list-style-type: none"> <li>• Requires additional heating</li> <li>• Extensive degradation of polymer backbone</li> </ul>
<b>Microwave</b>	<ul style="list-style-type: none"> <li>• Devulcanisation occurs throughout material</li> <li>• Fast, continuous process</li> </ul>	<ul style="list-style-type: none"> <li>• Difficult to control</li> <li>• More effective on polar compounds</li> <li>• Poorly researched</li> </ul>
<b>Ultrasound</b>	<ul style="list-style-type: none"> <li>• Fast, continuous process</li> <li>• Devulcanisation occurs throughout material</li> </ul>	<ul style="list-style-type: none"> <li>• Cavitation appears to damage equipment</li> </ul>
<b>Mechanochemical</b>	<ul style="list-style-type: none"> <li>• Improved selectivity for crosslink scission compared to mechanical</li> <li>• Some agents double as curatives for devulcanisation</li> </ul>	<ul style="list-style-type: none"> <li>• Mostly batch processes</li> <li>• Additional chemical costs</li> </ul>

While technical descriptions of many devulcanisation technologies are abundant in the academic literature, information (power consumption etc.) suitable for the detailed economic analysis of devulcanisation processes is largely absent. Therefore, the following descriptions will focus on the technical performance of various devulcanisation technologies.

### 2.4.1 Thermal reclamation

Some of the oldest technologies for reclaiming vulcanised rubber are based on holding rubber scraps at high temperature and pressure for extended periods of time (Winkelmann, 1926; Isayev, 2013). Technologies included in this category include the pan process and the digester process, both of which are apparently still in use in modified form (Isayev, 2013).

In the pan process (also known as the heater process) rubber scraps are loaded into pans, sometimes including reclaiming chemicals, and these pans are loaded into a devulcanisation reactor. The rubber is then subjected to high pressure steam for an extended period of time until it has been softened sufficiently (Boys & Naudain, 1957). This process is typically used for fibre-free rubber (Kirby & Steinle, 1942). A typical reclaim compound has been shown to exhibit poor tensile properties when revulcanised, achieving only 3.6 MPa at 400% elongation (Boys & Naudain, 1957).

The digester process is more commonly used for fibre-containing scrap and consists of treating the rubber in caustic solution at high temperature and pressure for a period of 6-24 hours (Kirby & Steinle, 1942). The caustic serves the purpose of breaking down the fibres and softening the rubber. Some of the more recent developments in the digester process are reported to produce RR with tensile properties of 4.7 MPa at 210% ultimate elongation when revulcanised (Bryson, 1979).

Both of these processes were first described over 100 years ago and improvements have since been made to the processes in order to partially overcome the very long batch times and excessive pollution of the digester process (Manuel & Dierkes, 1997). However, most of the information available for these processes comes from patents and there seems to be very little interest in academic journals, most likely due to increased concerns about the pollution associated with these processes.

### 2.4.2 Chemical probes

A number of chemicals, collectively known as chemical probes, have been shown to be selectively reactive to sulfur crosslinks, while leaving the polymer chains intact (Adhikari, De & Maiti, 2000; Myhre et al., 2012). The high selectivity of chemical probes for crosslink scission is expected to yield RR with properties, once revulcanised, very close to those of the original vulcanisate. Various chemical probes and their method of action are summarised in Table 2.3.

Table 2.3: Summary of chemical probes exhibiting selective reactivity to crosslinks

Chemical probe	Reaction mechanism
Triphenylphosphine	Polysulfide links converted to monosulfide
Sodium di-n-butyl phosphite	Polysulfide and disulfide links broken
Propane-thiol/piperidine	Polysulfide links broken
Hexane-1-thiol	Polysulfide and disulfide links broken
Dithiothreitol	Disulfide links split into two thiol groups
Lithium aluminium hydride	Polysulfide and disulfide links broken
Phenyl lithium in benzene	Polysulfide and disulfide links broken
Methyl iodide	Monosulfide links broken

Source: (Adhikari, De & Maiti, 2000)

While these chemicals show potential as highly selective devulcanisation agents under controlled laboratory conditions, their potential for commercial application is limited. The high cost, high toxicity and reaction conditions associated with chemical probes suggest that industrial-scale application is unlikely at present (Myhre et al., 2012).

### 2.4.3 Microbial devulcanisation

It has been shown that certain species of bacteria are capable of oxidising sulfur in polysulfidic bonds, thus showing the potential to act as selective devulcanisation agents. Initial work has been done that has identified a few key microorganisms capable of reducing sulfur to hydrogen sulfide or oxidising crosslinks to sulfate (Myhre et al., 2012).

A study by Li, Zhao and Wang (2011) has shown that *Thiobacillus ferrooxidans* is capable of oxidising crosslinks and elemental sulfur in GTR to sulfate or other oxygen-containing sulfur groups (Li, Zhao & Wang, 2011). During the microbial devulcanisation process the crosslinks near the surface of the particles were broken over a period of 30 days. Samples of treated and untreated GTR were blended with a model rubber compound at various loadings of 0-40 phr and vulcanised, revealing an improvement in the tensile strength of samples containing treated GTR in comparison with samples containing untreated GTR. At a GTR loading of 40 phr (40 parts RR to 100 parts virgin NR), the sample containing treated GTR gave a tensile strength of 18.3 MPa at 527% elongation, which is a substantial improvement over the 15.4 MPa at 454% elongation exhibited by the sample containing untreated GTR. It should however be noted that the particle size of the GTR used in this experiment was smaller than 74  $\mu\text{m}$  which is likely to be substantially more expensive than the raw material used in other devulcanisation technologies which use 20 – 40 mesh size (420 – 841  $\mu\text{m}$ ) (Isayev, 2013).

#### 2.4.4 Mechanical devulcanisation

Mechanical processes for rubber reclamation are designed on the premise that strong shearing forces can be used to break chemical bonds in the network structure. Since the bond energies of S-S and C-S bonds are lower than that of C-C bonds, mechanical devulcanisation could be expected to exhibit good selectivity for crosslink scission (Myhre et al., 2012). In practice, thermal inhomogeneity and small differences in bond energies result in undesirable main chain scission subsequent degradation of mechanical properties (Myhre et al. 2012). Two main methods of applying mechanical shearing are reported: two-roll milling and extrusion.

A shortcoming of two-roll mill reclamation is the inhomogeneous heating of the rubber being processed, resulting in inconsistent product quality (Myhre et al. 2012). Due to the poor properties of rubber processed by the two-roll milling method, it is rarely used without reclaiming agents (discussed in Section 2.4.5). The use of single-screw and twin-screw extruders for mechanical devulcanisation has gained popularity in the academic literature recently due to the precise temperature control achieved by extruders, resulting in more consistent product quality (Maridass & Gupta, 2004).

Partial devulcanisation has been achieved in a single-screw extruder operating at low temperature (Bilgili, Arastoopour & Bernstein, 2001a). Rubber granules were pulverised in the extruder at a temperature of 135°C and a screw speed of 30-80 RPM, resulting in a fine powder with slightly reduced crosslink density and higher sol fraction than the coarse granules fed into the extruder (Bilgili, Arastoopour & Bernstein, 2001b). The extrusion-processed powder was compression moulded in the absence of fresh rubber and additives, yielding rubber slabs with tensile properties of approximately 5.5 MPa at 380% ultimate elongation (Bilgili et al., 2003).

A twin-screw extruder has been designed and developed specifically for reclaiming crosslinked rubber (Matsushita et al., 2003). GTR from car tyres was reclaimed at a screw speed of 400 RPM and a barrel temperature of 220°C, which resulted in an 87.5% reduction of the crosslink density and a corresponding sol fraction of 37.5%. A model compound containing 20 phr of the RR showed a tensile strength of 15.8 MPa and ultimate elongation of 320%. The effects of varying screw speed and barrel temperature were not reported.

Maridass and Gupta (2004) investigated the effect of the screw speed and barrel temperature of a twin-screw extruder on the mechanical properties of a reclaimed rubber compound. The temperature of the barrel was varied between 200°C and 230°C and the screw speed varied between 18 RPM and 32 RPM. The sol fraction and crosslink density of the RR were not reported, although it was suggested that the crosslink density decreased with increasing barrel

temperature of the extruder. The RR was blended with a small amount of fresh NR (RR:NR = 70:30) and revulcanised for tensile testing, which did not show a clear relationship between the operating parameters and the tensile strength, although the ultimate elongation was found to increase with increasing barrel temperature. Overall, the tensile strength of the revulcanised samples was consistently above 15 MPa, rising to a maximum strength of 18.5 MPa at a barrel temperature of 225°C and screw speed of 30 rpm.

Tao and co-workers investigated the relationship between the extent of devulcanisation and the mechanical properties of the rubber reclaimed by twin-screw extrusion by varying the screw speed from 80 RPM to 160 RPM and varying the barrel temperature from 160°C to 240°C (Tao et al., 2013). The sol fraction of the RR was found to increase with increasing barrel temperature and with increasing screw speed, while the crosslink density of the RR was found to decrease with increasing barrel temperature and with increasing screw speed. The RR was revulcanised without the addition of fresh rubber, revealing a peak in the tensile strength of the revulcanised RR at a sol fraction of approximately 23% for the RR. The major findings of Tao *et al.* (2013) suggest that the tensile properties of the revulcanised RR can be optimised by targeting the appropriate extent of devulcanisation for the RR, although the ideal sol fraction and crosslink density of the RR are expected to be functions of the initial crosslink density and the selectivity for crosslink scission (Horikx, 1956).

#### 2.4.5 Mechanochemical devulcanisation

It has been found that the addition of various reclaiming agents, most notably disulfides, to rubber during mechanical reclamation increases the extent of devulcanisation when compared to the same process without reclaiming agents (Myhre et al., 2012). Two reaction mechanisms have been proposed: radical scavenging (Adhikari, De & Maiti, 2000) and hydrogen abstraction (Rajan et al., 2005).

The radical scavenging mechanism suggests that the mechanical shearing forces and high temperatures achieved during reclamation break the S-S bond of the disulfide, thus forming two radicals. The shearing forces and high temperature also break the crosslinks and polymer chains of the rubber network, forming radicals of network fragments. The polymer and crosslink radicals are scavenged by the disulfide radicals to prevent them from recombining or causing further breakages (Adhikari, De & Maiti, 2000).

It has also been suggested that disulfide radicals react with the rubber network by hydrogen abstraction at the allylic positions, due to the resonance stabilisation of the resultant radical (Rajan et al., 2005). The resultant radical in the rubber network ultimately results in chain

scission and crosslink scission, followed by subsequent stabilisation of the radicals by capping as mentioned previously.

Early tests by De and co-workers used diallyl disulfide (DADS) as a reclaiming agent in conjunction with two-roll milling to reclaim a carbon black filled NR compound (De, Maiti & Adhikari, 1999). The sol fraction of the RR was found to increase from 24% to 31% with increasing milling time from 15 minutes to 35 minutes, respectively. The effects of varying temperature (40°C to 60°C) and varying DADS concentration (2 to 4 g per 100 g rubber crumb) on the sol fraction were unclear. The tensile properties of the revulcanised RR were poor, showing a tensile strength of only 3.52 MPa at 300% ultimate elongation. Despite the poor properties of the revulcanised RR, a blended compound of RR:NR = 40:60 showed a vastly improved tensile strength of 19.13 MPa at 450% ultimate elongation.

Later work by De and co-workers used tetramethylthiuram disulfide (TMTD) as a reclaiming agent for devulcanising GTR with a two-roll mill at ambient temperature (De et al., 2006). As seen previously (De, Maiti & Adhikari, 1999), the sol fraction of the RR was found to increase with increased milling time but the effect of the TMTD concentration was unclear. The mechanical properties of the revulcanised RR were reported for various process conditions and TMTD concentrations, with the best result achieved being a tensile strength of 5.78 MPa and ultimate elongation of 213%, although the trend between process conditions and product properties was unclear.

Jana and Das used diaryl disulfide (DArDS) in conjunction with two-roll milling for devulcanising unfilled NR vulcanisates with varying amounts of sulfur in the original cure recipe (Jana & Das, 2005). While the sol fraction and crosslink density of the RR were not reported, the major finding was that the tensile properties of the revulcanised RR improved when increasing the concentration of DArDS in the reclaiming process from 0.7 phr to 1.0 phr.

Shi and co-workers used a proprietary reclaiming agent (RA 420) in three different mechano-chemical reclaiming processes: twin-screw extruder and two-roll milling at high (180°C) and low (<40°C) temperatures (Shi et al., 2013). A Horikx analysis of the RR produced by the various devulcanisation methods showed that lower temperatures favour more crosslink-selective breakdown of the rubber network. Furthermore, the RR samples exhibiting the higher selectivity for crosslink scission had superior tensile properties in comparison to the samples of lower crosslink selectivity, which can be seen as supporting evidence for the postulation that more selective breakdown of the rubber network leads to better preservation of the physical properties of the rubber (Myhre et al., 2012).

## 2.4.6 Ultrasonic devulcanisation

In the ultrasonic method of devulcanisation, the rubber is transported by an extruder through a die fitted with an ultrasonic horn. The powerful ultrasound waves cause acoustic cavitation in the rubber network, breaking overstressed chemical bonds around the rapidly oscillating bubbles (Isayev, Yushanov & Chen, 1996a). A small amount of mechanical devulcanisation could be expected to take place within the extruder, therefore the temperature of the extruder is usually kept low (~180°C) in order to ensure that the majority of devulcanisation takes place in the ultrasonic die.

An early paper (Tukachinsky, Schworm & Isayev, 1996) presented results of the ultrasonic devulcanisation of GTR at varying process conditions. It was found that the extent of devulcanisation was most comprehensively characterised by the specific energy delivered by the ultrasound horn. The study suggested that the optimum specific energy was 1 kJ/g which resulted in a reclaimed rubber with a tensile strength of up to 10.5 MPa and ultimate elongation of 250%.

Later work by Isayev's research group (Hong & Isayev, 2001) investigated the mechanical properties of reclaimed carbon black filled natural rubber and compared these results to the properties of the original vulcanisate. The study also investigated the effect of adding radical scavengers during devulcanisation and adding carbon black to the devulcanised rubber, to determine whether these additions could improve the mechanical properties of the final reclaimed vulcanisate. The best result showed a tensile strength of about 16 MPa and ultimate elongation of about 450%. The addition of radical scavengers and extra carbon black showed no positive effect on the mechanical properties of the reclaimed rubber. The results from (Hong & Isayev, 2001) were extended by another study (Hong & Isayev, 2002) on the strength of blends of the RR with virgin NR. The virgin rubber content of the compounds ranged from 0% to 75%, with tensile strengths ranging from 16-26 MPa, respectively.

It has been reported that the cavitation that occurs in the rubber during reclamation damages the ultrasonic horn (Isayev, Yushanov & Chen, 1996b). This may require regular replacement of the ultrasonic equipment, although the severity of the damage was not reported.

## 2.4.7 Microwave devulcanisation

A few patents describing microwave devulcanisation processes are available, but other literature on the subject is sparse. Microwave energy causes molecular vibration of polar molecules in the rubber resulting in more uniform heating than that offered by external heating, thus providing more selective scission of C-S and S-S bonds (Wicks et al., 2002). While the rubber used in tyres is generally non-polar, the carbon black blended with the rubber is sufficiently polar for the rubber to absorb microwave radiation (Novotny et al., 1978).

Novotny and co-workers devulcanised samples of EPDM rubber with their microwave process and blended it with virgin rubber at loadings of 10% and 25% recycled rubber for the manufacture of rubber hoses (Novotny et al., 1978). The hose samples containing 10% and 25% recycled rubber showed tensile strengths 20% and 33% lower than that of 100% virgin rubber, respectively. The same process was used to devulcanise tyre crumb, but this rubber became tacky and didn't flow as well as the EPDM, thus making it difficult to control the amount of radiation absorbed. The reclaimed tyre rubber from the best run had a tensile strength 41% lower than that of the original rubber.

Wicks and co-workers treated rubber crumb (particle size 40 mesh) with microwaves at various process conditions and blended the partially devulcanised crumb with virgin rubber at a loading of RR:NR = 20:100 (Wicks et al., 2002). These samples were compared with a virgin control as well as a sample of untreated crumb blended with virgin rubber, also loaded at 20%. The sample containing untreated crumb showed a tensile strength 24% lower than that of the control. The samples containing treated crumb were only marginally stronger, with the best case showing a tensile strength 20% lower than the control.

One important disadvantage of microwave devulcanisation is the control difficulty mentioned by Novotny *et al.* (1978). In addition to difficulty achieving constant flow, the dielectric loss factor of most materials (including rubber) increases with increasing temperature (Roussy et al., 1985), which means that as the material heats up, the rate of heating also increases, which could lead to temperature runaway.

## 2.5 Concluding remarks

Section 2.5 summarises the major findings and interpretation of the literature review.

### 2.5.1 Devulcanisation feedstock description

The literature study has shown that the majority of work on devulcanisation technologies uses a feedstock of approximately 20 – 40 mesh size. It has also shown that truck tyre compounds use natural rubber as the main rubber component while passenger car tyres typically include large amounts of various synthetic rubbers. In order to avoid complications with the devulcanisation chemistry and characterisation of blends of NR and SBR, truck tyre crumb will be used in this study due to the high NR content.

### 2.5.2 Selection of devulcanisation technologies

A variety of devulcanisation technologies have been discussed in Section 2.4, including descriptions of the processes and examples of the technical performance of the revulcanised reclaims produced by each method. A summary of the technical performance of the RR produced by various processes is given in Table 2.4.

*Table 2.4: Summary of the technical performance of vulcanisates containing RR produced via various devulcanisation technologies.*

Process	Reference	Rubber type and reaction conditions	Original properties		Reclaim content (RR:NR)	Reclaim properties	
			Strength (MPa)	Elongation (%)		Strength (MPa)	Elongation (%)
Thermal	(Boys & Naudain, 1957)	Rubber: GTR (NR/SBR blend) Pan process with coal tar oil T=218C; P=1.7MPa; t=16h	-	-	100:0	3.6	400
	(Bryson, 1979)	Rubber: GTR (NR/SBR/BR blend) Digester process with aryl disulfides T=190C; P=1.5MPa; t=90min	-	-	100:0	4.7	210
Microbial	(Li, Zhao & Wang, 2011)	Rubber: GTR <i>T. ferrooxidans</i> in water pH=2.5; T=30C; t=30days	-	-	40:100	18.3	527
Mechanical	(Matsushita et al., 2003)	Rubber: GTR (NR/SBR blend) Twin-screw extrusion in air T=220C; R=400 rpm	-	-	20:100	15.8	320
	(Matsushita et al., 2003)	Rubber: GTR (NR/SBR blend) Twin-screw extrusion in N <sub>2</sub> T=220C; R=400 rpm	-	-	20:100	19.7	530
	(Maridass & Gupta, 2004)	Rubber: Vulcanised NR scraps Twin-screw extrusion T=225C; R=32 rpm	-	-	70:30	18.5	840
	(Tao et al., 2013)	Rubber: GTR Twin-screw extrusion T=180C; R=100 rpm	-	-	100:0	12.9	351
	(Bilgili et al., 2003)	Rubber: CB filled NR Single screw extrusion T=135C; R=80 rpm	16.5	470	100:0	5.5	380

Table 2.4, cont.: Summary of the technical performance of vulcanisates produced via various devulcanisation technologies

Process	Reference	Rubber type and reaction conditions	Original properties		Reclaim content (RR:NR)	Reclaim properties	
			Strength (MPa)	Elongation (%)		Strength (MPa)	Elongation (%)
Mechano-chemical	(De, Maiti & Adhikari, 1999)	Rubber: Carbon black filled NR Two-roll mill with DADS T=40-60C; DADS dose = 2-4 phr; t=15-35 min	22.88	500	100:0	4.34	283
	(De, Maiti & Adhikari, 1999)	Rubber: Carbon black filled NR Two-roll mill with DADS T=40-60C; DADS dose = 2-4 phr t=15-35 min	22.88	500	40:60	19.13	450
	(De et al., 2006)	Rubber: GTR (NR/SBR blend) Two-roll mill with TMTD T=30C; TMTD dose = 1.5 phr; t=40 min	-	-	100:0	5.78	213
	(Jana & Das, 2005)	Rubber: Unfilled NR Two-roll mill with DARdS T=110C; DARdS dose = 1 phr; t=10min	16.87	1300	100:0	14.4	1011
	(Shi et al., 2013)	Rubber: GTR Two-roll mill with RA420 T<40C; RA420 dose = 0.5%; t=5min	-	-	100:0	11.4	324
	(Shi et al., 2013)	Rubber: GTR Two-roll mill with RA420 T=180C; RA420 dose = 0.5%; t=5min	-	-	100:0	6.4	226
	(Shi et al., 2013)	Rubber: GTR Twin screw extruder with RA420 T=200C; RA420 dose = 0.5% Residence time=5min	-	-	100:0	6.0	221
Ultrasound	(Tukachinsky, Schworm & Isayev, 1996)	Rubber: GTR (NR/SBR/BR blend) 20 kHz ultrasonic die extrusion Specific ultrasound energy = 1 kJ/g	-	-	100:0	10.5	250
	(Hong & Isayev, 2002)	Rubber: Carbon black filled NR 20 kHz ultrasonic die extrusion T=120C; Amplitude A=5 µm	32	600	25:75	26	545
	(Hong & Isayev, 2002)	Rubber: Carbon black filled NR 20 kHz ultrasonic die extrusion T=120C; Amplitude A=5 µm	32	600	50:50	24	520
	(Hong & Isayev, 2002)	Rubber: Carbon black filled NR 20 kHz ultrasonic die extrusion T=120C; Amplitude A=5 µm	32	600	75:25	21	475
	(Hong & Isayev, 2002)	Rubber: Carbon black filled NR 20 kHz ultrasonic die extrusion T=120C; Amplitude A=5 µm	32	600	100:0	16	450
Microwave	(Novotny et al., 1978)	Rubber: GTR (Tread material) Continuous microwave reactor Power=750W; Frequency=2450MHz Feed rate=8kg/h	15.3	740	100:0	9	200
	(Wicks et al., 2002)	Rubber: GTR (Mostly SBR) Batch microwave reactor Frequency=2450MHz; t=8min	21.51	421	20:100	17.28	425

Owing to the complexity of rubber and the wide variety of potential applications, it is difficult to give a single quantitative indication of product quality. While the tensile properties of compounds containing reclaimed rubber can serve as a useful indication of the quality of the reclaim, this measurement depends on the composition of the rubber feedstock as well as the compounding formulation used to revulcanise the reclaim, amongst other factors. This makes it difficult to compare the technical performance between processes, as this would require that the same feedstock, characterisation methods and compound formulation be used between publications. Furthermore, a superior technical performance does not necessarily suggest superior economic performance of the process that produces the reclaim. For this reason it is useful to compare the qualitative advantages and disadvantages of the processes, as shown in Table 2.2.

Thermal devulcanisation processes have a long history of industrial application, but these technologies appear to yield relatively poor products compared to some of the more recently developed technologies such as extrusion-based mechanical and mechanochemical devulcanisation and ultrasonic devulcanisation. Thermal devulcanisation was excluded from further analysis due to the poor product properties of rubber reclaimed by this method, along with the absence of any significant research in recent literature.

Microwave devulcanisation was excluded from further analysis due to the minimal interest in the academic literature, along with the reports of control difficulties associated with this process.

Microbial devulcanisation and chemical probes show the potential to be highly selective devulcanisation processes, however these processes were excluded from further analysis as both processes are still in the early stages of development. Chemical probes also have the disadvantage of being dangerous and expensive, which further limits their application beyond the laboratory.

The remaining devulcanisation processes (mechanical, mechanochemical and ultrasonic devulcanisation) were considered to show promise for industrial application in the near future, or have already reached initial industrial application recently. While ultrasonic devulcanisation was initially included in the list of technologies to be studied in this thesis, extensive difficulties with the ultrasonic die were encountered during experimental work, resulting in insufficient useful data being generated for ultrasonic devulcanisation. Therefore this thesis will focus on mechanical and mechanochemical devulcanisation, and ultrasonic devulcanisation is to be recommended for a follow-up project.

It is of interest to evaluate the techno-economic performance of the newer technologies as they are typically continuous processes yielding a finished product without the need for

subsequent refining as in the case of the older thermal devulcanisation processes. If the newer technologies show promise from an economic perspective, this could open a pathway to significantly higher levels of recycling of waste tyre rubber back into tyres where mechanical properties are very important.

### 2.5.3 Product characterisation

Sol-gel and crosslink density measurements give a good indication of the extent of the breakdown of the rubber network, and these measurements are commonly reported in devulcanisation literature. In practice the measurements are made by soxhlet extraction and swelling of a rubber sample in appropriate solvents. In the case of natural rubber, acetone is used for soxhlet extraction and toluene is used for swelling (ASTM D6814).

The sol fraction and crosslink density can be analysed further with the Horikx method in order to give an estimate of how selective the devulcanisation process was for crosslink scission. Horikx analysis will be of interest in comparing the selectivity between processes and how process parameters affect the selectivity.

### 2.5.4 Novel research contribution

There is a clear lack of comparable technical and economic data in the devulcanisation field. While the effects of varying operating parameters on the properties of devulcanised rubber have been investigated for various technologies, these quantitative findings are often not comparable between technologies due to each study using a different feedstock and equipment. Furthermore, no power consumption data has been identified in the literature for any of the devulcanization processes. This study aims to address the lack of comparable techno-economic data by generating this data using a single source of crumb rubber feedstock, using the same equipment and characterisation methods for all experiments.

The objectives listed in Section 1.3 were updated subsequent to satisfying objective 1 during the literature review in Chapter 2. The further objectives to be addressed are:

2. Design and conduct experiments for mechanical and mechanochemical devulcanisation such that response surface models can be generated for power consumption as well as the sol fraction and crosslink density of the reclaimed rubber.
3. Use response surface models to generate technical (sol fraction and crosslink density) and economic data within the experimental domain of each devulcanisation technology and compare the advantages and disadvantages of the devulcanisation technologies from a technical and economic point of view.

In order to address these objectives, experiments were designed using a central composite design (CCD) such that subsequent analysis and optimisation using response surface methodology (RSM) could be done. In order to put a reasonable limit on the number of experimental runs required, the experiments were limited to two important operating parameters for each devulcanisation process, identified from literature as follows:

- Mechanical devulcanisation: Extruder barrel temperature and screw speed
- Mechanochemical devulcanisation: Extruder barrel temperature and concentration of the reclaiming agent.

Based on the literature review, mechanical devulcanisation is typically conducted in twin-screw extruders at temperatures of 150-300°C, using screw speeds of 20-400 RPM depending on the design of the equipment used. Mechanochemical devulcanisation is typically conducted using a two-roll mill at 30-110°C, although mechanochemical devulcanisation conducted in a twin-screw extruder has been conducted at higher temperatures of 200-240°C. Concentration of various disulfide reclaiming agents are typically varied between 5-40 g/kg.

Based on the typical operating parameters used in literature, the following parameters were expected to provide a suitable experimental domain for the subsequent experimental work:

- Mechanical devulcanisation:
  - Temperature: 150-275°C
  - Screw speed: 30-80 RPM (for single screw extruder (Bilgili, Arastoopour & Bernstein, 2001b))
- Mechanochemical devulcanisation:
  - Temperature: 125-200°C
  - Disulfide concentration: 5-30 g/kg

The initial experimental domain identified from literature values was used to guide preliminary exploratory experiments in order to confirm the suitability of these operating parameters in the single screw extruder used in this study. The purpose of preliminary experiments was to define the experimental domain of the CCD experiments for mechanical and mechanical devulcanisation such that the properties of the reclaimed rubber were amenable to Horikx analysis. Horikx analysis requires that the relative decrease in crosslink density of samples lies approximately between 50% and 95% in order to avoid the small margin of error outside of this range, in terms of the low precision of both sol fraction and crosslink density measurements.

### 3 Experimental

The following chapter gives a detailed discussion of the experimental procedures followed in this study. This chapter is broken down into four sections describing the materials, equipment, experimental procedures and analytical methods used.

#### 3.1 Materials used

The materials used in this study are summarized in Table 3.1. The materials were used as received without further purification.

*Table 3.1: Summary of materials used in this study*

Material	Supplier	Specifications	Use
Rubber	Dawhi, Germiston	20 mesh (841 $\mu$ m) 100% truck tyre GTR	Feedstock for devulcanisation experiments
Diphenyl disulfide (DPDS)	Sigma Aldrich	Reagent grade (99%)	Devulcanisation agent for mechanochemical devulcanisation
Process oil	H&R, Durban	Distillate Aromatic Extract (DAE)	Distributing agent for mechanochemical devulcanisation agent
Acetone	Kimix, Cape Town	Reagent grade ( $\geq 99.5\%$ )	Soxhlet extraction of soluble compounds in rubber
Toluene	Kimix, Cape Town	Reagent grade ( $\geq 99.8\%$ )	Swelling of rubber crumb

#### 3.2 Devulcanisation equipment and methodology

Devulcanisation experiments were carried out in a Brabender (model PLE 651) single-screw extruder (SSE). The extruder consists of a 19 mm diameter screw with a length of 475 mm ( $L/D = 25$ ) in a barrel with four heating zones, including the die. The temperature can be manipulated between 125°C and 350°C and the screw speed can be manipulated between zero and 100 RPM. The extruder was starve-fed by a screw feeder with a 35 mm screw. The experimental setup is shown in Figure 3.1, Figure 3.2 and Figure 3.3. A 6 mm strand die was attached to the extruder for all experiments.

The power consumption of the extruder was monitored using 3 CT sensors (one over each live phase) coupled to an Efergy e2 3-phase wattmeter. The total power consumption of the heaters on the extruder barrel was monitored using an Efergy EMS 2.0 wattmeter socket.

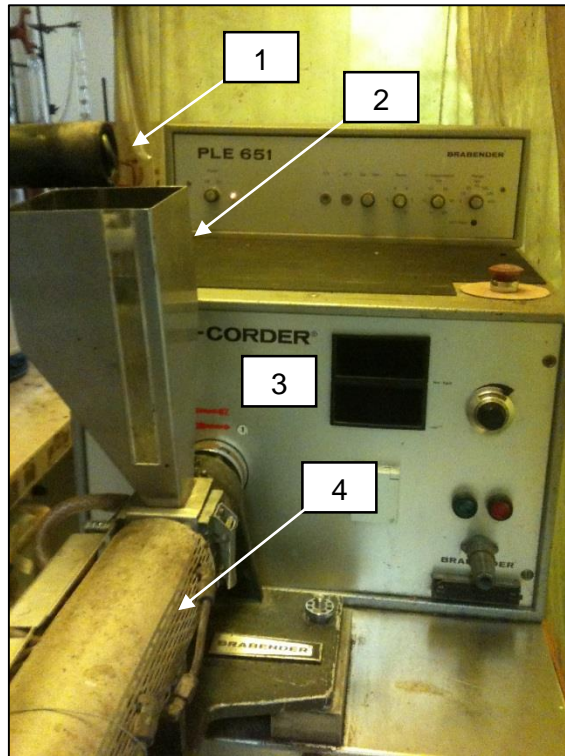


Figure 3.1: Brabender Plasti-Corder PLE 651 used for devulcanisation experiments.  
(1: Feeder outlet; 2: Extruder hopper; 3: Extruder driver; 4: Extruder)

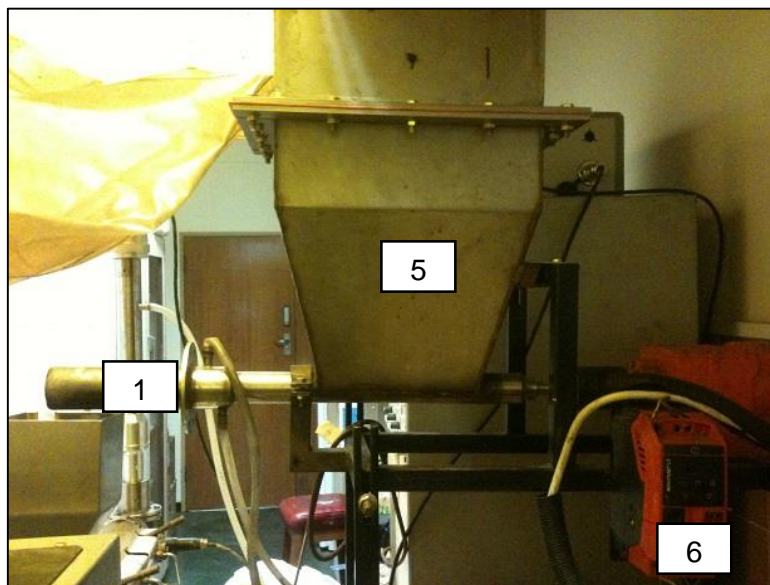


Figure 3.2: Screw feeder used to feed GTR into the extruder.  
(1: Feeder outlet; 5: Feeder hopper; 6: Feeder speed controller)

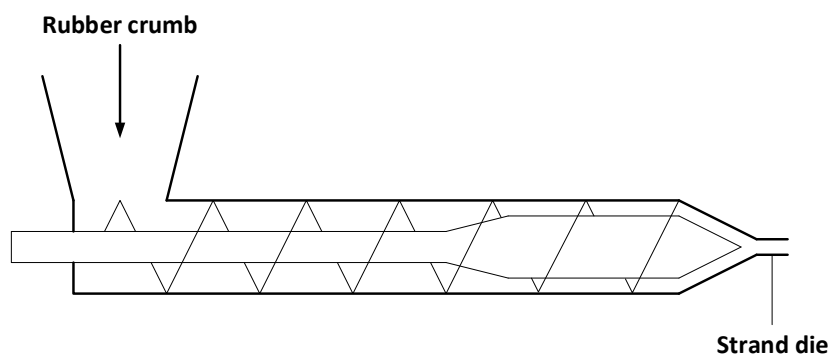


Figure 3.3: Diagram of the single screw extruder used for experimental work.

### 3.2.1 Mechanical devulcanisation methodology

The die and the three barrel heaters of the extruder (4) were preheated to the set point temperature of a particular run. The feeder hopper (5) was filled with approximately 1 kg of GTR. Once the extruder had achieved the desired temperature, the extruder screw driver (3) was started and adjusted to the required speed. The feeder was then started and adjusted using the speed controller (6) to a frequency of 2.5 Hz corresponding to a feed rate of 6 g/min. The extruder was allowed to run for 10 minutes in order to ensure that steady state had been achieved. Power data logging was carried out over the next 10 minutes. A reclaimed rubber sample of approximately 10 g was collected in a glass jar during the last 2 minutes of the data logging period and allowed to cool to room temperature before sealing the jar.

### 3.2.2 Mechanochemical devulcanisation methodology

In preparation for mechanochemical devulcanisation, the rubber was premixed with process oil and DPDS in the proportions shown in Table 3.2. The DPDS was dissolved in the process oil prior to adding the crumb, in order to facilitate DPDS dispersion within the rubber matrix (Saiwari & Dierkes, 2013).

Table 3.2: Mechanochemical devulcanisation preparation recipe

Material	Quantity
Rubber crumb	1000 g
Process oil	100 g
DPDS	Varied

After premixing the crumb with reclaiming agents, the rubber was allowed to absorb the oil mixture for 30 minutes before being loaded into the feeder hopper. The 6 mm strand die and the three zones of the extruder were preheated to the set point temperature of a particular run such that the experiment could be started 30 minutes after premixing the GTR and oil mixture. Once the correct temperature had been achieved, the screw driver was started and adjusted to a speed of 30 rpm before starting the feeder. The feed rate was adjusted to 6 g/min based on total mass flow rate of the mixture described by Table 3.2. After waiting for 10 min to ensure steady state, data logging and sample collection were carried out as described in Section 3.2.1.

### 3.3 Experimental design and planning

In order to determine the maximum and minimum values of the operating parameters to be used in the full experiments, preliminary exploratory experiments were conducted in the form of  $2^2$  factorial experiments as discussed in Section 2.5.4. The development of experimental designs for the mechanical and mechanochemical devulcanisation experiments is discussed in Section 3.3.1 and Section 3.3.2 respectively.

#### 3.3.1 Mechanical devulcanisation experiment design

The preliminary experiments for mechanical devulcanisation used barrel temperatures of 150°C and 275°C and screw speeds of 30 rpm and 80 rpm in order to test a wide range of the screw speeds available to the equipment used in this study. The results of the preliminary experiments suggested that the minimum temperature should be increased slightly in order to avoid the low precision area of the Horikx plot (<50% devulcanisation), as discussed in Section 2.5.4.

The final central composite design (CCD) of the mechanical devulcanisation experiment is summarised in Table 3.3.

Table 3.3: Full central composite design for mechanical devulcanisation experiment.

Experiment	Coded experimental conditions		Experimental conditions	
	Temperature	Screw Speed	Temperature (°C)	Screw speed (rpm)
M1	-1.414	0	175	55
M2	-1	-1	190	37
M3	-1	+1	190	73
M4	0	-1.414	225	30
M5	0	0	225	55
M6	0	1.414	225	80
M7	+1	-1	260	37
M8	+1	+1	260	73
M9	+1.414	0	275	55
M10	0	0	225	55
M11	0	0	225	55
M12	0	0	225	55

### 3.3.2 Mechanochemical devulcanisation experiment design

The preliminary mechanochemical devulcanisation experiments were conducted at extruder temperatures of 125°C and 200°C and DPDS concentration of 5 g/kg and 30 g/kg while the screw speed was kept constant at 30 rpm in order to avoid an excessive number of experimental runs. The results of the preliminary experiment suggested that both the minimum and maximum temperature should be increased in order to ensure a similar distribution of points on the Horikx plot for mechanical and mechanochemical devulcanisation.

The final design for the mechanochemical devulcanisation experiment is given in Table 3.4.

Table 3.4: Full central composite design for mechanochemical devulcanisation experiment.

Experiment	Coded experimental conditions		Experimental conditions	
	Temperature	DPDS	Temperature (°C)	DPDS (g/kg rubber)
C1	-1.414	0	150	17.5
C2	-1	-1	160	8.70
C3	-1	+1	160	26.3
C4	0	-1.414	185	5.00
C5	0	0	185	17.5
C6	0	+1.414	185	30.0
C7	+1	-1	210	8.70
C8	+1	+1	210	26.3
C9	+1.414	0	220	17.5
C10	0	0	185	17.5
C11	0	0	185	17.5
C12	0	0	185	17.5

## 3.4 Analytical equipment and methodology

The sol fraction and crosslink density measurements for the untreated GTR as well as the RR from all experiments were made using soxhlet extraction and swelling procedures described in Section 3.4.1 and Section 3.4.2.

### 3.4.1 Soxhlet extraction equipment and procedure

Three samples of approximately 1 gram each were taken from the RR collected from each experimental run for triplicate measurement of the sol fraction and crosslink density in order to account for the error associated with sol fraction and crosslink density measurements. Each sample was wrapped in pre-weighed filter paper and weighed again to ascertain the precise mass of each sample ( $m_{sample}$ ). The three individually wrapped samples for triplicate analysis were placed in a single soxhlet extractor<sup>2</sup> and extracted with acetone for a total of 16 hours in order to remove the majority of the low molecular weight compounds in the sample.



*Figure 3.4: Soxhlet extractors used for rubber analysis.*

---

<sup>2</sup> The soxhlet extraction of multiple GTR samples in a single soxhlet extractor showed no apparent error in the measurements in comparison to triplicate measurement in three separate extractors. Therefore the procedure for extracting three samples per soxhlet extractor was used in order to reduce the amount of time and solvent used for sample characterisation.

After soxhlet extraction, the samples were allowed to dry in a fume hood overnight before proceeding with the swelling procedure.

### 3.4.2 Swelling procedure

The dried acetone-extracted samples (still in filter paper) were placed in toluene at room temperature in order to swell the rubber network and to remove any residual soluble components from the sample. The samples were kept in toluene for a total of 72 hours, changing the solvent every 24 hours in order to ensure maximum extraction of the soluble components from the samples.

After swelling, the samples were removed from the toluene and dabbed with absorbent paper to remove excess toluene. The samples were transferred quickly to pre-weighed foil and weighed in order to determine the mass of the swollen sample ( $m_{swollen}$ ). The weighing of each swollen sample was completed within 60 seconds of removing the sample from the toluene.

The swollen samples were dried in a vacuum oven overnight at 60°C in order to remove the toluene from the rubber. The samples were allowed to cool to room temperature before they were weighed again in order to determine the dry mass of each sample ( $m_{dry}$ ).

Results from the soxhlet extraction and swelling procedures were used to determine the sol fraction and crosslink density of samples.

## 3.5 Statistical analysis

Data from the experimental work were analysed using Statistica (Dell Inc., 2015) version 12 for the development of response surface models. Initially a quadratic model was generated including a linear interaction term, as appropriate. The general form of the initial model is described by Equation (3.1) (Dell Inc., 2015):

$$Z = a_0 + a_1X + a_2X^2 + a_3Y + a_4Y^2 + a_5XY + \varepsilon \quad (3.1)$$

where  $Z$  is the response variable,  $X$  and  $Y$  are independent variables,  $a_0$  to  $a_5$  are regression coefficients, and  $\varepsilon$  is the error term.

The initial model was refined by removing statistically insignificant factors one-by-one from the model, using analysis of variance (ANOVA) tables generated by Statistica as a guide.

### 3.6 Error analysis

Each experimental code in Table 3.3 and Table 3.4 (M1, M2, etc.) represented a single experimental run consisting of a 10 minute wait for steady state, followed by 10 minutes of power data logging and 1 minute of sample collection. Therefore, each physical sample of RR represented 1 minute of steady state operation. The sample analysis (sol fraction and crosslink density) was done by triplicate measurement of the sample from each experimental run, thus accounting for measurement error. Variation of results with repeated experimental runs (experimental error) was estimated by repetitions of the centre point (M10 to M12 and C10 to C12).

Power consumption measurements were taken every 30 seconds with the average power consumption reported over 10 minutes of operation.

## 4 Results and Discussion

This chapter presents and discusses the results from the experiments conducted as set out in Chapter 3. This chapter begins by describing the characterisation of the crumb rubber in Section 4.1 before describing the experimental results of mechanical devulcanisation and mechanochemical devulcanisation in Section 4.2 and Section 4.3 respectively.

### 4.1 Crumb characterisation

In order to develop a baseline for further analysis, the crumb feedstock was characterised in terms of the crosslink density and sol fraction by the data generated by the soxhlet extraction and swelling procedures described in Section 3.4. The equations used to calculate the crosslink density and sol fraction are fairly straightforward for pure vulcanised rubber (Horikx, 1956), but their application to GTR requires a number of corrections and assumptions, as discussed in Section 4.1.1 and Section 4.1.2.

#### 4.1.1 Fundamental assumptions

For the purpose of the analysis of rubber samples, GTR (crumb) was described as consisting of the following composition: rubber polymer, carbon black, ash and the extractable non-rubber components consisting of soluble compounding ingredients such as process oil and residual vulcanisation agents. In a highly vulcanised rubber compound (crosslink density > 100 mol/ton) the soluble fraction (sol) of the rubber polymer is very low (<0.2% of the polymer) (Charlesby, 1954) and was therefore assumed to be negligible. The extractable non-rubber portion of the GTR was assumed to be constant during devulcanisation and was referred to as the “crumb extract”. Figure 4.1 shows an estimated composition of GTR.

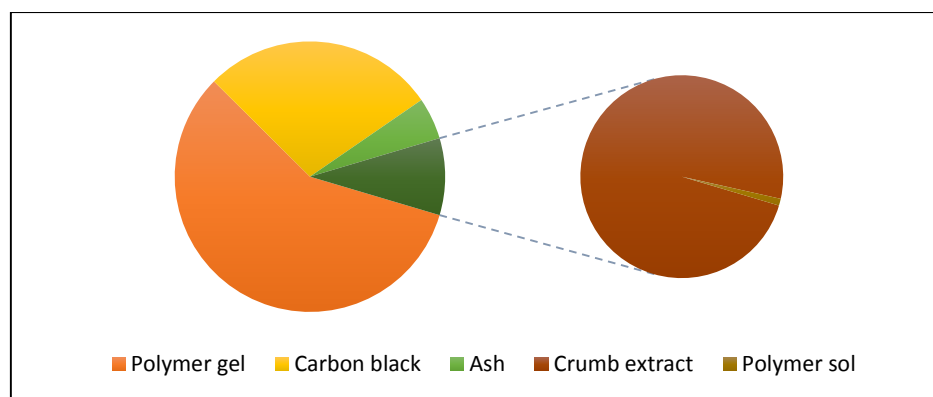


Figure 4.1: Fractional composition of GTR. The dark green section is the total extractable portion composed of crumb extract and the negligible sol fraction of the polymer.

During devulcanisation the polymer network is broken down by scission of crosslinks and the polymer backbone. The freed chain fragments increase the sol fraction (and decrease the gel fraction) while the crumb extract remains constant, resulting in an overall increase in extractable portion of the crumb, as shown in Figure 4.2. While the polymer network of the GTR undergoes chemical and structural changes during devulcanisation, the carbon black and ash portions were assumed to be unaffected by devulcanisation.

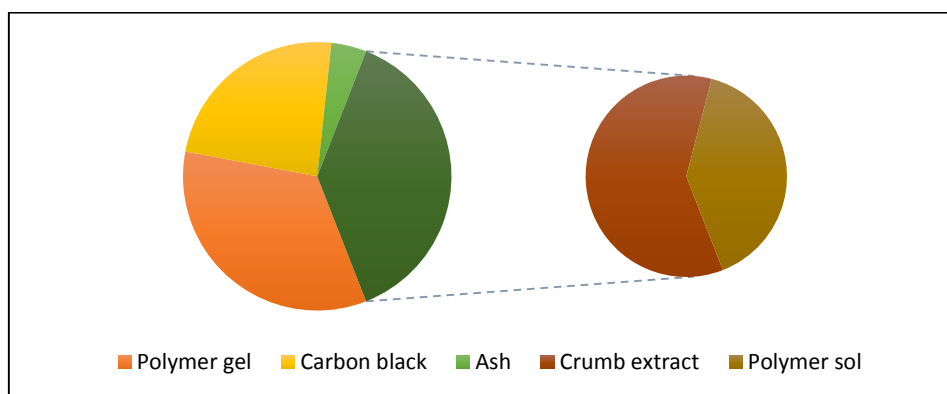


Figure 4.2: Fractional composition of reclaimed rubber. The dark green section is the extractable portion of the sample composed of crumb extract and the sol fraction

In order to achieve good estimates of the approximate composition of the GTR, a sample was subjected to thermogravimetric analysis (TGA) which revealed the volatile matter, fixed carbon and ash contents of the crumb.

Another sample of GTR was also subjected to soxhlet extraction with acetone followed by swelling in toluene at room temperature, as described in Section 3.4, in order to determine the crumb extract. The initial mass of the sample ( $m_{sample}$ ), swollen mass of the sample ( $m_{swollen}$ ) and dried mass of the sample ( $m_{dry}$ ) were determined. Using the data from the analysis of the GTR, the fraction of extractable non-rubber compounds ( $e_N$ ) was calculated as the soluble mass fraction of the GTR such that the sol fraction of the remaining highly vulcanised polymer fraction of the crumb was approximately zero. The residual mass of the GTR after accounting for the ash, fixed carbon and crumb extract was taken to be the crosslinked polymer network.

The approximate composition of the crumb was determined using the TGA data and extraction data, the results of which are presented in Table 4.1.

Table 4.1: Composition of the GTR feedstock

Property	Mass percentage	Notes
Proximate analysis (TGA)		
<i>Moisture</i>	0.5%	
<i>Volatiles</i>	63.4%	Consists of rubber + oils etc.
<i>Fixed carbon</i>	29.9%	
<i>Ash</i>	6.3%	
Crumb composition		
<i>Crumb extract (non-rubber)</i>	7.6%	Acetone extract + toluene extract
<i>Carbon black</i>	29.9%	Equal to fixed carbon by TGA
<i>Ash</i>	6.3%	Equal to ash by TGA
<i>Crosslinked rubber network</i>	56.2%	100% – CB – Ash - extractables

The results reported in Table 4.1 are very similar to results reported by other authors using GTR from truck tyres (Mangili et al., 2014).

#### 4.1.2 Crosslink density and sol fraction of the crumb rubber

Since the Flory-Rehner equation was derived from a model rubber network consisting of only polymer chains and sulfur crosslinks, it does not account for the presence of carbon black fillers which are present in GTR. The presence of carbon black results in an error in the apparent volume fraction of rubber in the swollen network since the bonds between polymer chains and carbon black particles restrict the swelling, thus leading to an overestimate of the crosslink density (Kraus, 1963). Kraus' correction (Kraus, 1963) is commonly employed to calculate a corrected volume fraction of the rubber to be used in the Flory-Rehner equation.

The apparent volume fraction of the rubber in the swollen sample ( $V_R$ ) was calculated as the ratio of the volume occupied by the rubber network in the swollen sample to the total volume of swollen network, according to Equation (4.1):

$$V_R = \frac{m_R}{m_R + m_S \frac{\rho_R}{\rho_S}} \quad (4.1)$$

where  $m_R$  is the mass of rubber polymer in the swollen sample,  $m_S$  is the mass of the solvent taken up at equilibrium swelling, and  $\rho_R$  and  $\rho_S$  are the densities of the rubber and solvent, respectively.

The Kraus correction described by Equation (4.2) (Kraus, 1963) was solved iteratively for the corrected volume fraction to be used in the Flory-Rehner equation.

$$\frac{V_{R0}}{V_R} = 1 - \frac{\phi [3c(1 - \sqrt[3]{V_{R0}}) + V_{R0} - 1]}{1 - \phi} \quad (4.2)$$

In Equation (4.2),  $V_R$  is the apparent volume fraction of rubber in the swollen network (as calculated using equation (4.1) and  $V_{R0}$  is the corrected volume fraction of rubber to be used in the Flory-Rehner calculation. The parameter  $\phi$  denotes the volume fraction of filler in the unswollen rubber and  $c$  is an empirical parameter depending only on the type of filler. The value of  $c$  was taken as 1.17, corresponding to the assumption of HAF N330 as the type of carbon black (Mangili et al., 2014). The volume fraction of filler in the dried sample ( $\phi$ ) was calculated from the mass of rubber and filler in the dried sample after swelling:

$$\phi = \frac{m_F}{m_F + m_R \frac{\rho_F}{\rho_R}} \quad (4.3)$$

where  $m_F$  is the mass of the filler in a sample and  $\rho_F$  is the density of the filler.

Further assumptions required for the calculation of the crosslink density included the following, based on previous work using GTR from truck tyres (Mangili et al., 2014):

- Polymer-solvent interaction parameter  $\chi = 0.39$  assuming the polymer is mostly NR.
- Density of rubber  $\rho_R = 920 \text{ kg/m}^3$  assuming NR.
- Density of the filler  $\rho_F = 1800 \text{ kg/m}^3$  assuming HAF N330 carbon black.

Applying the measurements of  $m_{sample}$ ,  $m_{swollen}$  and  $m_{dry}$  generated by the soxhlet extraction and swelling procedure described in Section 3.4, along with assumptions made in Section 4.1, the crosslink density of the GTR was found to be 117 mol/ton.

Due to the difficulty of obtaining a precise experimental measurement of the initial sol fraction in rubber compounds containing extractable non-rubber components, the sol fraction was estimated according to Equation (4.4) (Charlesby, 1954; Horikx, 1956):

$$s_1 = \frac{(2 + \gamma_1) - (\gamma_1^2 + 4\gamma_1)^{0.5}}{2\gamma_1} \quad (4.4)$$

where  $\gamma_1$  is the initial value of the crosslinking index of the rubber network, calculated according to Equations (4.5), (4.6) and (4.7) (Horikx, 1956), assuming an initial number-average molecular weight of the rubber polymer chains to be  $M = 200000 \text{ g/mol}$  (Horikx, 1956).

$$N = \frac{1}{M} \quad (4.5)$$

$$v_0 = v_e + 2N \quad (4.6)$$

$$\gamma = \frac{v_0}{N} \quad (4.7)$$

The results of the crosslink density and sol fraction calculations for the GTR are summarised in Table 4.2, along with typical values published by other authors.

*Table 4.2: Sol fraction and crosslink density measurements of vulcanised rubber*

Source	Sol fraction	Crosslink density (mol/ton)	Material
This work	0.0014	117	GTR
(Horikx, 1956)	0.0006	190	Unfilled NR
(Yun, Oh & Isayev, 2001)	0.18	109	GTR
(Tao et al., 2013)	0.13	161	GTR
(Mangili et al., 2014)	0.001	89	GTR

As seen in Table 4.2, the crosslink density of the polymer network in the GTR used in this work corresponds to a theoretical sol fraction of 0.0014, thus supporting the prior assumption of negligible initial sol fraction in the crumb, as mentioned in Section 4.1.1.

The majority of authors in the devulcanisation field appear to define the sol fraction as the mass fraction of soluble components in the whole rubber compound which does not make any correction for extractable non-rubber components, resulting in overestimated sol fraction as seen in Table 4.2 (Yun, Oh & Isayev, 2001; Tao et al., 2013). More recently, attempts have been made to measure the sol fraction by first extracting low molecular weight compounds with acetone, followed by extraction of unbound rubber by swelling in toluene, resulting in a more realistic measure of the sol fraction (Mangili et al., 2014).

It should be noted that the crosslink density measurements were reported on a volume basis ( $\text{mol/m}^3$ ) by other authors in the devulcanisation field (Yun, Oh & Isayev, 2001; Tao et al., 2013; Mangili et al., 2014). These values are converted to mass basis using a polymer density of  $920 \text{ kg/m}^3$  in order to allow comparison with the mass basis method used in this work.

Having established a baseline estimate for the sol fraction and crosslink density of the GTR, subsequent sections will focus on the results of mechanical devulcanisation experiments in Section 4.2 and mechanochemical devulcanisation experiments in Section 4.3.

## 4.2 Mechanical devulcanisation

To the author's knowledge, mechanical devulcanisation has never been performed in a single screw extruder, apart from low-temperature extrusion (<135°C) which resembled pulverisation more than devulcanisation (Bilgili, Arastoopour & Bernstein, 2001b). Furthermore, valid comparison of sol fraction and crosslink density data of devulcanisation processes to values achieved by other authors requires that similar feedstocks are used in the processes being compared, along with comparable assumptions in the calculations used to generate the data. Therefore, the data presented in Section 4.2 will be compared qualitatively to other reports in the academic literature, where possible.

Section 4.2 begins with a discussion of the RR product properties in Sections 4.2.1 to 4.2.3 before describing the power consumption of the process in Section 4.2.4

### 4.2.1 Sol fraction

The sol fraction of the RR samples was determined using the procedure described in Section 3.4, taking account of the extractable non-rubber components as discussed in Section 4.1. The measurements are reported in Table 4.3 below.

*Table 4.3: Sol fraction measurements of samples produced by mechanical devulcanisation*

Run	Temperature °C	Screw speed (RPM)	Sol Fraction	
			Mean	SD <sup>3</sup>
M1	175	55	0.063	0.011
M2	190	37	0.099	0.019
M3	190	73	0.158	0.024
M4	225	30	0.337	0.009
M5	225	55	0.359	0.013
M6	225	80	0.441	0.017
M7	260	37	0.475	0.015
M8	260	73	0.457	0.007
M9	275	55	0.534	0.013
M10	225	55	0.328	0.028
M11	225	55	0.366	0.023
M12	225	55	0.334	0.022

<sup>3</sup> Standard deviation of the measurement

A Pareto chart using the results obtained in Table 4.3 suggested that the linear and quadratic temperature effects were significant effects in modelling the sol fraction of the samples produced in the mechanical devulcanisation experiment, as shown in Figure 4.3.

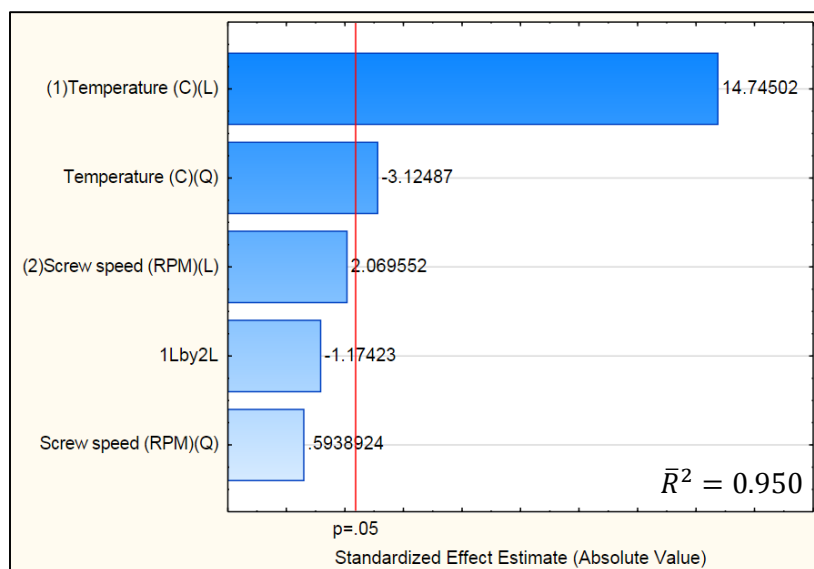


Figure 4.3: Pareto chart indicating the significance of operating parameters on modelling the sol fraction of samples produced by mechanical devulcanisation

The Pareto chart in Figure 4.3 shows that the linear screw speed effect could be a significant factor to include in the model. Analysis of variance (ANOVA) revealed a p-value of 0.077 for the effect of the linear screw speed factor in the original quadratic model for the sol fraction. The p-value of the linear screw speed factor was not considered to be large enough to warrant its exclusion from the sol fraction model, so linear screw speed factor was retained in the revised model while the quadratic screw speed and linear interaction factors were excluded from the model. The correlation coefficients were estimated and reported in Equation (4.8)

$$S_{mech} = -2.36 + 1.88 \times 10^{-2} \cdot T - 3.12 \times 10^{-5} \cdot T^2 + 1.33 \times 10^{-3} \cdot \omega + \varepsilon \quad (4.8)$$

where  $S_{mech}$  is the sol fraction of the RR produced by mechanochemical devulcanisation, as predicted as a function of screw speed in RPM and temperature in degrees Celsius.

A surface plot of the sol fraction model described by Equation (4.8) is given in Figure 4.4 along with the experimental measurements of the sol fraction.

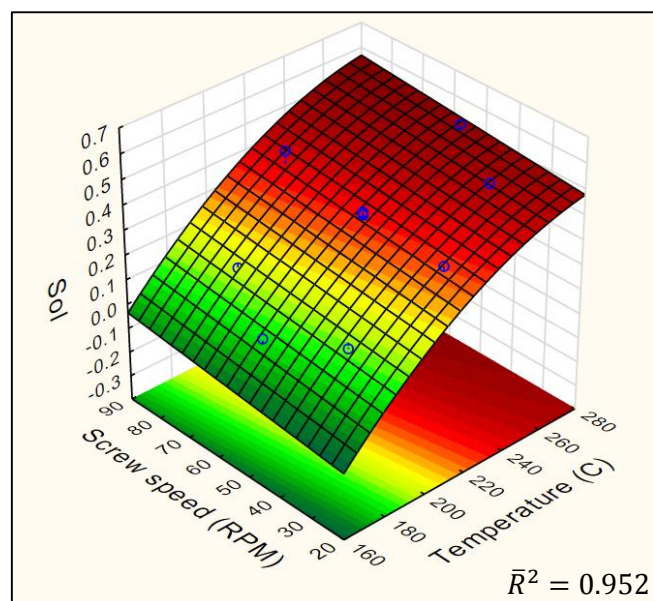


Figure 4.4: Surface plot of the sol fraction model for mechanical devulcanisation

As shown in Figure 4.4, the sol fraction increases strongly with increasing temperature, with the gradient tapering off at higher temperatures. The reducing gradient of increasing sol fraction versus temperature at high temperatures could reflect the tangential approach to the theoretical maximum sol fraction of unity, although this would be expected to occur at a higher sol fraction than observed in Figure 4.4. An alternative explanation for the reducing gradient of the sol fraction could be that devolatilisation of non-rubber components occurs at high extrusion temperatures ( $>250^{\circ}\text{C}$ ), as suggested by TGA data in Figure 4.5.

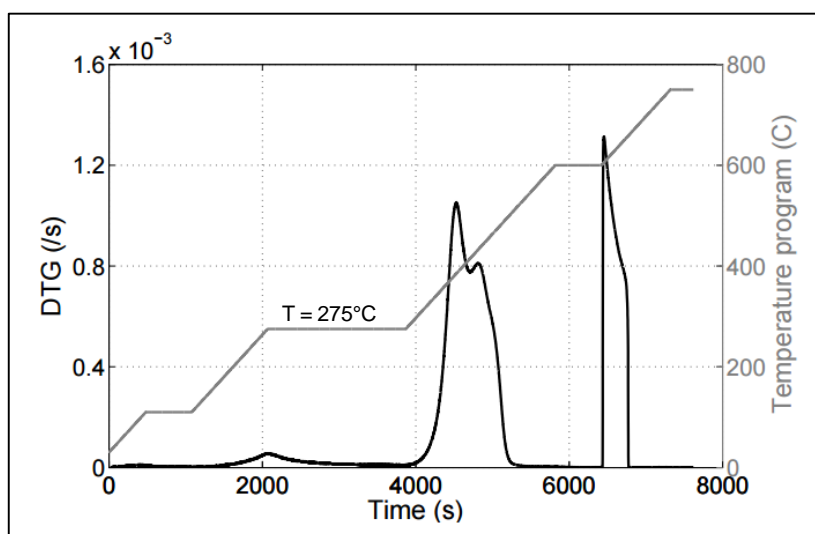


Figure 4.5: TGA data confirming partial devolatilisation of the GTR used in experiments at  $T > 250^{\circ}\text{C}$

Figure 4.5 shows a peak in the differential thermogravimetric (DTG) curve at the beginning of the second isothermal segment at a temperature of 275°C, although an appreciable rate of devolatilisation can be seen by the time the temperature reaches approximately 240°C. The peak at the beginning of the second isothermal segment is probably due to devolatilisation of the extractable non-rubber components since the moisture is removed at around 100°C and typical rubber polymers present in GTR have been shown to devolatilise at temperatures beyond 300°C (Danon, de Villiers & Görgens, 2015). Devolatilisation of the extractable non-rubber components could cause  $e_N$  (assumed to be constant during devulcanisation) to be greater than the true value for RR produced at high temperatures, thus leading to a sol fraction lower than the true value. To the author's knowledge, devolatilisation during devulcanisation has not been taken into account in the characterisation of RR in the literature.

In comparison to a mechanical devulcanisation process in a twin screw extruder where the sol fraction was reported (Si, Chen & Zhang, 2013), a similar trend of increasing sol fraction with increasing barrel temperature was observed within the range of 180°C to 260°C, which also showed a reducing gradient at  $T > 240^\circ\text{C}$ . The study found the sol fraction of the product to increase strongly with increasing screw speed in the range of 400 to 1000 RPM, while in the present thesis the sol fraction increased very slowly with increasing screw speed as seen in Figure 4.4. The difference in the strength of the screw speed effect could be attributed to significantly higher screw speed achieved by their extruder, along with the significant differences in shear and mixing behaviour between single-screw and twin-screw extruders (van Zuilichem, Stolp & Janssen, 1983).

In order to corroborate the findings of the sol fraction analysis, crosslink density analysis was also conducted as discussed in the following section.

## 4.2.2 Crosslink density

The crosslink density was calculated using the Flory-Rehner equation including the Kraus correction as discussed in Section 4.1.2, and the results are summarised in Table 4.4.

*Table 4.4: Crosslink density measurements of samples generated by mechanical devulcanisation*

Run	Temperature °C	Screw speed (RPM)	Crosslink density (mol/g)x10 <sup>-6</sup>	
			Mean	SD
M1	175	55	65.9	2.5
M2	190	37	52.1	4.9
M3	190	73	44.2	3.0
M4	225	30	26.2	1.3
M5	225	55	22.4	2.1
M6	225	80	13.8	2.9
M7	260	37	07.6	2.1
M8	260	73	10.2	1.3
M9	275	55	0.0	0.66
M10	225	55	26.1	3.8
M11	225	55	20.7	0.90
M12	225	55	25.3	1.7

The crosslink density of the sample from run M9 could not be calculated precisely due to the Kraus correction equation having no non-negative solution for the corrected volume fraction of rubber ( $V_{R0}$ ) at the required conditions. Possible explanations for the problem encountered with the Kraus correction include the following:

- The description of polymer-filler adhesion in the Kraus correction becomes invalid in RR due to the breakage of C-C bonds near the carbon black particles (Kraus, 1963).
- Application of Kraus correction to RR becomes invalid at high levels of devulcanisation due to extrapolation errors in terms of the experimental values of  $\frac{\phi}{1-\phi}$  and  $V_{R0}$  lying far outside the original correlation range investigated by Kraus, as shown in Table 4.5.

Table 4.5: Validity of Kraus correction

Factor	Correlation range (Kraus, 1963)	Sample M2	Sample M9
$\frac{\phi}{1 - \phi}$	0 – 0.45	0.30	0.55
$V_{R0}$	0.15 – 0.55	0.12	~0.01

The difficulty in calculating the crosslink density of sample M9 could indicate a serious problem with the applicability of Kraus correction to RR. However, for the purpose of the present analysis, the crosslink density of sample M9 was taken to be zero.

The Pareto chart associated with the data in Table 4.4 is given in Figure 4.6.

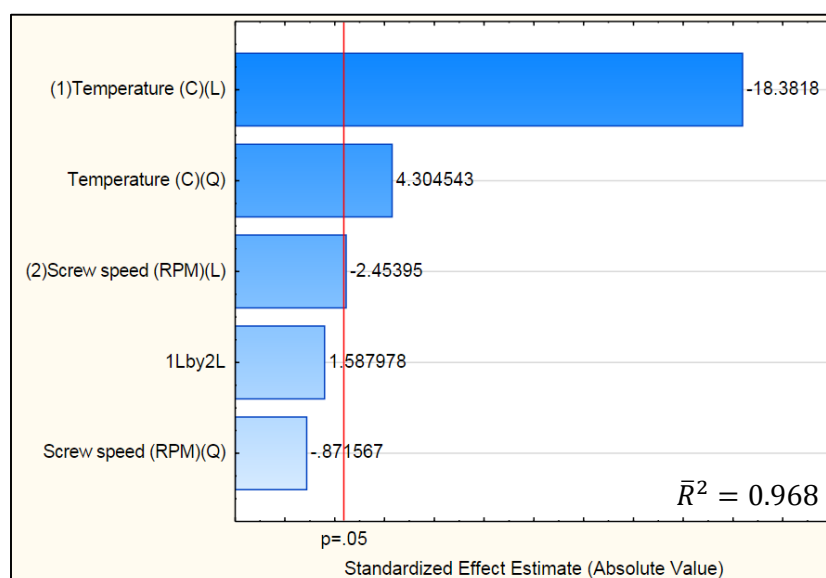


Figure 4.6: Pareto chart indicating the statistical significance of operating parameters on modelling the crosslink density of samples produced by mechanical devulcanisation

The crosslink density model was refined by removing the insignificant quadratic screw speed and linear interaction factors, resulting in the model described by Equation (4.9)

$$v_{e,mech} = 3.92 \times 10^{-4} - 2.60 \times 10^{-6} \cdot T + 4.43 \times 10^{-9} \cdot T^2 - 1.62 \times 10^{-7} \cdot \omega + \varepsilon \quad (4.9)$$

where  $v_{e,mech}$  is the crosslink density (mol/g) of the gel fraction of the RR samples produced by mechanical devulcanisation.

A surface plot for the refined crosslink density model described by Equation (4.9) is given in Figure 4.7 along with experimental data.

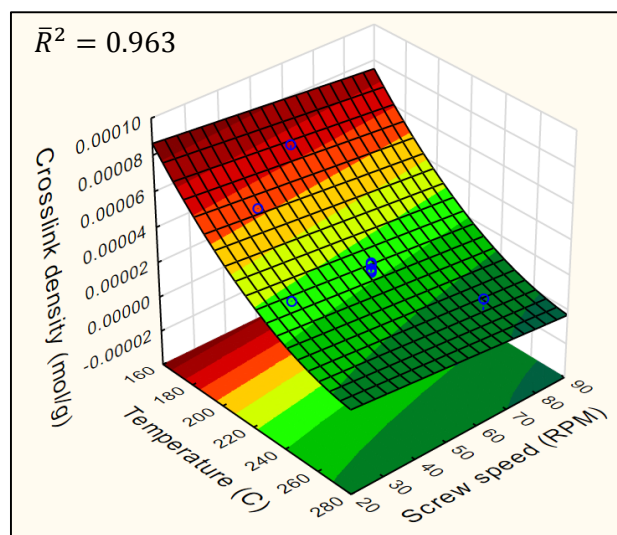


Figure 4.7: Surface plot of the crosslink density model for mechanical devulcanisation

Figure 4.7 shows that increasing the barrel temperature of the extruder strongly reduces the crosslink density of the gel fraction of the reclaimed rubber product. Higher screw speeds also result in lower crosslink density of the product, although the effect of screw speed is not as strong as the temperature effect. The reduction in crosslink density indicates a higher extent of network breakdown with increasing temperature and screw speed, which is in agreement with the sol fraction analysis (Figure 4.4).

Yazdani and co-workers (Yazdani et al., 2011) reported the relative decrease in crosslink density of GTR from truck tyres in a twin screw extruder at screw speeds of 30 RPM to 120 RPM and barrel temperatures of 220°C to 280°C. Their results showed that the extent of network breakdown increased with increasing temperature and increasing screw speed. Their results are similar to the findings shown in Figure 4.7, except that the effect of screw speed in Figure 4.7 is much weaker than that described in literature for twin-screw extruders (Yazdani et al., 2011; Si, Chen & Zhang, 2013).

While the sol fraction and crosslink density measurements in Section 4.2.1 and Section 4.2.2 have given an indication of the extent of network breakdown, a correlation of the sol fraction against the relative decrease in crosslink density can give further information in the form of a Horikx plot, as discussed in the following section.

### 4.2.3 Horikx analysis

The sol fraction and crosslink density measurements reported in Table 4.3 and Table 4.4, respectively, were analysed further using Horikx analysis. A plot of the experimental data along with the theoretical Horikx curves appears in Figure 4.8.

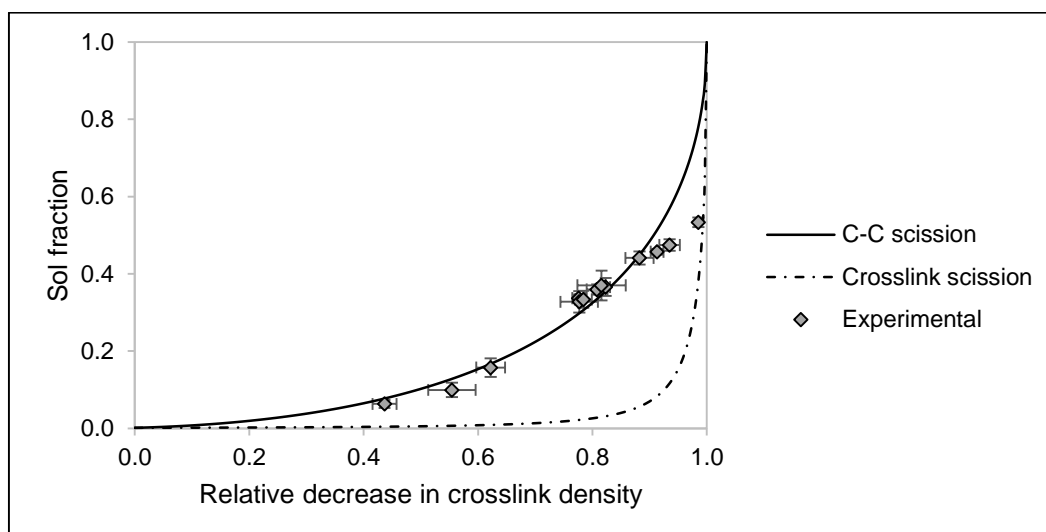


*Figure 4.8: Horikx plot of data from the mechanical devulcanisation experiment along with theoretical curves*

In Figure 4.8 the experimental points are clustered around the C-C scission line which suggests that the network breakdown proceeded mostly by breakage of the carbon-carbon bonds in the polymer chains. While the breakdown of the network by C-C scission rapidly softens the rubber due to the rapid generation of sol, the mechanical properties of the devulcanised rubber are expected to be poor due to the shortening of polymer chains. Shorter polymer chains (lower molecular weight) have been shown to exhibit inferior mechanical properties when subjected to the same extent of vulcanisation (Flory, 1944).

While Horikx analysis has been applied in literature reports of mechanical devulcanisation in twin-screw extruders (Yazdani et al., 2011; Formela, Cysewska & Haponiuk, 2014), it is not possible to provide a good critical comparison with Figure 4.8 due to the wide variety of assumptions affecting the generation of both the experimental data and the theoretical curves. It should be noted that neither of the authors accounted for the extractable non-rubber compounds in the GTR when calculating the sol fraction, which I believe to be a major shortcoming in terms of the characterisation of RR throughout the devulcanisation literature. The sol fraction referred to in the Horikx analysis is strictly the soluble mass fraction of the rubber polymer component of a rubber compound (Horikx, 1956).

#### 4.2.4 Power consumption

Previous work has suggested that the RR product quality (in terms of the physical properties of the revulcanised rubber) can be optimised by targeting specific values of the sol fraction and crosslink density of the RR (Tao et al., 2013). However, technical optimisation of the physical properties of the RR does not necessarily translate to an economic optimum, since the power consumption is expected to vary along with RR properties.

In the interest of developing economic data for devulcanisation, the power consumption was recorded and reported along with technical data already reported in Section 4.2. The power consumption of the mechanical devulcanisation process at various experimental conditions is summarised in Table 4.6.

*Table 4.6: Electrical power consumption measurements from the mechanical devulcanisation experiment.*

Run	Temperature (°C)	Screw speed (RPM)	Power consumption (kW)		
			Extruder	Ancillary	Total
M1	175	55	1.068	0.468	1.536
M2	190	37	0.918	0.552	1.470
M3	190	73	1.165	0.529	1.694
M4	225	30	0.847	0.744	1.591
M5	225	55	1.028	0.720	1.748
M6	225	80	1.174	0.702	1.876
M7	260	37	0.830	0.918	1.748
M8	260	73	1.081	0.912	1.993
M9	275	55	0.962	1.014	1.976
M10	225	55	1.034	0.744	1.778
M11	225	55	1.057	0.732	1.789
M12	225	55	1.023	0.720	1.743

A preliminary analysis of the power consumption data looked at the variation of the power consumption of the extruder driver and the ancillary equipment (barrel heaters) at varying operating conditions. Figure 4.9 shows the variation of power consumption with varying barrel temperature at a constant screw speed of 55 RPM. Figure 4.10 shows the variation of power consumption with varying screw speed at a constant temperature of 225°C.

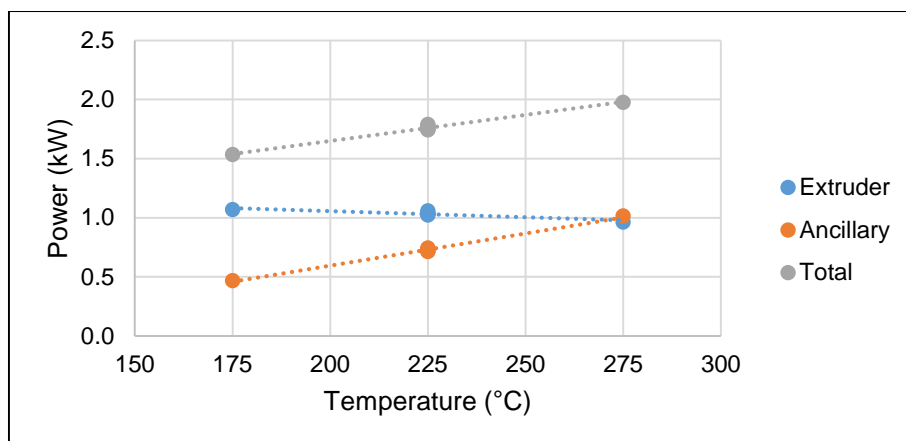


Figure 4.9: Power consumption of the mechanical devulcanisation process at a constant screw speed (55 RPM)

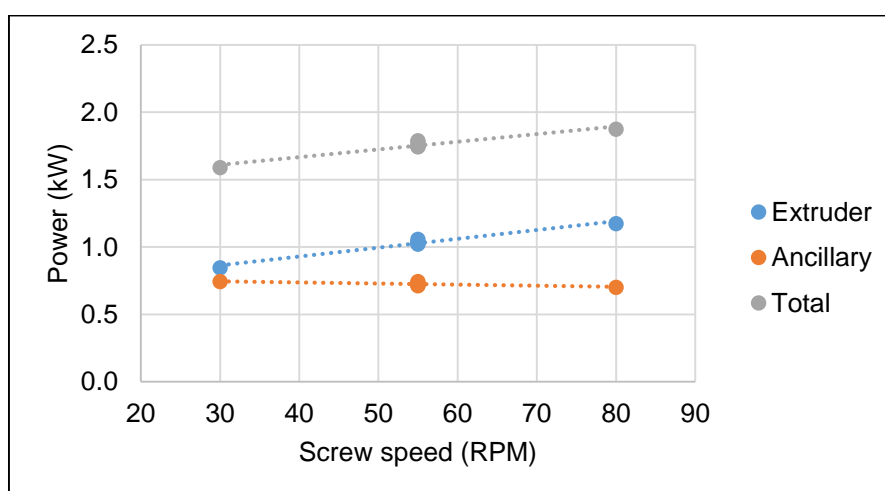


Figure 4.10: Power consumption of the mechanical devulcanisation process at a constant temperature (225°C)

Figure 4.9 shows that the power consumption of the screw driver tends to decrease slightly with increasing temperature, probably due to the reduced viscosity of the rubber at higher temperature. However, the increased power consumption of the barrel heaters at higher temperatures caused an overall increase in total power consumption of the mechanical devulcanisation process when operating at higher temperatures.

Figure 4.10 shows that the extruder screw power consumption increases with increasing screw speed at a constant barrel temperature of 225°C. This resulted in a slight decrease in the power consumption of the barrel heaters with increasing screw speed due to the additional heat generated by friction at higher screw speeds. The net effect was that the total power consumption increased with increasing screw speed.

To the best of the author's knowledge, only one paper has reported the power consumption of the extrusion processing of vulcanised rubber (Bilgili, Arastoopour & Bernstein, 2001b), although the paper only reports the power consumption of the screw driver via torque measurements and neglects the power consumption of the heaters. The results of Bilgili *et al.* (2001b) showed a reduction in the power required to drive the screw when increasing the barrel temperature, similar to that shown in Figure 4.9. They also showed that higher screw speeds demand a higher power requirement to drive the screw, as shown in Figure 4.10.

The Pareto chart in Figure 4.11 using the initial quadratic model gives an initial indication of the statistical significance of each of the potential factors in the quadratic model.

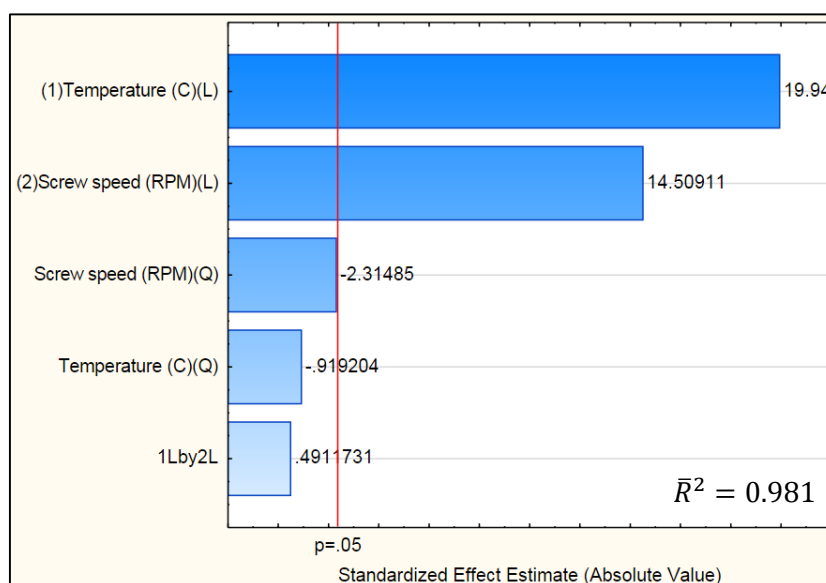


Figure 4.11: Pareto chart showing the statistical significance of the effects of operating parameters on the power consumption of the mechanical devulcanisation process.

The Pareto chart in Figure 4.11 shows that the linear factors of temperature and screw speed appear to be significant in modelling the power consumption of the mechanical devulcanisation process within the experimental domain under investigation. The quadratic screw speed factor could also be considered significant with a p-value of 0.053, however since the screw speed is expected to have a linear effect on power consumption (Bilgili, Arastoopour & Bernstein, 2001b) the quadratic screw speed factor was ultimately rejected from the model.

After reducing the initial model to include only linear temperature and screw speed effects, the correlation coefficients were estimated and summarised in Equation (4.10)

$$P_{mech} = 0.451 + 4.24 \times 10^{-3} \cdot T + 6.18 \times 10^{-3} \cdot \omega + \varepsilon \quad (4.10)$$

where  $P_{mech}$  is the power consumption (kW) of the mechanical devulcanisation process,  $T$  is the temperature set point of the barrel of the extruder in degrees Celsius ( $^{\circ}\text{C}$ ) and  $\omega$  is the screw speed of the extruder in revolutions per minute (RPM).

A surface plot of the model described by Equation (4.10) appears in Figure 4.12, along with experimental power consumption measurements.

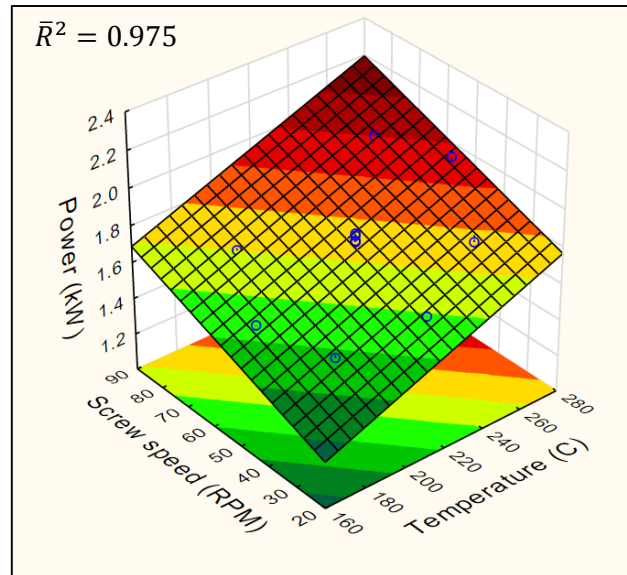


Figure 4.12: Surface plot of the power consumption model for the mechanical devulcanisation process.

As seen in Figure 4.12, the total power consumption tends to increase with increasing temperature and increasing screw speed. Therefore a higher specific energy consumption ( $\text{kWh}/\text{kg}_{\text{rubber}}$ ) could be expected at higher temperatures and screw speeds if the feed rate is kept constant, as was done in the mechanical devulcanisation experiment. From an economic standpoint it would be desirable to keep the specific energy consumption as low as possible without sacrificing product quality described by an appropriate sol fraction or crosslink density (Tao et al., 2013). Using the data generated in Section 4.2, the trade-off between technical and economic performance of the mechanical devulcanisation process with varying operating conditions could be investigated, as discussed in Chapter 5.

## 4.3 Mechanochemical devulcanisation

This section presents and discusses the results from the mechanochemical devulcanisation experiment as specified in Section 3.3.2. The mechanochemical devulcanisation process was similar to the mechanical devulcanisation process, except for the addition of a reclaiming agent (DPDS) dispersed in process oil, as well as operating at lower temperatures and a fixed screw speed of 30 RPM.

### 4.3.1 Sol fraction

The sol fraction of the rubber reclaimed by the mechanochemical method was measured as discussed in Section 3.4, but an additional correction was made for oil and reclaiming agent added prior to devulcanisation, resulting in an average value of  $e_N = 0.16$ . The experimental results are summarised in Table 4.7:

*Table 4.7: Sol fraction measurements of samples generated by mechanochemical devulcanisation*

Run	Temperature °C	DPDS Conc (g/kg)	Sol Fraction	
			Mean	SD
C1	150	17.5	0.014	0.001
C2	160	8.70	0.030	0.001
C3	160	26.3	0.035	0.015
C4	185	5.00	0.126	0.018
C5	185	17.5	0.230	0.013
C6	185	30.0	0.249	0.017
C7	210	8.70	0.405	0.020
C8	210	26.3	0.424	0.003
C9	220	17.5	0.453	0.003
C10	185	17.5	0.205	0.017
C11	185	17.5	0.265	0.010
C12	185	17.5	0.231	0.039

A Pareto chart (Figure 4.13) was generated using the data in Table 4.7, using a quadratic model including linear interaction between temperature and DPDS concentration.

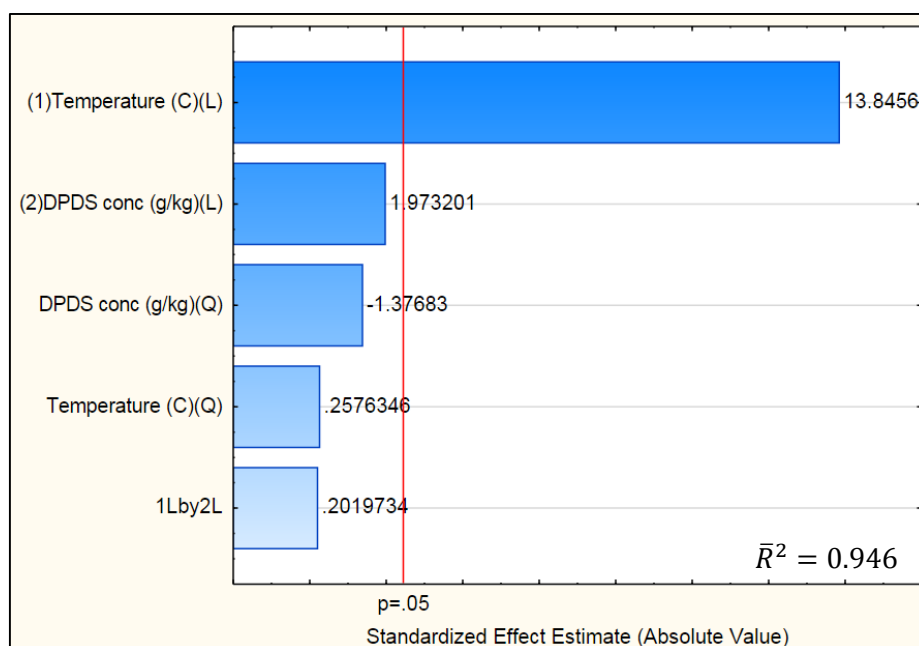


Figure 4.13: Pareto chart showing the statistical significance of various factors on modelling the sol fraction of samples generated by mechanochemical devulcanisation

The Pareto chart in Figure 4.13 suggests that only the linear temperature factor was significant in modelling the sol fraction of the samples produced by the mechanochemical devulcanisation experiment. The ANOVA calculation determined a reasonably low p-value of 0.096 for the linear DPDS concentration factor in the context of the quadratic model, which was deemed to be acceptable to justify the retention of the linear DPDS concentration factor in the revised model. The decision to retain the linear DPDS concentration factor was justified later by a higher adjusted coefficient of determination ( $\bar{R}^2$ ) for the model retaining the linear DPDS concentration factor over the model that rejected the linear DPDS concentration factor.

The final sol fraction model accepted for further analysis is given by Equation (4.11) below

$$S_{chem} = -1.12 + 6.99 \times 10^{-3} \cdot T + 2.79 \times 10^{-3} \cdot C_{DPDS} + \varepsilon \quad (4.11)$$

where  $S_{chem}$  is the sol fraction of the reclaimed rubber and  $C_{DPDS}$  is the concentration of DPDS (g/kg<sub>rubber</sub>).

A surface plot of the sol fraction model described by Equation (4.11) along with the experimental sol fraction measurements for the mechanochemical devulcanisation experiment appears in Figure 4.14 below.

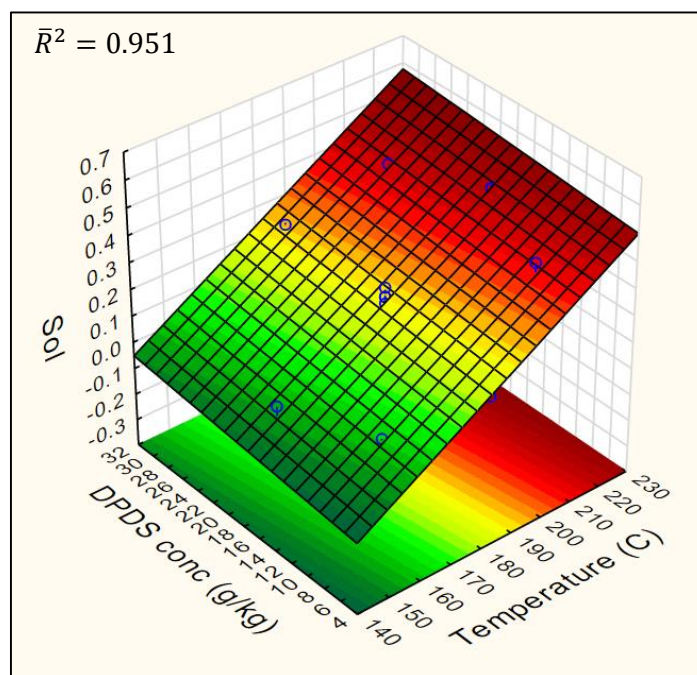


Figure 4.14: Surface plot of the sol fraction model for mechanochemical devulcanisation

The sol fraction was found to increase strongly with increasing temperature, but the effect of the DPDS concentration on the sol fraction was considerably weaker than that of temperature, as seen in Figure 4.14. Previous work has also shown a weak increase in the sol fraction with increasing disulfide concentration (Rajan et al., 2007) or unclear effects of varying disulfide concentration (De, Maiti & Adhikari, 1999). Other authors have also reported the strong influence of process temperature on the sol fraction of RR (Shi et al., 2013)

While the mechanical devulcanisation sol fraction model showed a tapering gradient of increasing sol fraction with increasing temperature (Figure 4.4), the mechanochemical devulcanisation sol fraction model did not show the same tapering behaviour within the experimental domain. The absence of the tapering behaviour in the case of mechanochemical devulcanisation is consistent with the postulation of devolatilisation at high temperature since the highest temperature used in mechanochemical devulcanisation was 220°C at which point there appears to be negligible devolatilisation shown by the TGA data in Figure 4.5.

Crosslink density analysis was also conducted on the reclaimed rubber samples generated by mechanochemical devulcanisation in order to augment the findings of the sol fraction analysis, as discussed in the following section.

### 4.3.2 Crosslink density

The crosslink density of each sample produced during the mechanochemical devulcanisation experiment was measured using the procedure described in Section 3.4 and the results thereof are summarised in Table 4.8.

*Table 4.8: Crosslink density measurements of samples from the mechanochemical devulcanisation experiment*

Run	Temperature °C	Screw speed (RPM)	Crosslink density (mol/g)x10 <sup>-6</sup>	
			Mean	SD
C1	150	17.5	79.3	0.51
C2	160	8.70	70.4	0.14
C3	160	26.3	63.6	2.10
C4	185	5.00	36.6	2.11
C5	185	17.5	23.5	0.95
C6	185	30.0	21.6	1.19
C7	210	8.70	13.3	0.73
C8	210	26.3	10.7	0.12
C9	220	17.5	07.8	0.07
C10	185	17.5	26.4	1.03
C11	185	17.5	21.3	1.18
C12	185	17.5	23.4	3.33

Statistical analysis of the crosslink density data in Table 4.8 was conducted in order to generate a response surface model for the purpose of predicting the crosslink density within the experimental domain of the experiment. As a first step toward simplifying the initial quadratic model, a Pareto chart (Figure 4.15) was generated from the data presented in Table 4.8.

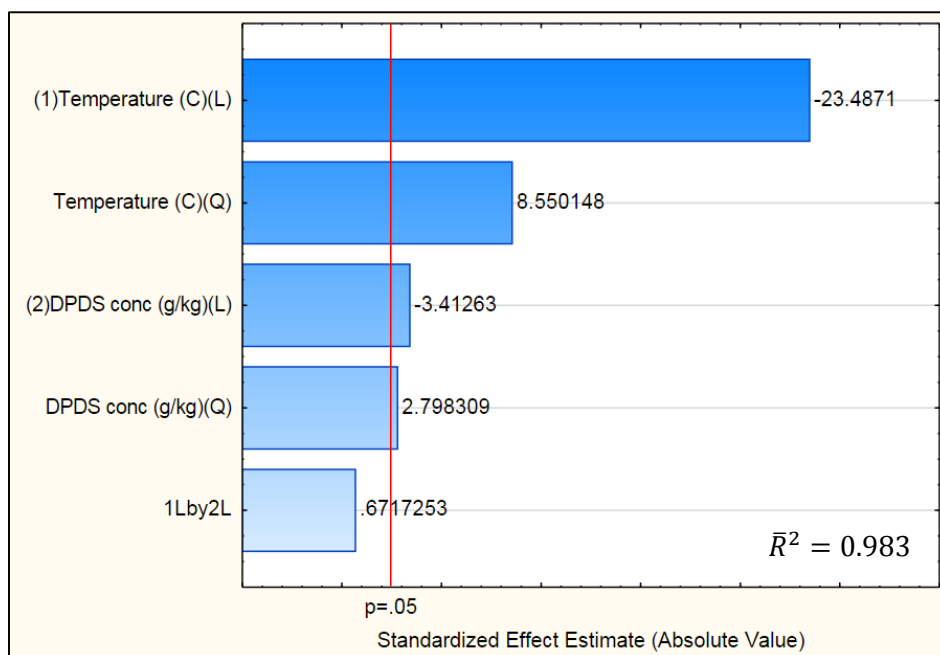


Figure 4.15: Pareto chart showing the significance of various factors on modelling the crosslink density of samples produced by mechanochemical devulcanisation

The Pareto chart in Figure 4.15 suggests that all factors except the linear interaction factor of the quadratic model are significant for predicting the crosslink density within the domain of the mechanochemical devulcanisation experiment. After removal of the linear DPDS and temperature interaction factor from the crosslink density model, the correlation coefficients were estimated and summarised in Equation (4.12)

$$v_{e,chem} = 8.42 \times 10^{-4} - 7.56 \times 10^{-6} \cdot T + 1.75 \times 10^{-8} \cdot T^2 - 2.01 \times 10^{-6} \cdot C_{DPDS} + 4.50 \times 10^{-8} \cdot C_{DPDS}^2 + \varepsilon \quad (4.12)$$

where  $v_{e,chem}$  is the crosslink density of the reclaimed rubber produced by mechanochemical devulcanisation, as predicted by the model generated from experimental measurements.

A surface plot of Equation (4.12) along with experimental measurements of the crosslink density at various reaction conditions of the mechanochemical devulcanisation experiment appears in Figure 4.16.

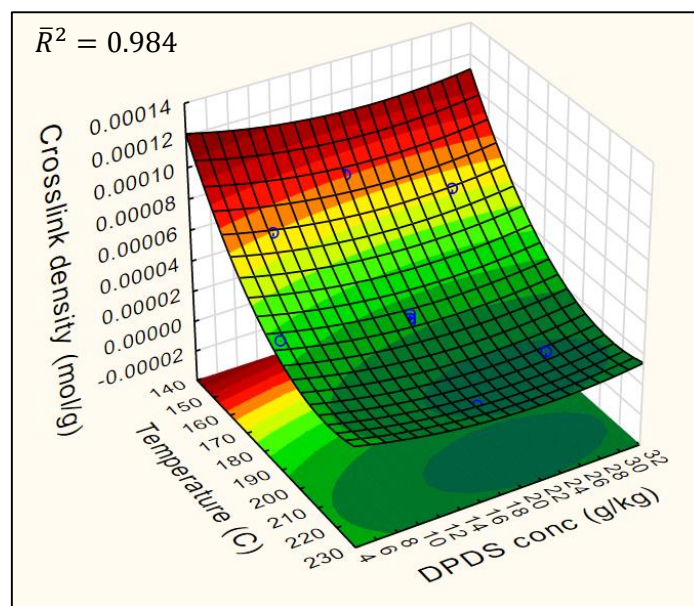


Figure 4.16: Surface plot of the crosslink density model for the mechanochemical devulcanisation process

The crosslink density model in Figure 4.16 shows that the crosslink density decreases strongly with increasing extruder barrel temperature and decreases weakly with increasing DPDS concentration. The decreased crosslink density indicates a higher extent of network breakdown at higher temperatures and higher DPDS concentration which is in agreement with the findings of the sol fraction analysis in Section 4.3.1.

Previous work has identified the strong influence of increasing process temperature on the reduction of crosslink density in mechanochemical devulcanisation conducted in both a milling process and a TSE process (Shi et al., 2013) which corroborates the experimental results shown in Figure 4.16. The weak effect of varying DPDS concentration on network breakdown shown in Figure 4.16 has also been observed previously (Rajan et al., 2007).

The crosslink density model shows a tangential approach to the theoretical minimum crosslink density of zero as the temperature increases beyond 200°C. The fact that the sol fraction model in Figure 4.14 does not show the tangential behaviour exhibited by the crosslink density model may seem contradictory, but this behaviour can be explained with the use of Horikx analysis.

### 4.3.3 Horikx analysis

The sol fraction and crosslink density data from the mechanochemical devulcanisation experiment were analysed further using a Horikx plot in order to give a qualitative indication of the selectivity for crosslink scission. A plot of experimental data from the mechanochemical devulcanisation experiment along with the theoretical Horikx curves appears in Figure 4.17 below.

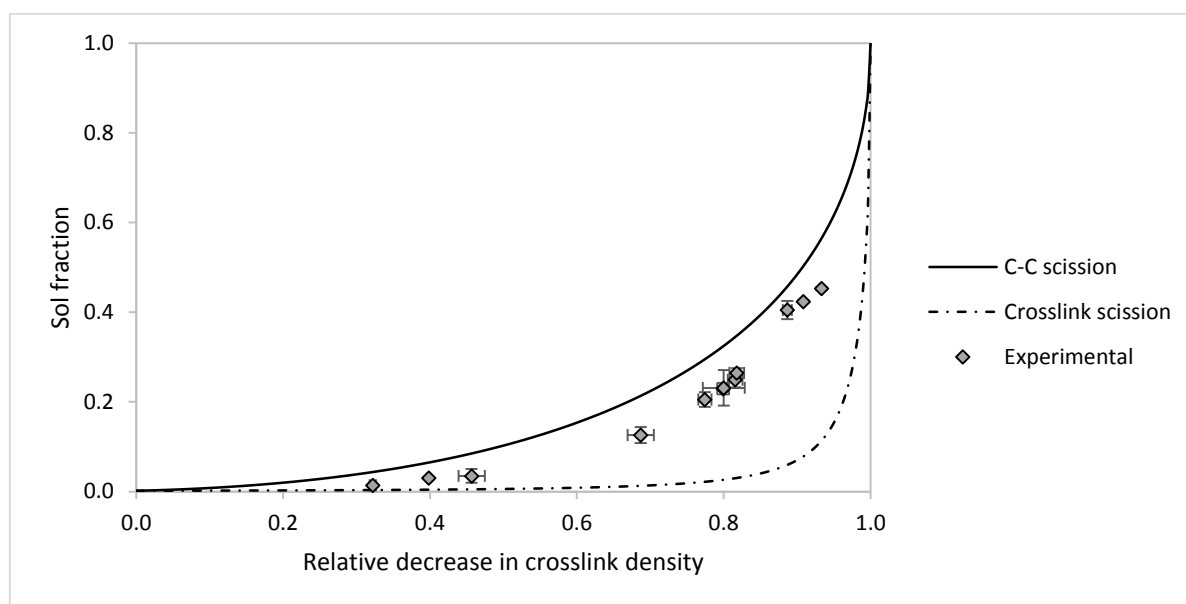


*Figure 4.17: Horikx plot of experimental data from the mechanochemical devulcanisation experiment along with theoretical curves*

In comparison with the Horikx plot of data from the mechanical devulcanisation experiment (Figure 4.8), the data generated by mechanochemical devulcanisation showed a higher selectivity for crosslink scission, as suggested by experimental points generally lying closer to the crosslink scission line in Figure 4.17. An improved selectivity for crosslink scission indicates better preservation of the chain length of the original rubber polymer chains during devulcanisation, which is expected to result in less reduction in mechanical properties of the reclaimed rubber, leading to a potentially higher-value product.

The improved selectivity is not necessarily due to the presence of DPDS, since even the point with the lowest concentration (5 g DPDS per kilogram of rubber) shows a similar selectivity to the point with the highest concentration (30 g/kg) generated at the same temperature. Although the relationship is unclear at this stage, it is possible that the process oil added along with the DPDS acts to swell the rubber network, and it is the swollen state rather than the DPDS that accounts for the increased selectivity.

The Horikx plot also shows that the experimental points with the highest degree of network breakdown (far right in Figure 4.17) show a reduction in crosslink density very close the theoretical maximum which explains the tangential behaviour in Figure 4.16. By comparison to the reduction in crosslink density, the sol fraction of the points representing a high degree of network breakdown (far right in Figure 4.17) is still quite far from the theoretical limit, thus explaining the absence of tangential behaviour in Figure 4.14.

While the work of Rajan and co-workers (Rajan et al., 2007) suggests a significant improvement in the selectivity for crosslink scission by comparison to typical Horikx plots for mechanical devulcanisation processes in the literature, their work used vulcanised NR in the form of rubber gloves, which is unlikely to yield similar results to typical GTR compounds. Furthermore, the assumptions used to generate the Horikx curves and experimental data could also have a strong influence on the interpretation and comparison of Horikx plots of mechanical and mechanochemical devulcanisation reported in the literature. The comparison of Figure 4.8 and Figure 4.17 gives a significantly more convincing argument for the increased selectivity of the mechanochemical devulcanisation process over mechanical devulcanisation, due to the consistency of materials, methods, calculations and assumptions used to generate the Horikx plots and experimental data in this thesis.

The work of Shi and co-workers (Shi et al., 2013) presents the results from LTSR (batch milling at 12°C) and HTSR (batch milling at 180°C), which can be seen as evidence of increasing selectivity for crosslink scission at lower processing temperatures.

Having described the RR properties at varying operating conditions, the power consumption data for the mechanical devulcanisation process is discussed in the following section.

### 4.3.4 Power consumption

The power consumption measurements for the mechanochemical devulcanisation experiment are summarised in Table 4.9 below. To the author's knowledge, there have been no reports in the literature regarding the power consumption of mechanochemical devulcanisation processes.

*Table 4.9: Power consumption measurements from the mechanochemical devulcanisation experiment*

Run	Temperature °C	DPDS Conc. (g/kg)	Power consumption (kW)		
			Extruder	Ancillary	Total
C1	150	17.5	0.854	0.450	1.304
C2	160	8.70	0.860	0.522	1.382
C3	160	26.3	0.878	0.516	1.394
C4	185	5.00	0.851	0.594	1.445
C5	185	17.5	0.831	0.595	1.426
C6	185	30.0	0.831	0.595	1.426
C7	210	8.70	0.809	0.700	1.509
C8	210	26.3	0.808	0.720	1.528
C9	220	17.5	0.785	0.736	1.522
C10	185	17.5	0.845	0.612	1.457
C11	185	17.5	0.832	0.600	1.432
C12	185	17.5	0.833	0.594	1.427

Previous studies (Rajan et al., 2005, 2007) have shown that the addition of higher quantities of disulfide reclaiming agents leads to higher extents of devulcanisation, which is associated with a reduced viscosity of the rubber. It was therefore expected that increasing the amount of DPDS added to the rubber would lead to a reduction in the torque required to drive the screw, and therefore to a lower power consumption at higher DPDS levels. As shown in Figure 4.18 below, the power consumption was found to be constant with varying DPDS concentration at fixed temperature.

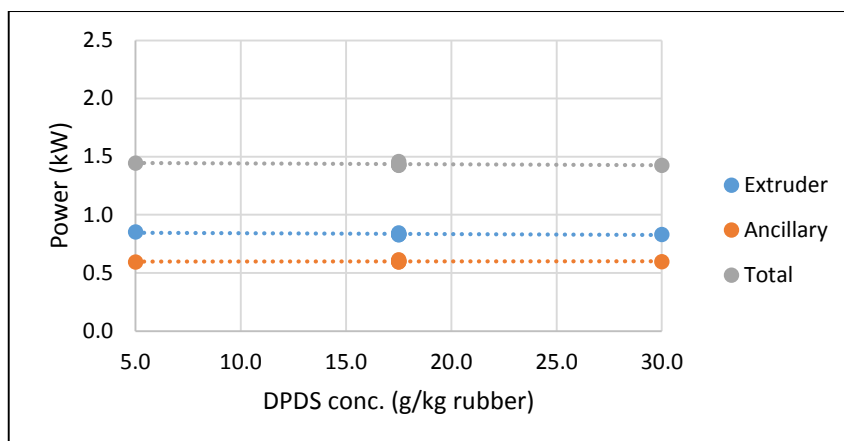


Figure 4.18: Power consumption of the mechanochemical devulcanisation experiments at constant temperature of 185°C

While varying DPDS concentration did not affect the power consumption of the mechanochemical devulcanisation process, increasing the barrel temperature at constant DPDS concentration caused a net increase in the total power consumption of the process as seen in Figure 4.19.

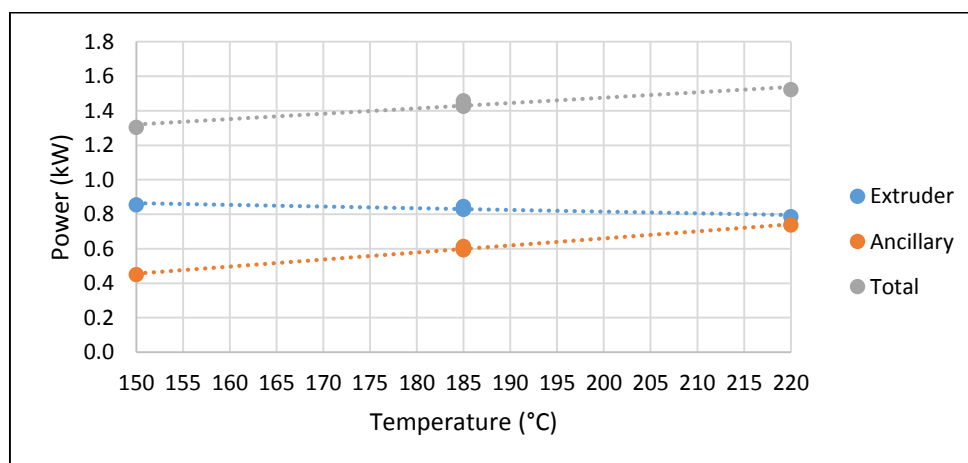


Figure 4.19: Power consumption of the mechanochemical devulcanisation at constant DPDS concentration of 17.5 g/kg rubber

Statistical analysis of the power consumption data in Table 4.9 was conducted in order to develop response surface models for use in further economic analysis. The initial model took account of linear and quadratic factors of the temperature and DPDS concentration, as well as a linear interaction factor between temperature and DPDS concentration. As shown in the Pareto chart in Figure 4.20 below, only the linear temperature factor was significant in modelling the power consumption within the range of experimental conditions investigated.

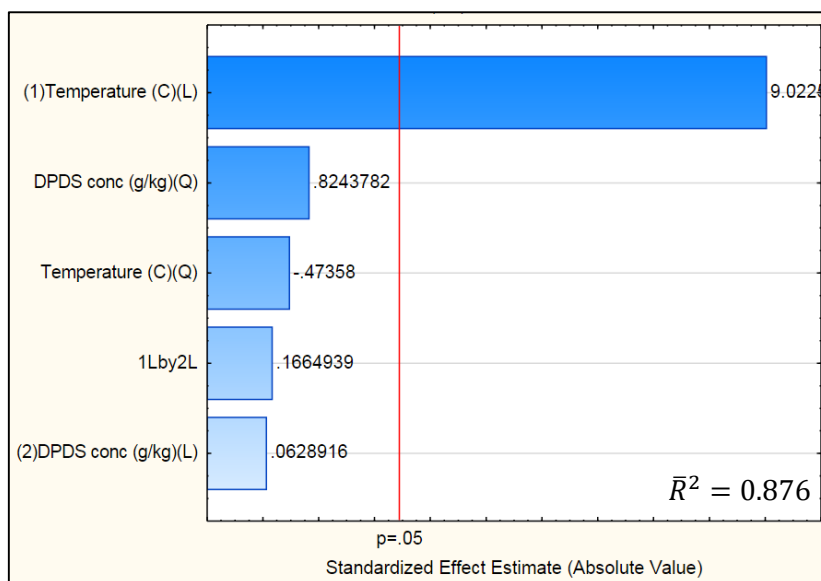


Figure 4.20: Pareto chart showing the statistical significance of the various factors of the full quadratic model in terms of modelling the power consumption of the mechanochemical devulcanisation process

After elimination of the insignificant factors, the reduced model was fitted to the data which resulted in the model described by Equation (4.13)

$$P_{chem} = 0.906 + 2.88 \times 10^{-3} \cdot T + \varepsilon \tag{4.13}$$

where  $P_{chem}$  is the total power consumption of the mechanochemical devulcanisation process.

A surface plot of Equation (4.13) along with experimental data appears in Figure 4.21.

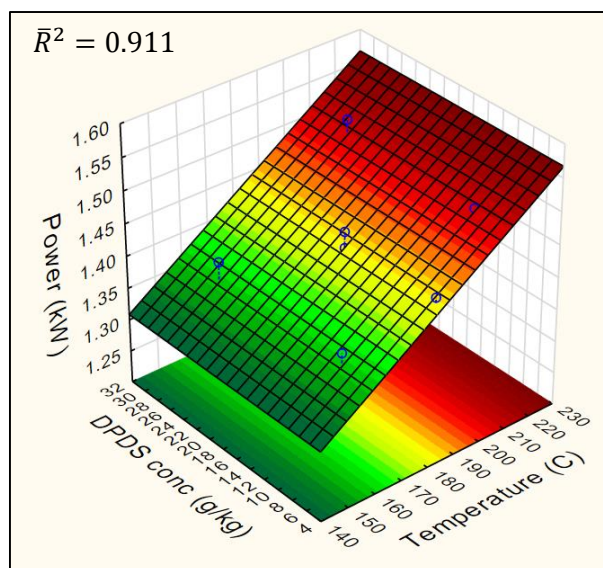


Figure 4.21: Surface plot of the power consumption model for mechanochemical devulcanisation process

As could be expected from the interpretation of Figure 4.18 and Figure 4.19, the power consumption of the mechanochemical devulcanisation depends only on the barrel temperature within the domain of the experimental work, as seen in Figure 4.21.

While the variation of the DPDS concentration has no apparent effect on the power consumption at constant temperature, higher concentrations have been shown to slightly increase the extent of network breakdown. The accelerating effect of the DPDS could lead to an economic trade-off between the costs of DPDS and power consumption, which is discussed in the economic analysis in Chapter 5

A summary of the findings from the experimental work is given in Section 4.4.

## 4.4 Concluding remarks

The major findings of the experimental portion of the work are as follows:

- The power consumption of the mechanical devulcanisation process increased linearly with increasing screw speed and barrel temperature, causing an overall higher specific energy consumption (kWh/kg) at higher temperatures and screw speeds at a constant feed rate.
- The power consumption of the mechanochemical devulcanisation process increased linearly with increasing temperature and was independent of DPDS concentration.
- The extent of network breakdown, as indicated by the sol fraction and crosslink density, increased strongly with increasing barrel temperature and increased weakly with increasing screw speed in the mechanical devulcanisation process.
- In the mechanochemical devulcanisation process, the extent of network breakdown increased strongly with increasing extruder barrel temperature, but increasing DPDS concentration only slightly increased the extent of network breakdown.
- The mechanochemical devulcanisation process exhibited a significantly higher selectivity for crosslink scission than the mechanical devulcanisation process.

## 5 Economic Analysis

Chapter 5 discusses the scale-up and economic analysis of the mechanical devulcanisation and mechanochemical devulcanisation processes based on the experimental results reported in Chapter 4.

The primary objective of the economic analysis is to compare the relative economic viability of mechanical devulcanisation versus mechanochemical devulcanisation at an industrial scale. The secondary objectives are to investigate the potential economies of scale of mechanical and mechanochemical devulcanisation processes as well as their sensitivity to changes in operating conditions, product specification and estimated economic parameters.

### 5.1 Economic modelling strategy

In order to achieve the objectives of the economic analysis, an economic model that could be manipulated as required was developed. The economic model was designed in such a way as to account for the influence of the devulcanisation operating parameters on the variable costs as well as the product characteristics of the reclaimed rubber. An overview of the proposed economic model is provided in Figure 5.1 below. The numbers in brackets refer to the sections of this thesis in which the components of the model are discussed.

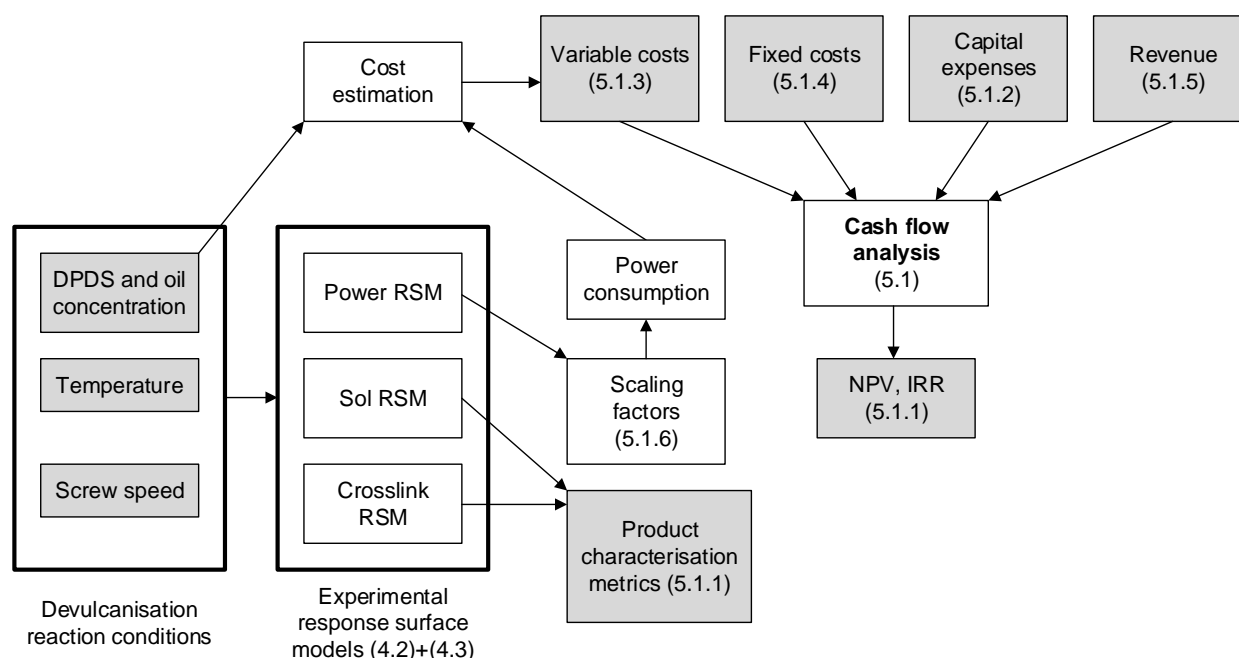


Figure 5.1: Overview of the economic model for a devulcanisation plant including the flow of numerical information (shaded blocks) through calculations (unshaded blocks)

Figure 5.1 shows how the power consumption models developed in Chapter 4 were used to predict power consumption of the scaled up process and this power consumption information then feeds into the variable cost estimates. The DPDS and oil concentrations were also used to calculate variable costs in the case of mechanochemical devulcanisation. The predicted variable costs were then used along with fixed cost and capital investment estimates in the generation of a discounted cash flow (DCF) analysis.

A discounted cash flow (DCF) analysis takes account of the time-value of money by discounting future cash flows so that they are representative of the present value of the future cash flows. The discount rate used in the DCF analysis depends on the costs of equity and debt taken to fund the project.

The DCF analysis in this study neglected the effects of inflation, also known as a real DCF analysis. The real discount rate used for the DCF analysis was 9.3%, assuming a debt-to-equity ratio of 60:40. The DCF analysis also applied a company tax rate of 28% (SARS, 2015) and assumed that fixed capital was depreciated at 10% per year using the straight line method. The DCF analysis was conducted over an assumed plant life of 15 years.

The sol fraction and crosslink density models were also included in the model in order to determine the product characteristics associated with the economic outcomes as a function of operating parameters. The sol fraction and crosslink density predictions as functions of operating conditions were assumed to be independent of scale, as discussed in Section 5.1.6.

Section 5.1 first describes the key performance indicators (5.1.1) required as outputs of the economic model and then proceeds to describe the methods used to estimate the capital costs (5.1.2), variable costs (5.1.3), fixed costs (5.1.4) and revenue (5.1.5) required as inputs for the economic analysis. Methods for scaling experimental data are also discussed in Section 5.1.6 before presenting the base case analysis in Section 5.2.

### 5.1.1 Key performance indicators

The internal rate of return (IRR) was selected as the primary indicator of economic viability of the devulcanisation processes. An IRR greater than the discount rate associated with the investment typically indicates that an investment could be profitable, although the IRR should be substantially greater than the discount rate in order to justify an investment in an unproven field (Couper, 2003).

The IRR is independent of scale, so a small-scale project and a large scale project might have the same IRR and can therefore not be distinguished from each other using the IRR. Therefore, the net present value (NPV) should also be reported in order to assist with the appropriate interpretation of the IRR.

The NPV and IRR depend on the selling price of the reclaimed rubber, which can be difficult to determine for a particular reclaimed rubber product due to the spectrum of properties associated with reclaimed rubber. In order to avoid attempting to determine a likely selling price as a function of reclaim properties, the minimum acceptable selling price (MASP) was defined as the selling price of the reclaimed rubber that would yield an acceptable economic return indicated by a targeted IRR hurdle rate. For the purposes of the economic analyses conducted in this thesis, the hurdle rate was chosen as 10%, which is just higher than the discount rate of 9.3%.

The MASP would probably be a function of operating parameters which will also affect product properties. Therefore the product properties were also considered to be important outputs of the economic model. The product properties that were reported were the sol fraction and the extent of devulcanisation based on the relative decrease in crosslink density calculated by Equation (2.2).

The estimation of the inputs required for the DCF analysis are discussed in Section 5.1.2 to Section 5.1.6.

### 5.1.2 Capital cost estimations (TCI)

The initial total capital investment (TCI) was calculated as the sum of major equipment costs, minor equipment costs, installation costs and working capital. A contingency factor of 10% was added to the expected total capital expenditure (Towler & Sinnott, 2013).

Major equipment included the purchase of the single-screw extruder(s) (SSE), the prices of which were determined by confidential quotations for a 100 mm extruder (R 500 000) and a 180 mm extruder (R 630 000) from the same supplier. Minor equipment costs were estimated at R 500 000 which included the purchase of a forklift and other minor equipment such as packaging equipment, assumed to be independent of the scale of the devulcanisation plant. In the case of mechanochemical devulcanisation, an additional 5% of the major equipment cost was added to the minor equipment cost in order to account for any mixing equipment required for feed preparation. Installation costs were estimated as 30% of the major equipment costs (Towler & Sinnott, 2013) to account for equipment erection, but excluding the costs of piping, civil engineering and other factors that are irrelevant for a devulcanisation plant.

A common engineering estimate of working capital for a chemical plant is 15-25% of the fixed capital investment (Perry, Green & Maloney, 1997), however this results in an unreasonably low estimate of working capital for a devulcanisation plant where the raw material costs are rather high in comparison to fixed capital costs, particularly in the case of mechanochemical devulcanisation. Working capital was therefore estimated as the sum of variable and fixed costs for two months' worth of operation (Towler & Sinnott, 2013).

The capital expenditure factors for the devulcanisation model are summarised in Table 5.1.

*Table 5.1: Estimated capital costs associated with a devulcanisation plant*

<b>Capital cost factor</b>	<b>Estimated value</b>	<b>Source</b>
Major equipment:		
<i>100 mm extruder</i>	R 500 000	Quote
<i>180 mm extruder</i>	R 630 000	Quote
Minor equipment:		
<i>Forklift + packaging</i>	R 500 000	Estimate
<i>Mixing equipment</i>	5% of major equipment	Estimate
Installation costs	30% of major equipment	(Towler & Sinnott, 2013)
Working capital	2 months' fixed and variable costs	(Towler & Sinnott, 2013)
Contingency	10% of estimated TCI	(Towler & Sinnott, 2013)

### 5.1.3 Variable cost estimations

The variable costs were calculated as the sum of the electrical power consumption and raw material costs. For the mechanical devulcanisation process the only raw material was the rubber crumb. The mechanochemical devulcanisation model included the costs of process oil (TDAE, as DAE is currently being phased out due to environmental concerns), loaded at 0.1 ton TDAE per ton of rubber, along with DPDS at variable concentration. The variable costs taken into account by the economic model are listed in Table 5.2 below.

*Table 5.2: Summary of variable costs associated with the devulcanisation economic model*

<b>Variable cost</b>	<b>Unit cost</b>	<b>Unit</b>	<b>Source</b>
Crumb	R 2 800	ton	Quote
TDAE	R 14 000	ton	Quote
DPDS	R 373	kg	Quote
Electricity	R 1.12	kWh	Estimate

### 5.1.4 Fixed costs

The annual fixed costs considered for the devulcanisation plant included labour, rent and maintenance of equipment. Annual labour costs were estimated using PayScale (PayScale, 2015) assuming three shifts per day. Each shift was assumed to include one extruder operator at R 160 000, one forklift driver at R 60 000 and one labourer at R 60 000. In addition to the shift workers, one manager was included in the labour costing at R 300 000 per year. Labour costs were assumed to be independent of the scale of the operation due to the high degree of automation of extrusion processes. Rent of an industrial warehouse was estimated to be R 600/m<sup>2</sup> per year, adjusted according to the scale of the operation as discussed in Appendix B. The annual equipment maintenance cost was estimated as 11% of the purchase cost of the major equipment (Levy & Carley, 1989), as discussed in Appendix B.

The fixed costs applied to the DCF analysis are summarised in Table 5.3 below.

*Table 5.3: Annual fixed costs associated with the devulcanisation economic model*

<b>Fixed cost</b>	<b>Annual cost</b>	<b>Source</b>
Labour	R 1 140 000	(PayScale, 2015)
Rent	R 600/m <sup>2</sup>	Estimate
Maintenance	11% of major equipment cost	(Levy & Carley, 1989)

### 5.1.5 Revenue

Revenue was calculated as the product of the selling price per ton of product and the annual production output. In the case of mechanical devulcanisation, the mass of reclaimed rubber produced each year was equal to the mass of rubber crumb fed to the process. In the mechanochemical devulcanisation process, the RR consisted of the devulcanised GTR along with the added TDAE oil and DPDS. The mass of DPDS added to the mechanochemical process was considered negligible in calculating the production output, thus the output was calculated as the mass of rubber crumb plus 10% for the TDAE added.

The GTR feed rate in the economic model was adjusted accordingly in order to ensure that the output of the mechanical devulcanisation process (GTR only) matched the output of the mechanochemical devulcanisation process (GTR plus TDAE), as was done for experimental work.

### 5.1.6 Scale-up considerations

Scale-up of extruder operations is not straightforward, depending on the material properties, design of the extruder, as well as desired functionality of the extrusion operation. Scale-up parameters have been described for common cases, as well as parameters specifically for heat transfer and mixing operations, as summarised in Table 5.4 below (Rauwendaal, 2014). These scale-up parameters typically attempt to specify the design and required combination of operating parameters of a larger extruder in such a way as to satisfy the requirements of a particular extrusion process such as a desired melt temperature, shear rate or residence time.

The properties and performance of the extruder are calculated according to Equation (5.1) (Rauwendaal, 2014):

$$\frac{K_L}{K_S} = \left(\frac{D_L}{D_S}\right)^\alpha \quad (5.1)$$

where  $D_S$  and  $D_L$  are the screw diameters of the small (known) extruder and large extruder, respectively;  $K_S$  is the property of the small extruder to be scaled up, and  $K_L$  is the same property predicted for the larger extruder according to the scaling parameter,  $\alpha$ , listed in Table 5.4 (Rauwendaal, 2014).

*Table 5.4: Summary of scale-up parameters for plastic extrusion processes*

<b>Extruder property</b>	<b>Common scale-up</b>	<b>Scale-up for heat transfer</b>	<b>Scale-up for mixing</b>
Channel depth	0.5	0.5	1
Screw speed	-0.5	-1	0
Output	2	1.5	3
Shear rate	0	-0.5	0
Tip speed	0.5	0	1
Residence time	0.5	1	0
Melting rate	1.75	1.5	2
Solids conveying	2	1.5	3
Screw power	2.5	1.5	3
Specific energy	0.5	0	0

In the case of devulcanisation, the rubber behaves differently from typical melt polymers due to its crosslinked nature, at least until the crosslinked polymer network has been broken down substantially. At present there has been little discussion, if any, about the scale-up of extrusion-based devulcanisation processes, which makes the scaling parameters of devulcanisation processes particularly difficult to predict without conducting detailed scale-up studies.

For the purposes of the economic analyses, the devulcanisation processes were scaled according to the parameters for scale-up for mixing, as shown in Table 5.4. Scale-up for mixing was selected since it offers constant shear rate and residence time which are speculated to be the important parameters for devulcanisation. It was also assumed that the technical performance of the larger extruder, in terms of product properties as a function of operating parameters, would be identical to the experimental results discussed in Chapter 4. The scaling of devulcanisation processes will need to be studied further to confirm this assumption, or to develop more reliable scaling methods.

Scale-up for mixing results in constant specific energy consumption (kWh/kg), which allows the power consumption models described in Section 4.2.4 and Section 4.3.4 to be linked to the DCF analysis as portrayed in the overview of the economic model in Figure 5.1.

## 5.2 Preliminary economic analysis

The purpose of the preliminary analysis was to give an initial comparison of the potential profitability between mechanical and mechanochemical devulcanisation as indicated by the MASP. The initial analysis assumed a small scale devulcanisation operation using a 100 mm single-screw extruder operating at a throughput of 416 ton/year, according to the scale-up method discussed in Section 5.1.6, using a throughput of 0.36 kg/h for the 19 mm lab-scale extruder used in experiments, and assuming continuous operation for 330 days per year.

The analysis was optimised by solving for the MASP by varying the operating parameters subject to the constraints of the IRR being fixed at 10%, and the extent of devulcanisation being fixed at 75%, which has been suggested as a good estimate for optimum RR properties (Tao et al., 2013). The operating parameters were also constrained to within the experimental domain in order to avoid extrapolation errors in the experimental response surface models.

The results of the preliminary analysis are summarised in Table 5.5.

*Table 5.5: Summary of the preliminary economic analysis of a devulcanisation plant*

<b>Parameter</b>	<b>Mechanical</b>	<b>Mechanochemical</b>
Fixed capital	R 1 150 000	R 1 175 000
Working capital	R 752 000	R 916 000
TCl contingency	R 190 000	R 209 000
Annual fixed costs	R 1 315 000	R 1 315 000
Annual variable costs	R 3 198 000	R 4 178 000
NPV (15 years)	R 92 700	R 102 000
IRR (15 years)	10%	10%
MASP	R 11 600 per ton	R 14 100 per ton
Payback period	8 years	8 years
Temperature (°C)	220.6	192.3
Screw speed (RPM)	30	30
TDAE loading (ton/ton)	0	0.1
DPDS loading (kg/ton)	0	5
Sol fraction	30.2%	23.8%
Extent of devulcanisation	75%	75%

As seen in Table 5.5, the MASP of reclaimed rubber is substantially higher in the case of mechanochemical devulcanisation. The higher MASP for mechanochemical devulcanisation could make mechanical devulcanisation a more attractive investment, unless a higher perceived value of the reclaimed rubber can be linked to the higher selectivity for crosslink scission exhibited by the mechanochemical devulcanisation process discussed in Section 4.4.

Besides the difference in MASP between mechanical devulcanisation and mechanochemical devulcanisation, both processes exhibit MASPs higher than typical reclaimed rubber prices which vary between R 6 000 and R 10 000 based on quotes received from suppliers in India and South Africa.

The high MASP for the base case analysis is not too surprising considering the scale of the base case analysis was approximately 416 tons per year, and the MASP is expected to drop significantly with increasing scale as discussed in Section 5.3.

### 5.3 Effect of scale on MASP

The scale-up analysis was conducted as described in the preliminary analysis (Section 5.2) with the exception of increasing the scale of the operation for each iteration. The scale of the operation was varied by increasing the number and size of the extruders, as shown in Table 5.6 below. Iterations 1-4 use a varying number of 100 mm extruders and iterations 5-7 use a varying number of 180 mm extruders.

*Table 5.6: Throughput of devulcanisation processes with varying extruder configurations*

<b>Iteration</b>	<b>Extruder screw diameter</b>	<b>Number of extruders</b>	<b>Throughput (ton/year)</b>
1	100 mm	1	416
2	100 mm	2	831
3	100 mm	3	1247
4	100 mm	4	1663
5	180 mm	1	2424
6	180 mm	2	4848
7	180 mm	3	7273

The 7 extruder configurations in Table 5.6 were applied to the mechanical devulcanisation and mechanochemical devulcanisation models in order to test the response of each process to variation in scale. The results of the analysis are listed in Table 5.7 and Table 5.8 for mechanical devulcanisation and mechanochemical devulcanisation, respectively.

*Table 5.7: Effect of scale on MASP at 10% IRR for the mechanical devulcanisation process*

<b>Iteration</b>	<b>TCI</b>	<b>Variable costs per ton</b>	<b>MASP per ton</b>
1	R 2 092 000	R 7 693	R 11 600
2	R 3 426 000	R 7 693	R 10 100
3	R 4 759 000	R 7 693	R 9 590
4	R 6 092 000	R 7 693	R 9 340
5	R 5 120 000	R 7 693	R 8 560
6	R 9 481 000	R 7 693	R 8 300
7	R 13 843 000	R 7 693	R 8 200

*Table 5.8: Effect of scale on MASP at 10% IRR for the mechanochemical devulcanisation process*

<b>Iteration</b>	<b>TCI</b>	<b>Variable costs per ton</b>	<b>MASP per ton</b>
1	R 2 300 000	R 10 051	R 14 067
2	R 3 840 000	R 10 051	R 12 555
3	R 5 381 000	R 10 051	R 12 051
4	R 6 921 000	R 10 051	R 11 800
5	R 6 203 000	R 10 051	R 11 000
6	R 11 648 000	R 10 051	R 10 750
7	R 17 092 000	R 10 051	R 10 663

Graphical representations of the MASP for mechanical devulcanisation and mechanochemical devulcanisation as a function of throughput appear in Figure 5.2 and Figure 5.3, respectively.

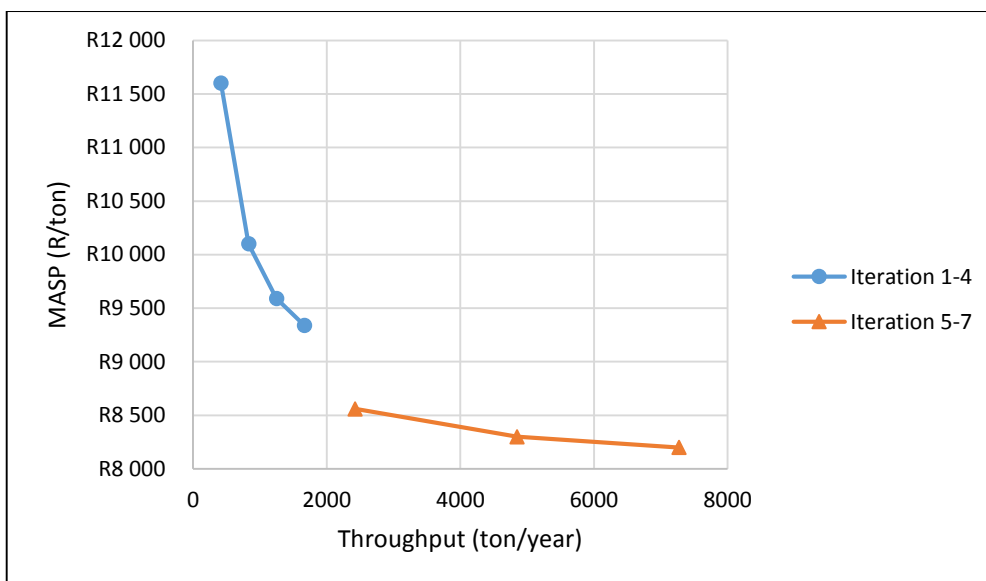


Figure 5.2: The MASP as a function of increasing throughput for mechanical devulcanisation

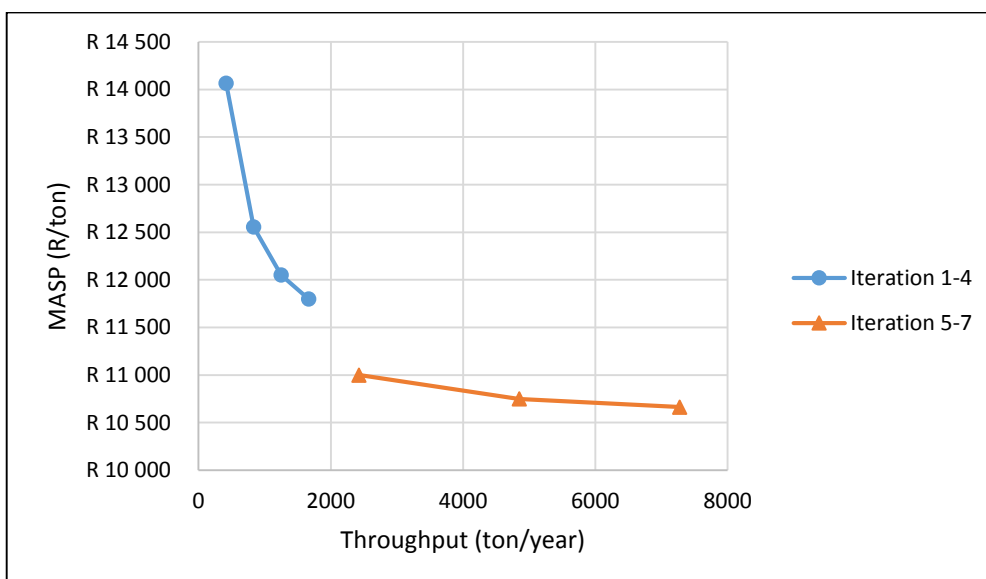


Figure 5.3: The MASP as a function of increasing throughput for mechanochemical devulcanisation

Figure 5.2 and Figure 5.3 show that there was a general trend of decreasing MASP with increasing scale for both mechanical devulcanisation and mechanochemical devulcanisation, reflecting the economies of scale related to the dilution of fixed costs over a higher throughput. There was a distinct drop in MASP between iteration 4 and iteration 5 which suggests that scaling up by using larger extruders is more economical than using multiple smaller extruders, which can be attributed to the large increase in throughput relative to the small increase in major equipment costs from small to larger extruders as discussed in Section 5.1.6.

Increasing the number of 100 mm extruders (iteration 1-4) caused a rapid drop in MASP while the effect of increasing the number of 180 mm extruders (iteration 5-8) was substantially weaker. The weaker effect of iterations 5-7 on the MASP was attributed to the MASP approaching the lowest value allowed by the constant value of the variable costs per ton of reclaimed rubber produced, as seen in Table 5.7 and Table 5.8. In reality, raw material prices are likely to vary with the magnitude and frequency of purchases which is likely to have an impact on the MASP.

During the preliminary analysis and scale-up analysis the operating parameters of the devulcanisation processes remained constant along with product properties due to the values of the operating parameters listed in Table 5.5 apparently being the most economical for achieving the specified extent of devulcanisation. The following analysis in Section 5.4 relaxes the constraint on the extent of devulcanisation in order to investigate the effect of varying operating parameters on the MASP and associated product properties.

## 5.4 Economic trade-off between operating parameters

The MASP of rubber reclaimed by mechanical devulcanisation and mechanochemical devulcanisation, subject to a specified extent of devulcanisation, was reached at the minimum value of screw speed for mechanical devulcanisation and minimum DPDS concentration for mechanochemical devulcanisation. The purpose of the present analysis is to clarify the poor economic performance at higher screw speed and higher DPDS concentration.

This analysis was conducted using iteration 5 in Table 5.6 defining the scale of the operation, since iteration 5 yields the lowest MASP without exceeding the typical production capacity of tyre crumbing plants in South Africa. As before, the IRR hurdle rate was kept constant at 10%, but this time the extent of devulcanisation was calculated along with the MASP by specifying the operating parameters. In the case of mechanical devulcanisation the temperature was varied at a constant screw speed of 30 RPM followed by varying the screw speed at a constant temperature of 200°C. For mechanochemical devulcanisation the temperature was varied at a constant DPDS concentration of 7 g/kg followed by varying the DPDS concentration at constant temperature of 180°C.

Results of the analysis appear in Figure 5.4 and Figure 5.5 below.

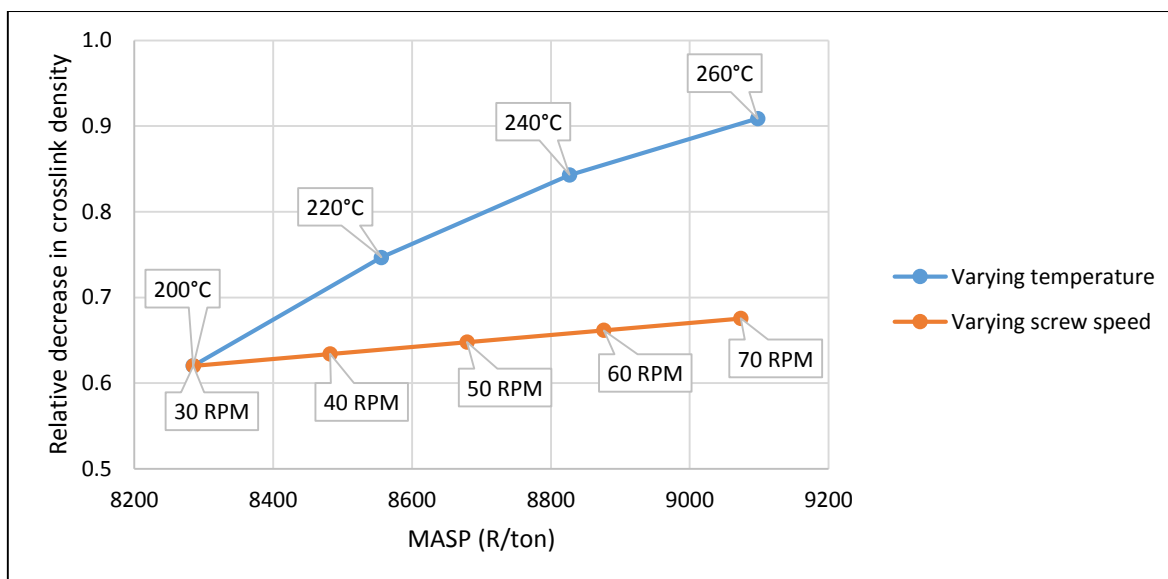


Figure 5.4: Effect of varying temperature and screw speed on the MASP and associated extent of devulcanisation for mechanical devulcanisation

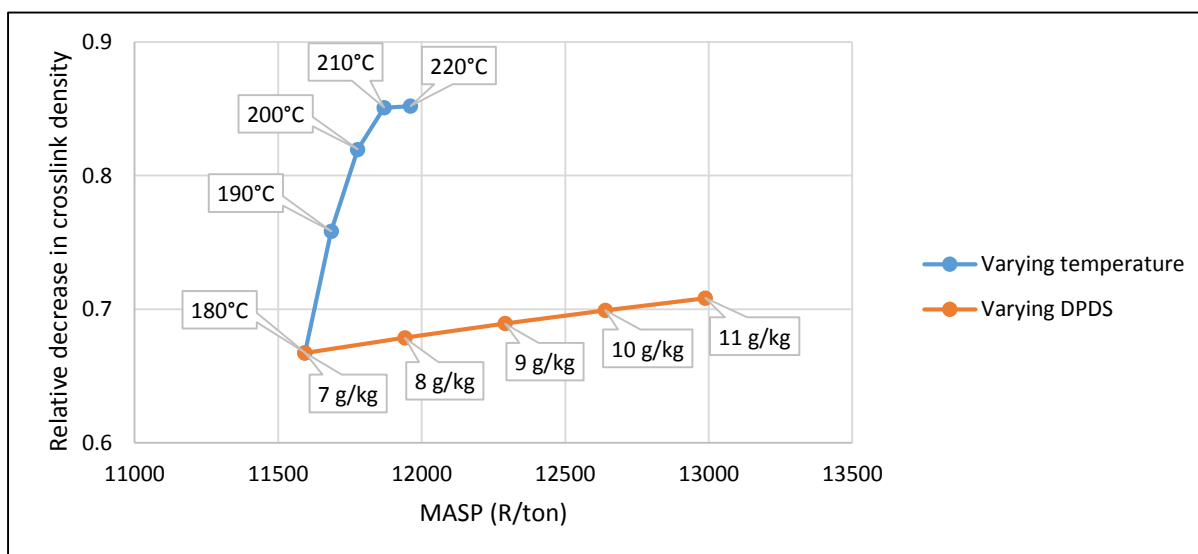


Figure 5.5: Effect of varying temperature and DPDS concentration on the MASP and associated extent of devulcanisation for mechanochemical devulcanisation

As discussed in Section 4.2, the weak effect of screw speed on network breakdown was expected to give rise to a situation where the screw speed should be kept as low as possible and the extent of devulcanisation should be controlled by barrel temperature. Figure 5.4 agrees with the statements made in Section 4.2, since attempting to increase the extent of devulcanisation by increasing the screw speed causes an increase in MASP but not much change in the extent of devulcanisation. Increasing the temperature also caused an increase

in MASP, but the effect of higher temperature on the extent of devulcanisation was greater than that of increasing screw speed.

In the case of the mechanochemical devulcanisation process model, even a small increase in the DPDS concentration caused a very strong increase in MASP and a comparatively small increase in the extent of devulcanisation, as shown in Figure 5.5. By comparison to the effect of DPDS concentration, the increase in temperature resulted in a very small increase in MASP and a very strong increase in the extent of devulcanisation.

The main conclusion to be drawn from Figure 5.4 and Figure 5.5 is that increasing the temperature of the devulcanisation processes is a more economical approach to increasing the extent of devulcanisation in comparison to varying screw speed and DPDS concentration.

Up to this point, the analyses have determined the MASP required to achieve an IRR of 10%. The actual selling price achieved for the RR product is likely to be strongly influenced by marketing and fluctuating prices of virgin rubber. The effect of uncertainties in the selling price for RR and other major components of the economic model are investigated and discussed in Section 5.5

## 5.5 Sensitivity analysis

The major factors influencing the outcome of the economic analysis were the selling price of the RR, fixed capital costs, fixed costs, variable costs and production rate (throughput). The deviation of actual values from estimations of these parameters could affect the economic performance of the plant, and it is important to identify the factors which could have a negative impact on the viability of the plant (Towler & Sinnott, 2013).

In order to identify critical economic parameters of the devulcanisation model, a sensitivity analysis was conducted by varying the major economic parameters of the model around their respective base case values, as summarised in Table 5.9 below. The sensitivity of the model to changes in the economic parameters was indicated by the strength of the resultant deviation of the IRR from the base case value. Iteration 5 in Table 5.6 was used to define the scale of the plant, and the extent of devulcanisation was fixed at 75% achieved by the operating parameters identified in Table 5.5.

Table 5.9: Base case values of the major economic parameters for the sensitivity analysis

Parameter	Base case value	
	Mechanical	Mechanochemical
RR selling price per ton	R 8 564	R 11 009
Fixed capital	R 1 319 000	R 1 350 000
Annual fixed costs	R 1 365 000	R 1 365 000
Annual variable costs	R 18 649 000	R 24 368 000
Throughput	2424 ton/year	2424 ton/year
Base case IRR	10%	10%

The results of the sensitivity analyses are summarised in Figure 5.6 and Figure 5.7 for mechanical devulcanisation mechanochemical devulcanisation, respectively.

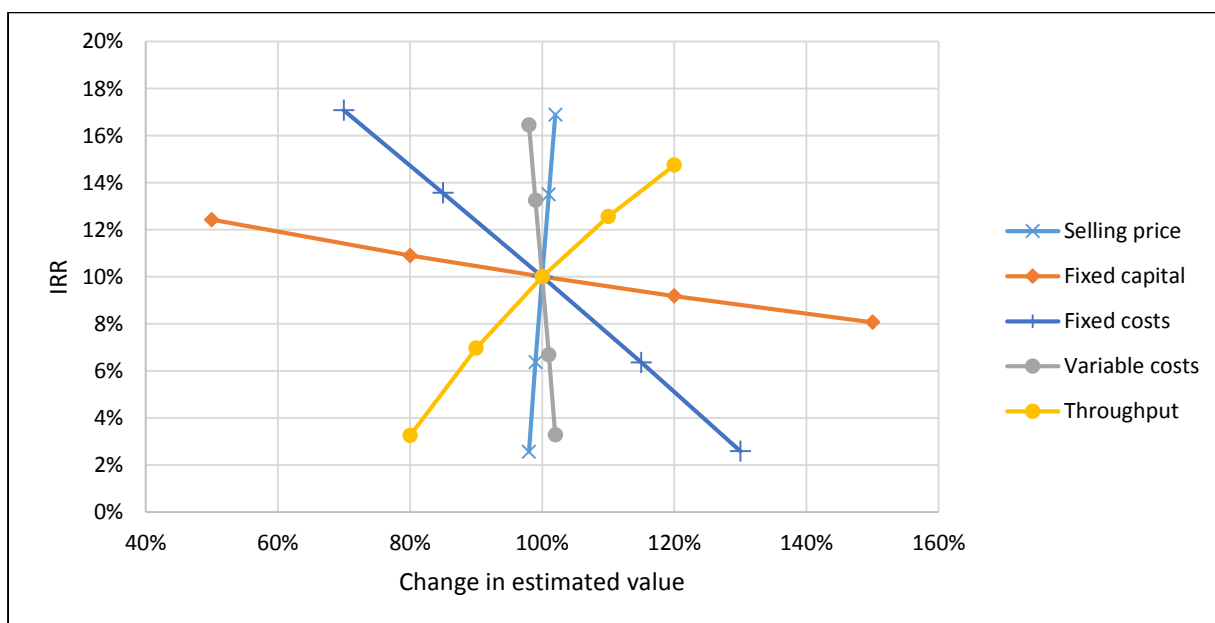


Figure 5.6: Sensitivity of the mechanical devulcanisation model to changes in economic factors

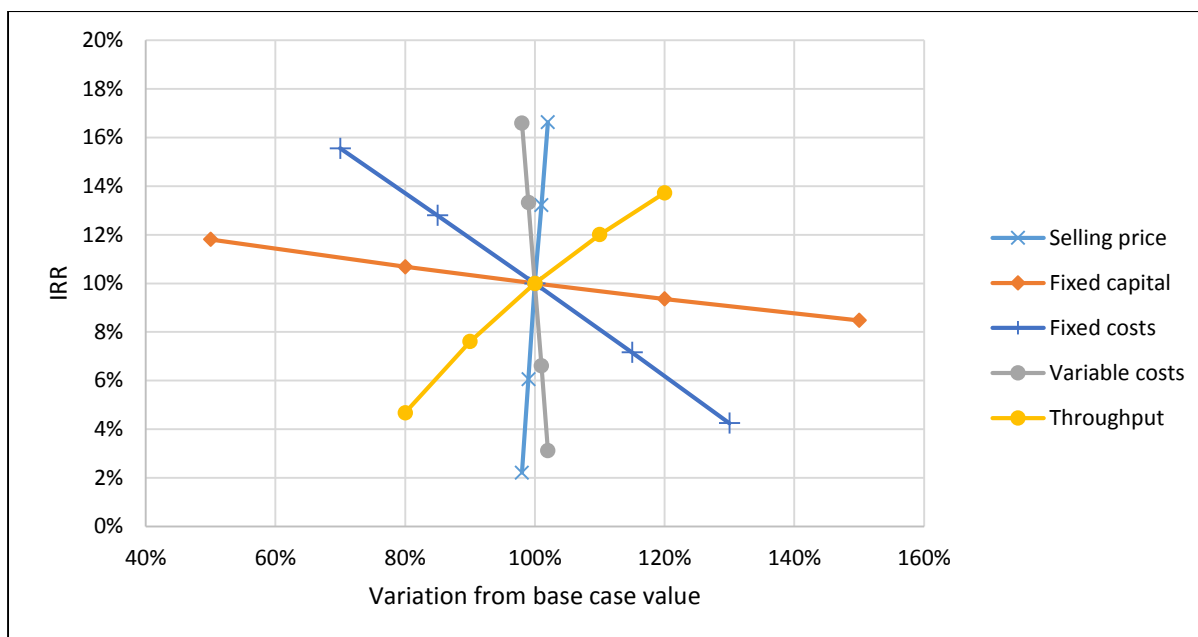


Figure 5.7: Sensitivity of the mechanochemical devulcanisation model to changes in economic parameters

Figure 5.6 and Figure 5.7 show no major difference between the sensitivity of the mechanical devulcanisation and mechanochemical devulcanisation processes. Both processes show very low sensitivity to fixed capital costs, probably as a result of the low capital costs in comparison to the operating costs. The sensitivity of the devulcanisation processes to variations in the production throughput and fixed costs is significantly higher than the sensitivity to fixed capital costs. The sensitivities of both devulcanisation processes to variations in selling price and variable costs are very high (critical factors), which could be an indication of low profit margins and high risk for the investment due to the high uncertainty of the selling price as a function of RR properties.

Due to the high sensitivity of the devulcanisation economic models to the variable costs, as shown in Figure 5.6 and Figure 5.7, it was deemed necessary to conduct a further investigation into the factors contributing to the total variable costs in order to identify the dominant factors (Towler & Sinnott, 2013). The variable costs were varied independently around their respective base case values, as summarised in Table 5.10, while constraining all other economic parameters to the base case values summarised in Table 5.9.

Table 5.10: Base case values for variable cost sensitivity analysis

Variable cost	Base case value	Unit
Crumb	R 2 800	ton
TDAE	R 14 000	ton
DPDS	R 373	kg
Electricity	R 1.12	kWh

The results of the variable cost sensitivity analysis are summarised in Figure 5.8 and Figure 5.9 for mechanical devulcanisation and mechanochemical devulcanisation, respectively.

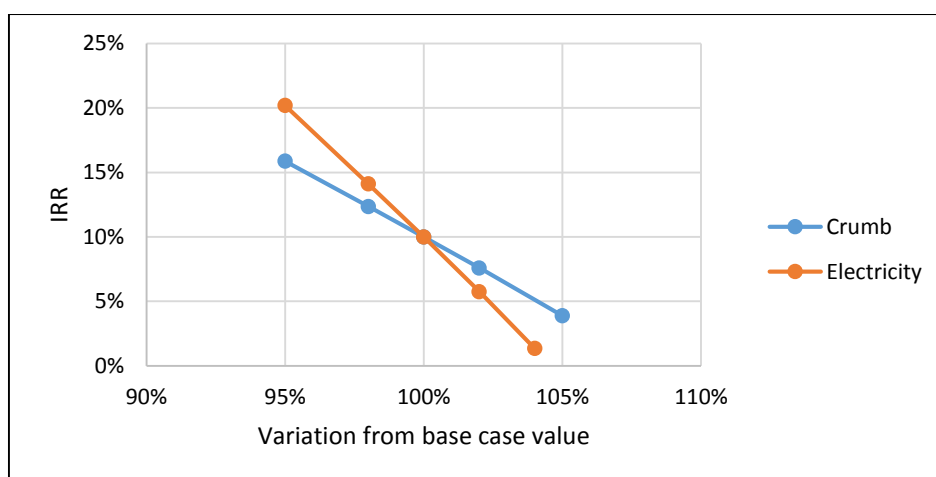


Figure 5.8: Sensitivity of IRR to variation of variable cost factors in the case of mechanical devulcanisation

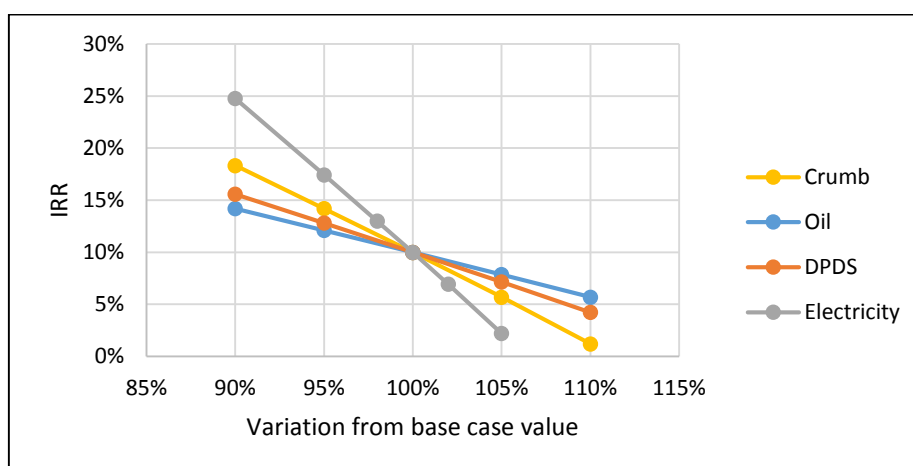


Figure 5.9: Sensitivity of IRR to variation of variable cost factors in the case of mechanochemical devulcanisation

Based on the results of the variable cost sensitivity analyses presented in Figure 5.8 and Figure 5.9, variation of the electrical power cost has the strongest effect on the potential profitability of both the mechanical and mechanochemical devulcanisation processes. The strong influence of the electrical power cost on the IRR of a devulcanisation process raises two major concerns regarding the economic viability of devulcanisation as an appropriate technology for rubber recycling in South Africa. Firstly, Eskom electricity prices have been increasing rapidly over the past few years in an attempt to recover capital costs of new generation capacity (Eskom, 2015), which could lead to a poor economic climate for devulcanisation processes in South Africa in the near future. Secondly, uncertainty in the predicted specific energy consumption used in the devulcanisation model creates further uncertainty around the potential viability of devulcanisation processes in South Africa and in general.

Since the economic performance of devulcanisation processes depend so strongly on power consumption, the lack of reports of power consumption of devulcanisation processes in the literature can be seen as a major shortcoming in the devulcanisation field. Future work in the field should focus on reporting power consumption at various scales and operating conditions in order to develop a clearer understanding of the power consumption of devulcanisation processes, and how the energy-efficiency of devulcanisation processes could be improved.

While variation of the electrical power cost has been shown to have the strongest effect on the IRR of the model, all of the other variable costs also show strong influences on the IRR, as shown in Figure 5.8 and Figure 5.9. The high sensitivity of the devulcanisation processes could indicate a high risk of investing in devulcanisation technology. Therefore, future efforts should focus on identifying more cost-effective modifications to the devulcanisation processes investigated in this thesis.

## 5.6 Conclusions from economic analysis

The following subsections summarise the important findings of the economic analyses described in this chapter.

### 5.6.1 Mechanical vs mechanochemical devulcanisation

A major finding of the economic analysis was that the mechanochemical devulcanisation process demanded a substantially higher selling price of the RR in order to achieve a satisfactory IRR, when compared to the mechanical devulcanisation process. Typical values of the MASP per ton of the RR were R 8 600 for mechanical devulcanisation and R 11 000 for mechanochemical devulcanisation which are comparable with typical selling prices of RR currently on the market (R 6 000 – R 10 000). In the absence of significant technical advantages of the rubber reclaimed by mechanochemical devulcanisation, which would result in a different market value, the more cost-effective mechanical devulcanisation process is more likely to be profitable.

### 5.6.2 Economies of scale

Both devulcanisation processes responded well to increased scale of the operation, up to a scale of approximately 2500 ton/year, beyond which any further increase in scale appeared to offer no further benefit under the assumed absence of improved energy-efficiency and discounts on raw material costs at the scales investigated.

### 5.6.3 Effect of operating conditions on economics

The higher operating costs associated with using a higher screw speed in the mechanical devulcanisation process were found to be outweighed by the benefits in terms of extent of devulcanisation. Instead of manipulating screw speed to increase the extent of devulcanisation, increasing the temperature was found to be a more economical method of increasing the extent of devulcanisation. It should be noted that the possible variation of throughput with screw speed was not investigated in this study.

Increasing DPDS concentration was found to cause a strong increase in the MASP of the RR produced by the mechanochemical devulcanisation process, while providing little increase in the extent of devulcanisation. Increasing the operating temperature of the mechanochemical devulcanisation process was found to be a far more economical means of increasing the extent of devulcanisation.

#### 5.6.4 Economic sensitivity

At a designed throughput of approximately 2500 ton/year, both devulcanisation processes showed critical sensitivity of the IRR to the product selling price and variable costs. Sensitivity to variation of fixed costs and throughput was also significant, while the processes showed low sensitivity to variation in fixed capital costs.

The most important parameter influencing the potential viability of devulcanisation plants in South Africa was identified as the electrical power consumption costs.

## 6 Conclusions and Recommendations

The following chapter provides a summary of the important conclusions drawn from the experimental work reported in Chapter 4 and the economic analysis presented in Chapter 5. The conclusions are presented in Section 6.1, followed by recommendations for further work in Section 6.2.

### 6.1 Conclusions

#### 6.1.1 Identification of promising devulcanisation technologies

Of the seven major devulcanisation processes identified in the literature, mechanical, mechanochemical and ultrasonic devulcanisation seem to show the most potential for industrial application at present or in the near future. Older processes such as thermal devulcanisation have a proven track record, but are likely to be replaced by more modern processes due to the poor mechanical properties of reclaimed rubber produced by older technologies. This study, therefore, focused on investigating the technical and economic feasibility of mechanical and mechanochemical devulcanisation processes.

#### 6.1.2 Technical performance modelling

Both the mechanical and the mechanochemical devulcanisation processes produced reclaimed rubber with varying properties depending on the operating conditions of each process. In both of the investigated devulcanisation processes, the extent of rubber network breakdown, measured by the sol fraction and change in crosslink density, tended to increase strongly with increasing temperature of the extruder barrel. The secondary independent variables for the mechanical devulcanisation process (screw speed) and mechanochemical devulcanisation process (DPDS concentration) also caused an increase in the extent of network breakdown, although the effects of the secondary variables were far weaker than the effect of temperature on the extent of network breakdown.

The power consumption of the mechanical devulcanisation process increased linearly with increasing temperature and increasing screw speed. The power consumption of the mechanochemical devulcanisation process was independent of DPDS concentration, but increased linearly with increasing temperature.

### 6.1.3 Techno-economic comparison

In general, the mechanical devulcanisation process was found to be more economical than the mechanochemical devulcanisation process due to the high cost of the process oil and DPDS used in the mechanochemical devulcanisation process.

Assuming an IRR hurdle rate of 10% for a devulcanisation plant operating at approximately 2400 tons per year, the mechanical devulcanisation plant would require a minimum selling price of R 8 600 per ton of RR in order to be profitable. On the other hand, the mechanochemical devulcanisation process required a minimum selling price of R 11 000 per ton of RR, assuming the same IRR and extent of devulcanisation achieved by the mechanical devulcanisation plant.

Variation of the screw speed in mechanical devulcanisation process showed an insignificant effect on the extent of devulcanisation in comparison to the associated increase in operating costs. For the mechanochemical devulcanisation process, the concentration of DPDS was found to have a very strong effect on the MASP while offering very little benefit in terms of increasing the extent of devulcanisation. Therefore, the extrusion temperature was found to be the most cost-effective method for achieving a desired extent of devulcanisation in both devulcanisation technologies.

A sensitivity analysis revealed the selling price and variable costs to be critical factors to the potential economic viability of extrusion-based devulcanisation technologies in South Africa. A more detailed sensitivity analysis of the variable costs suggested that the electrical power consumption was the most important parameter affecting the profitability of the devulcanisation processes.

In general, the mechanochemical devulcanisation process achieved a greater selectivity for crosslink scission than the mechanical devulcanisation process. The improved selectivity of the mechanochemical devulcanisation process could lead to a higher perceived value of the reclaimed rubber than that produced by mechanical devulcanisation, although further market research will be required in order to identify which of the two technologies would be more desirable from an economic perspective.

## 6.2 Recommendations

The following recommendations are based on the main findings of the experimental work and economic analyses presented in Chapter 4 and Chapter 5 respectively. The recommendations made in Section 6.2.1 are extensions and improvements to the experimental work conducted as discussed in this thesis while Section 6.2.2 and Section 6.2.3 recommend novel research that could lead to a better understanding of devulcanisation processes in general.

### 6.2.1 Experimental work

The findings of the mechanochemical devulcanisation experiment showed that the costs of higher concentrations of DPDS outweigh the expected benefits in terms of increasing the extent of network breakdown, at least within the experimental domain. Therefore, the mechanochemical devulcanisation experiments should be repeated with lower DPDS concentrations varying from 0 g/kg to 5 g/kg in order to investigate the possibility of identifying a DPDS concentration beyond which any further addition results in diminishing benefits of adding DPDS.

The reclaimed rubber produced by mechanochemical devulcanisation showed a higher selectivity for crosslink scission, which was tentatively attributed to the presence of process oil due to varying DPDS concentration having no apparent effect on the selectivity for crosslink scission. Varying the quantity of process oil added to the rubber would help with conclusive identification of whether the DPDS or process oil is responsible for the increased selectivity for crosslink scission in the mechanochemical devulcanisation process.

Higher extruder screw speeds led to higher specific power consumption in the mechanical devulcanisation process due to the feed rate being kept constant in the experimental work. It is expected that higher feed rates would be possible at higher extruder screw speeds, which may result in an overall reduction in specific energy consumption at higher screw speeds. Thus, studying the effect of varying screw speed and feed rate on the power consumption and associated product properties of extrusion-based devulcanisation processes in general could yield useful information for improving the energy-efficiency of both mechanical and mechanochemical devulcanisation processes.

## 6.2.2 Scale-up methodology

The scaling of plastic extrusion processes is conducted according to the desired functionality of the extrusion process as well as the properties of the material being extruded. The scaling method used in this thesis was designed for the scale-up for mixing of melt polymers. Owing to the differences in properties between thermoset rubber and typical thermoplastics processed by extrusion, commonly available scaling methods are likely to yield a poor prediction of the design and performance of scaled-up devulcanisation processes. Furthermore, the extrusion parameters that should be considered important for devulcanisation are currently poorly understood. Therefore, research into the fundamental parameters affecting the scaling of extrusion-based devulcanisation processes would allow more reliable design and prediction of the performance of large-scale devulcanisation plants.

## 6.2.3 Fundamental research into RR characterisation

The relationship between the properties of devulcanised rubber (RR) and the physical properties of new rubber compounds containing RR is currently poorly understood, which is believed to be one of the major barriers to the more widespread acceptance of RR as a truly valuable raw material. The experiments already described in Section 6.2.1 are expected to yield reclaimed rubber of varying extents of devulcanisation and selectivity for crosslink scission. Revulcanisation and subsequent testing of physical properties of the RR, along with blends of RR with fresh rubber, could provide invaluable information on how the selectivity for crosslink scission and extent of devulcanisation affect the physical properties of compounds containing reclaimed rubber.

Furthermore, fundamental research and development of a new reliable characterisation methodology developed specifically for RR could further the understanding of the important properties of RR as they pertain to important properties required for high-value applications of rubber, such as automotive tyres. This recommendation is made considering the errors that were encountered and discussed in Chapter 4, along with the large number of assumptions required for the application of current methods. A rigorous, standardised methodology for characterising RR would lead to greater comparability between future publications, thereby leading to more rapid advancement of the fundamental understanding of RR performance and process optimisation.

## References

- Adhikari, B., De, D. & Maiti, S. 2000. Reclamation and recycling of waste rubber. *Progress in Polymer Science (Oxford)*. 25(7):909–948. DOI: 10.1016/S0079-6700(00)00020-4.
- Alemán, J. V., Chadwick, A. V., He, J., Hess, M., Horie, K., Jones, R.G., Kratochvíl, P., Meisel, I., et al. 2007. Definitions of terms relating to the structure and processing of sols, gels, networks, and inorganic-organic hybrid materials (IUPAC Recommendations 2007). *Pure and Applied Chemistry*. 79(10). DOI: 10.1351/pac200779101801.
- Bilgili, E., Arastoopour, H. & Bernstein, B. 2001a. Pulverization of rubber granulates using the solid state shear extrusion process. Part II. Powder characterization. *Powder Technology*. 115(3):277–289.
- Bilgili, E., Arastoopour, H. & Bernstein, B. 2001b. Pulverization of rubber granulates using the solid-state shear extrusion (SSSE) process: Part I. Process concepts and characteristics. *Powder Technology*. 115(3):265–276.
- Bilgili, E., Dybek, A., Arastoopour, H. & Bernstein, B. 2003. A new recycling technology: Compression molding of pulverized rubber waste in the absence of virgin rubber. *Journal of Elastomers and Plastics*. 35(July 2003):235–256. DOI: 10.1177/0095244303035003004.
- Boys, C.H. & Naudain, E.A. 1957. Google Patents. Available: <https://www.google.com/patents/US2794006>.
- Bryson, J.G. 1979. Google Patents. Available: <https://www.google.com/patents/US4148763>.
- Charlesby, A. 1954. Gel formation and molecular weight distribution in long-chain polymers. *Proceedings of the Royal Society of London. Series A. Mathematical and Physical Sciences*. 222(1151):542–557.
- Coran, A.Y. 2013. Vulcanization. In *The Science and Technology of Rubber*. Elsevier. 337–381. DOI: 10.1016/B978-0-12-394584-6.00007-8.
- Couper, J.R. 2003. *Process engineering economics*. CRC Press.
- Danon, B., van der Gryp, P., Schwarz, C.E. & Görgens, J.F. 2015. A review of dipentene (dl-limonene) production from waste tire pyrolysis. *Journal of Analytical and Applied Pyrolysis*. 112:1–13. DOI: 10.1016/j.jaap.2014.12.025.
- Danon, B., de Villiers, a. & Görgens, J.F. 2015. Elucidation of the different devolatilisation zones of tyre rubber pyrolysis using TGA-MS. *Thermochimica Acta*. 614:59–61. DOI: 10.1016/j.tca.2015.05.012.
- De, D., Maiti, S. & Adhikari, B. 1999. Reclaiming of rubber by a renewable resource material (RRM). II. Comparative evaluation of reclaiming process of NR vulcanizate by RRM and diallyl disulfide. *Journal of applied polymer science*. 73(14):2951–2958.
- De, D., Das, A., De, D., Dey, B., Debnath, S.C. & Roy, B.C. 2006. Reclaiming of ground rubber tire (GRT) by a novel reclaiming agent. *European Polymer Journal*. 42(4):917–927.
- Dell Inc. 2015. STATISTICA (data analysis software system), version 12. [www.statsoft.com](http://www.statsoft.com).

Erman, B. & Mark, J.E. 2013. The Molecular Basis of Rubberlike Elasticity. In *The Science and Technology of Rubber*. Elsevier. 167–192. DOI: 10.1016/B978-0-12-394584-6.00004-2.

Eskom. 2015. *Integrated Report*. Available: <http://www.eskom.co.za/IR2015/Documents/EskomIR2015spreads.pdf> [2015, November 23].

Ferrer, G. 1997. The economics of tire remanufacturing. *Resources, Conservation and Recycling*. 19(4):221–255. DOI: 10.1016/S0921-3449(96)01181-0.

Flory, P.J. 1944. Network Structure and the Elastic Properties of Vulcanized Rubber. *Chemical Reviews*. 35(1):51–75. DOI: 10.1021/cr60110a002.

Flory, P.J. & Rehner, J. 1943. Statistical Mechanics of Cross-Linked Polymer Networks II. Swelling. *The Journal of Chemical Physics*. 11(11):521. DOI: 10.1063/1.1723792.

Formela, K., Cysewska, M. & Haponiuk, J. 2014. The influence of screw configuration and screw speed of co-rotating twin screw extruder on the properties of products obtained by thermomechanical reclaiming of ground tire rubber. *Polimery*. 59(02):170–177. DOI: 10.14314/polimery.2014.170.

Hong, C.K. & Isayev, A.I. 2001. Continuous ultrasonic devulcanization of carbon black-filled NR vulcanizates. *Journal of applied polymer science*. 79(13):2340–2348.

Hong, C.K. & Isayev, A.I. 2002. Blends of ultrasonically devulcanized and virgin carbon black filled NR. *Journal of materials science*. 37(2):385–388.

Horikx, M.M. 1956. Chain Scissions in a Polymer Network. *Rubber Chemistry and Technology*. 29(4):1166–1173. DOI: 10.5254/1.3542617.

Isayev, A.I. 2013. Recycling of Rubbers. In *The Science and Technology of Rubber*. Elsevier. 697–764. DOI: 10.1016/B978-0-12-394584-6.00020-0.

Isayev, A.I., Yushanov, S.P. & Chen, J. 1996a. Ultrasonic devulcanization of rubber vulcanizates. I. Process model. *Journal of Applied Polymer Science*. 59(5):803–813.

Isayev, A.I., Yushanov, S.P. & Chen, J. 1996b. Ultrasonic devulcanization of rubber vulcanizates. II. Simulation and experiment. *Journal of applied polymer science*. 59(5):815–824.

Isayev, A.I., Liang, T. & Lewis, T.M. 2013. Effect of Particle Size on Ultrasonic Devulcanization of Tire Rubber in Twin-Screw Extruder. *Rubber Chemistry and Technology*. 00(0):130806110153001. DOI: 10.5254/RCT.13.87926.

Jana, G.K. & Das, C.K. 2005. Devulcanization of natural rubber vulcanizates by mechanochemical process. *Polymer-Plastics Technology and Engineering*. 44(8-9):1399–1412.

Kirby, W.G. & Steinle, L.E. 1942. Available: <http://www.google.com/patents/US2279047>.

Kraus, G. 1963. Swelling of filler-reinforced vulcanizates. *Journal of Applied Polymer Science*. 7(3):861–871. DOI: 10.1002/app.1963.070070306.

Levy, S. & Carley, J.F. 1989. *Plastics Extrusion Technology Handbook*. 2nd ed. Industrial Press, Inc.

Li, Y., Zhao, S. & Wang, Y. 2011. Microbial desulfurization of ground tire rubber by *Thiobacillus ferrooxidans*. *Polymer Degradation and Stability*. 96(9):1662–1668. DOI: 10.1016/j.polymdegradstab.2011.06.011.

Mangili, I., Collina, E., Anzano, M., Pitea, D. & Lasagni, M. 2014. Characterization and supercritical CO<sub>2</sub> devulcanization of cryo-ground tire rubber: Influence of devulcanization process on reclaimed material. *Polymer Degradation and Stability*. 102:15–24. DOI: 10.1016/j.polymdegradstab.2014.02.017.

Mangili, I., Lasagni, M., Anzano, M., Collina, E., Tatangelo, V., Franzetti, A., Caracino, P. & Isayev, A.I. 2015. Mechanical and rheological properties of natural rubber compounds containing devulcanized ground tire rubber from several methods. *Polymer Degradation and Stability*. 121:369–377. DOI: 10.1016/j.polymdegradstab.2015.10.004.

Manuel, H.J. & Dierkes, W. 1997. *Recycling of rubber*. V. 99. iSmithers Rapra Publishing.

Maridass, B. & Gupta, B.R. 2004. Performance optimization of a counter rotating twin screw extruder for recycling natural rubber vulcanizates using response surface methodology. *Polymer Testing*. 23(4):377–385. DOI: 10.1016/j.polymertesting.2003.10.005.

Matsushita, M., Mouri, M., Okamoto, H., Fukumori, K., Sato, N., Fukuta, M., Honda, H., Nakashima, K., et al. 2003. Available: <https://www.google.com/patents/US6632918>.

Myhre, M., Saiwari, S., Dierkes, W. & Noordermeer, J. 2012. Rubber Recycling: Chemistry, Processing, and Applications. *Rubber Chemistry and Technology*. 85(3):408–449. DOI: 10.5254/rct.12.87973.

Novotny, D.S., Marsh, R.L., Masters, F.C. & Tally, D.N. 1978. Available: <https://www.google.com/patents/US4104205>.

PayScale. 2015. *South Africa Salary Survey*. Available: [http://www.payscale.com/research/ZA/Country=South\\_Africa/Salary](http://www.payscale.com/research/ZA/Country=South_Africa/Salary) [2015, October 19].

Perry, R.H., Green, D.W. & Maloney, J.O. 1997. *Perry's handbook of chemical engineering*. Mc Graw-Hill.

Rajan, V. V., Dierkes, W.K., Noordermeer, J.W.M. & Joseph, R. 2005. Comparative Investigation on the Reclamation of NR Based Latex Products with Amines and Disulfides. *Rubber Chemistry and Technology*. 78(5):855–867. DOI: 10.5254/1.3547918.

Rajan, V. V., Dierkes, W.K., Joseph, R. & Noordermeer, J.W.M. 2007. Effect of diphenyldisulfides with different substituents on the reclamation of NR based latex products. *Journal of Applied Polymer Science*. 104(6):3562–3580. DOI: 10.1002/app.25925.

Rauwendaal, C. 2014. Extruder Screw Design. In *Polymer Extrusion*. München: Carl Hanser Verlag GmbH & Co. KG. 509–652. DOI: 10.3139/9781569905395.008.

Rodgers, B. & Waddell, W. 2013a. Tire Engineering. In *The Science and Technology of Rubber*. Elsevier. 653–695. DOI: 10.1016/B978-0-12-394584-6.00014-5.

- Rodgers, B. & Waddell, W. 2013b. The Science of Rubber Compounding. In *The Science and Technology of Rubber*. Elsevier. 417–471. DOI: 10.1016/B978-0-12-394584-6.00009-1.
- Roussy, G., Mercier, A., Thiébaud, J.-M. & Vaubourg, J.-P. 1985. Temperature runaway of microwave heated materials: Study and control. *J. Microwave Power*. 20(1):47–51.
- Saiwari, S. & Dierkes, W.K. 2013. Devulcanization of whole passenger car tire material. 20–25.
- SARS. 2015. Tax Guide for Small Business. *South African Revenue Service*.
- Shi, J., Jiang, K., Ren, D., Zou, H., Wang, Y., Lv, X. & Zhang, L. 2013. Structure and performance of reclaimed rubber obtained by different methods. *Journal of Applied Polymer Science*. 129(3):999–1007. DOI: 10.1002/app.38727.
- Si, H., Chen, T. & Zhang, Y. 2013. Effects of high shear stress on the devulcanization of ground tire rubber in a twin-screw extruder. *Journal of Applied Polymer Science*. 128(4):2307–2318. DOI: 10.1002/app.38170.
- Tao, G., He, Q., Xia, Y., Jia, G., Yang, H. & Ma, W. 2013. The effect of devulcanization level on mechanical properties of reclaimed rubber by thermal-mechanical shearing devulcanization. *Journal of Applied Polymer Science*. 129(5):2598–2605. DOI: 10.1002/app.38976.
- Towler, G.P. & Sinnott, R.K. 2013. *Chemical Engineering Design: Principles, Practice, and Economics of Plant and Process Design*. Elsevier.
- Tukachinsky, A., Schworm, D. & Isayev, A.I. 1996. Devulcanization of Waste Tire Rubber by Powerful Ultrasound. *Rubber Chemistry and Technology*. 69(1):92–103. DOI: 10.5254/1.3538362.
- Waddell, W.H., Bhakuni, R.S., Barbin, W.W. & Sandstrom, P.H. 1990. *Pneumatic tire compounding*.
- Wicks, I.G.G., Schulz, R.L., Poll, D.C., Us, G.F.L., Romine, M.F. & Swan, L.S. 2002.
- Winkelman, H.A. 1926. The Present and Future of Reclaimed Rubber. *Industrial & Engineering Chemistry*. 18(11):1163–1168. DOI: 10.1021/ie50203a018.
- Yazdani, H., Karrabi, M., Ghasmi, I., Azizi, H. & Bakhshandeh, G.R. 2011. Devulcanization of Waste Tires Using a Twin-Screw Extruder : The Effects of Processing Conditions. DOI: 10.1002/vnl.
- Yun, J., Oh, J.S. & Isayev, a. I. 2001. Ultrasonic Devulcanization Reactors for Recycling of GRT: Comparative Study. *Rubber Chemistry and Technology*. 74(2):317–330. DOI: 10.5254/1.3544953.
- Yun, J., Isayev, A.I., Kim, S.H. & Tapale, M. 2003. Comparative analysis of ultrasonically devulcanized unfilled SBR, NR, and EPDM rubbers. *Journal of Applied Polymer Science*. 88(2):434–441.

Van Zuilichem, D.J., Stolp, W. & Janssen, L.P.B.M. 1983. Engineering aspects of single- and twin-screw extrusion-cooking of biopolymers. *Journal of Food Engineering*. 2(3):157–175.  
DOI: 10.1016/0260-8774(83)90008-0.

## Appendix A: Calculation of Horikx curves

The purpose of Appendix A is to describe the details of the interpretation and assumptions made in the calculation of the theoretical Horikx curves. This discussion is important due to the lack of consensus around the interpretations and assumptions used by other authors in the field of rubber devulcanisation.

In the case of random C-C bond scission, the relationship between the relative decrease in crosslink density and the final sol fraction is described by equation A.1 (Horikx, 1956):

$$1 - \frac{\nu_{e2}}{\nu_{e1}} = 1 - \frac{(1 - \sqrt{s_2})^2}{(1 - \sqrt{s_1})^2} \quad (\text{A.1})$$

where  $\nu_{e1}$  is the crosslink density of the gel fraction before devulcanisation,  $\nu_{e2}$  is the crosslink density of the gel fraction after devulcanisation,  $s_1$  is the initial sol fraction of the crumb before devulcanisation and  $s_2$  is the sol fraction measured after devulcanisation. Due to the difficulty of obtaining a precise experimental measurement of the initial sol fraction,  $s_1$  was estimated according to Equation A.2 (Charlesby, 1954; Horikx, 1956):

$$s_1 = \frac{(2 + \gamma_1) - (\gamma_1^2 + 4\gamma_1)^{0.5}}{2\gamma_1} \quad (\text{A.2})$$

where  $\gamma_1$  is the initial value of the crosslinking index of the rubber network, calculated according to Equations A.3, A.4 and A.5, assuming an initial number-average molecular weight of the rubber polymer chains to be  $M = 200000 \text{ g/mol}$  (Horikx, 1956).

$$N = \frac{1}{M} \quad (\text{A.3})$$

$$\nu_0 = \nu_e + 2N \quad (\text{A.4})$$

$$\gamma = \frac{\nu_0}{N} \quad (\text{A.5})$$

Finally, for selective crosslink scission, the relationship between the relative decrease in crosslink density and the sol fraction after devulcanisation is described by:

$$1 - \frac{\nu_{e2}}{\nu_{e1}} = 1 - \frac{\gamma_2(1 - \sqrt{s_2})^2}{\gamma_1(1 - \sqrt{s_1})^2} \quad (\text{A.6})$$

where  $\gamma_1$  is the crosslinking index of the crumb before devulcanisation and  $\gamma_2$  is the crosslinking index of the sample after devulcanisation, calculated according to Equations A.3, A.4 and A.5 using the measured value of the final crosslink density in Equation A.4.

## Appendix B: Economics

Appendix B.1 gives an overview of some of the assumptions and clarifications to the economic analysis reported in Chapter 5, while Appendix B.2 consists of DCF analysis tables and cumulative DCF curves for selected scenarios.

### B.1. Assumptions and clarifications

The area required for the plant was estimated from the equipment footprint of extruders: the 100 mm extruder requires 20 m<sup>2</sup> per extruder and the 180 mm extruder requires 26 m<sup>2</sup> per extruder. The footprint was multiplied by the number of extruders required, and then further multiplied by 10 in order to allow sufficient room for safe operation, raw material storage and offices.

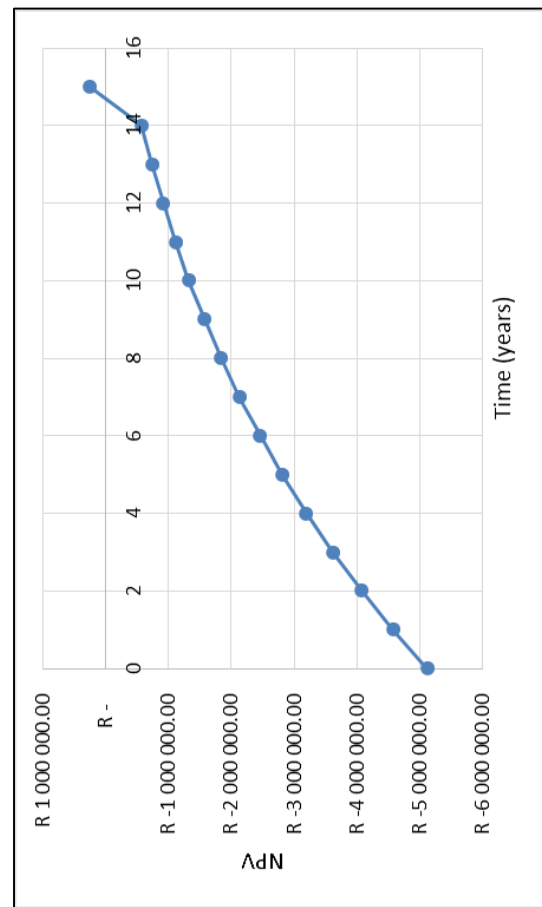
Maintenance costs for a typical plastic extrusion process using a 64 mm single-screw extruder are listed as US\$ 0.54 per hour of operation in 1989 (Levy & Carley, 1989) which amounts to approximately US\$ 1.04 per hour in 2015, or roughly US\$ 2750 per year. Scaling the quoted equipment costs of the 180 mm extruder and 100 mm down to a 64 mm extruder using the “six tenths rule” (found to be valid between the 100 mm and 180 mm extruders) suggested that the annual maintenance costs amount to approximately 11% of the purchase cost of the extruder. In the absence of any more reliable method for estimating maintenance costs, this rough estimate was used for the preliminary economic analysis.

The scrap value of the extruders was neglected in the DCF analysis, although the recovery of the relatively large working capital was accounted for, as seen in year 15 of the DCF sheets in Appendix B.2.

## B.2. Selected DCF sheets

Mechanical devulcanisation: Iteration 5

Year	Revenue	Expenses	Depreciation	Net profit/loss	Tax	Cash flow	DCF	NPV
0	R -	R 5 120 221.86	R -	R -5 120 221.86	R -	R -5 120 221.86	R -5 120 221.86	R -5 120 221.86
1	R 20 761 602.01	R 20 014 482.89	R 131 900.00	R 615 219.13	R 147 652.59	R 599 466.54	R 548 459.78	R -4 571 762.08
2	R 20 761 602.01	R 20 014 482.89	R 131 900.00	R 615 219.13	R 147 652.59	R 599 466.54	R 501 793.03	R -4 069 969.06
3	R 20 761 602.01	R 20 014 482.89	R 131 900.00	R 615 219.13	R 147 652.59	R 599 466.54	R 459 097.01	R -3 610 872.05
4	R 20 761 602.01	R 20 014 482.89	R 131 900.00	R 615 219.13	R 147 652.59	R 599 466.54	R 420 033.86	R -3 190 838.20
5	R 20 761 602.01	R 20 014 482.89	R 131 900.00	R 615 219.13	R 147 652.59	R 599 466.54	R 384 294.47	R -2 806 543.72
6	R 20 761 602.01	R 20 014 482.89	R 131 900.00	R 615 219.13	R 147 652.59	R 599 466.54	R 351 596.04	R -2 454 947.68
7	R 20 761 602.01	R 20 014 482.89	R 131 900.00	R 615 219.13	R 147 652.59	R 599 466.54	R 321 679.82	R -2 133 267.87
8	R 20 761 602.01	R 20 014 482.89	R 131 900.00	R 615 219.13	R 147 652.59	R 599 466.54	R 294 309.07	R -1 838 958.80
9	R 20 761 602.01	R 20 014 482.89	R 131 900.00	R 615 219.13	R 147 652.59	R 599 466.54	R 269 267.22	R -1 569 691.58
10	R 20 761 602.01	R 20 014 482.89	R 131 900.00	R 615 219.13	R 147 652.59	R 599 466.54	R 246 356.10	R -1 323 335.47
11	R 20 761 602.01	R 20 014 482.89	R -	R 747 119.13	R 179 308.59	R 567 810.54	R 213 492.03	R -1 109 843.44
12	R 20 761 602.01	R 20 014 482.89	R -	R 747 119.13	R 179 308.59	R 567 810.54	R 195 326.65	R -914 516.79
13	R 20 761 602.01	R 20 014 482.89	R -	R 747 119.13	R 179 308.59	R 567 810.54	R 178 706.91	R -735 809.88
14	R 20 761 602.01	R 20 014 482.89	R -	R 747 119.13	R 179 308.59	R 567 810.54	R 163 501.29	R -572 308.59
15	R 24 097 349.16	R 20 014 482.89	R -	R 4 082 866.28	R 979 887.91	R 3 102 978.37	R 817 478.46	R 245 169.87
	<b>NPV</b>	<b>IRR</b>	<b>PBP</b>					
	R 245 169.87	10%	8.54					



Mechanochemical devulcanisation: Iteration 5

Year	Revenue	Expenses	Depreciation	Net profit/loss	Tax	Cash flow	DCF	NPV
0	R -	R 6 203 402.85	R -	R -6 203 402.85	R -	R -6 203 402.85	R -6 203 402.85	R -6 203 402.85
1	R 26 689 080.48	R 25 733 742.83	R 135 050.00	R 820 287.65	R 229 680.54	R 725 657.11	R 663 913.18	R -5 539 489.67
2	R 26 689 080.48	R 25 733 742.83	R 135 050.00	R 820 287.65	R 229 680.54	R 725 657.11	R 607 422.86	R -4 932 066.81
3	R 26 689 080.48	R 25 733 742.83	R 135 050.00	R 820 287.65	R 229 680.54	R 725 657.11	R 555 739.12	R -4 376 327.69
4	R 26 689 080.48	R 25 733 742.83	R 135 050.00	R 820 287.65	R 229 680.54	R 725 657.11	R 508 452.99	R -3 867 874.70
5	R 26 689 080.48	R 25 733 742.83	R 135 050.00	R 820 287.65	R 229 680.54	R 725 657.11	R 465 190.29	R -3 402 684.41
6	R 26 689 080.48	R 25 733 742.83	R 135 050.00	R 820 287.65	R 229 680.54	R 725 657.11	R 425 608.69	R -2 977 075.72
7	R 26 689 080.48	R 25 733 742.83	R 135 050.00	R 820 287.65	R 229 680.54	R 725 657.11	R 389 394.96	R -2 587 680.77
8	R 26 689 080.48	R 25 733 742.83	R 135 050.00	R 820 287.65	R 229 680.54	R 725 657.11	R 356 262.54	R -2 231 418.23
9	R 26 689 080.48	R 25 733 742.83	R 135 050.00	R 820 287.65	R 229 680.54	R 725 657.11	R 325 949.26	R -1 905 468.97
10	R 26 689 080.48	R 25 733 742.83	R 135 050.00	R 820 287.65	R 229 680.54	R 725 657.11	R 298 215.24	R -1 607 253.73
11	R 26 689 080.48	R 25 733 742.83	R -	R 955 337.65	R 267 494.54	R 687 843.11	R 258 623.28	R -1 348 630.45
12	R 26 689 080.48	R 25 733 742.83	R -	R 955 337.65	R 267 494.54	R 687 843.11	R 236 617.82	R -1 112 012.63
13	R 26 689 080.48	R 25 733 742.83	R -	R 955 337.65	R 267 494.54	R 687 843.11	R 216 484.74	R -895 527.90
14	R 26 689 080.48	R 25 733 742.83	R -	R 955 337.65	R 267 494.54	R 687 843.11	R 198 064.72	R -697 463.18
15	R 30 978 037.62	R 25 733 742.83	R -	R 5 244 294.79	R 1 468 402.54	R 3 775 892.25	R 994 757.36	R 297 294.19
	<b>NPV</b>	<b>IRR</b>	<b>PBP</b>					
	R 297 294.19	10%	8.55					

